DESCRIPTIVE STUDY OF THE PHYSICAL OCEANOGRAPHY OF THE ALA WAI CANAL

BY
FRANK I. GONZALEZ, JR.
DEPARTMENT OF OCEANOGRAPHY
UNIVERSITY OF HAWAII

UNIVERSITY OF HAWAII
HAWAII INSTITUTE OF MARINE BIOLOGY
HONOLULU, HAWAII TECHNICAL REPORT NO. 26 MAY 1971

Descriptive Study of the Physical Oceanography of the Ala Wai Canal*

By

Frank I. Gonzalez, Jr.

May 1971

HAWAII INSTITUTE OF MARINE BIOLOGY

UNIVERSITY OF HAWAII

Technical Report Number 26

*Also issued as report HIG-71-7 of the
Hawaii Institute of Geophysics, University of Hawaii

A DESCRIPTIVE STUDY OF THE PHYSICAL OCEANOGRAPHY OF THE ALA WAI CANAL

A THESIS SUBMITTED TO THE GRADUATE DIVISION OF THE UNIVERSITY OF HAWAII IN PARTIAL FULFILLMENT OF THE REQUIREMENTS FOR THE DEGREE OF

MASTER OF SCIENCE

IN OCEANOGRAPHY

JUNE 1971

By

Frank I. Gonzalez, Jr.

Thesis Committee:

Brent S. Gallagher, Chairman
Edward D. Stroup
Robert A. Grace

ACKNOWLEDGMENTS

Dr. G. I. Murphy first suggested that this study be made; I am grateful to him and to Dr. B. S. Gallagher for their encouragement and guidance during this project. In addition, I am grateful to H. Santamore and D. Scott for their assistance.

This investigation was financed in part by the State of Hawaii, Division of Fish and Game, Department of Land and Natural Resources, who were supporting a general ecological study of the Ala Wai system. The study also received financial support from the Department of Oceanography, University of Hawaii.

I would like to acknowledge the organizations which made data available to me for use in this study: the U. S. Weather Bureau in Honolulu supplied wind and rain observations; the U. S. Geological Survey furnished stream discharge records.

The Water Resources Research Center of the University of Hawaii made their facilities available for the chemical and microbiological analyses. I am particularly grateful to K. Morphew of this organization who gave most generously of his time and experience in this task.

Finally, special thanks are due to my wife, Yolanda, for her moral support throughout this study and her cheerful assistance in the collection of data under frequently cheerless conditions.

ABSTRACT

From March through December 1969 a study of the circulation and temperature-salinity structure of the Ala Wai Canal was made. This man-made channel has an average depth of about 2 meters, and is about 70 meters wide and 3 kilometers long. It was constructed in two straight sections joined by a 45° elbow, and the landward section receives runoff from two major streams at about its midpoint. A circulation pattern typical of partially mixed, moderately stratified estuaries was found, and estimates were made of residence times. Heavy silting has altered the original bathymetry of the Canal into a channel, sill, and basin region. Deep water in the basin is virtually anoxic. Longitudinal sections of dissolved oxygen, phosphates, nitrates, and suspended load were obtained and an analysis was run on surface samples for fecal bacteria.

TABLE OF CONTENTS

LIST OF TABLES

LIST OF FIGURES

LIST OF FIGURES (CONTINUED)

LIST OF FIGURES (CONTINUED)

LIST OF FIGURES (CONTINUED)

LIST OF FIGURES (CONTINUED)

INTRODUCTION

The Waikiki resort area is separated almost entirely from the city of Honolulu by a long, narrow estuary called the Ala Wai Canal. The Canal was constructed by the Army Corps of Engineers in 1927 as part of a project to reclaim marsh lands in the Waikiki area (Bigelow, 1927). It is composed of two straight sections, each having near-vertical, parallel sides. These sections join at a 45° elbow. The shorter segment is 750 meters long and 50 meters wide and opens on the sea, while the inshore leg is 2350 meters long and 76 meters wide. The longer section receives the discharge from two major streams, the Manoa and the Palolo. The mean depth of the Canal is about two meters.

The purpose of the present study was to provide a description of circulation, mass transports, residence times, and temperature-salinity structure in the Canal under varying runoff, tide and wind conditions. Near the end of the investigation, it was decided to extend the study to include chemical and bacteriological parameters which would be useful in the analysis of pollution in the Ala Wai. Public Health regulations define ceilings on acceptable levels of phosphate and nitrate concentrations as well as the total suspended load in the Canal. Accordingly, these were chosen as the additional parameters which were to be examined.

It had already been established that the Ala Wai Canal and Yacht Harbor did not meet State Department of Health standards for microbiological contamination; Cox (1969) summarized the pertinent

data. The purpose of the present bacteriological sampling was to try to locate the source of this pollution in the Ala Wai; specifically, it was of interest to determine whether pollution from the harbor might extend upstream into the Canal. It had been suggested that the several hundred sailing vessels and houseboats moored in the harbor may introduce a significant amount of sewage into the water (Honolulu Advertiser, 1957). The information gathered on circulation patterns in the Canal aided in answering this question.

PRINCIPAL FINDINGS

Heavy silting since construction of the Ala Wai Canal in 1927 has drastically altered its original, more or less flat-bottomed bathymetry. The Canal is now divisible into several distinct topographic regions, each occupying roughly a third of the length of the entire Canal. Starting at the harbor and continuing landward, we have: a sloped-bottom channel, an extensive sill region and a relatively deep basin (Figure 20). A smaller basin is located at the curve of the Canal, between the sill and channel. The present rate of deposition on the sill is about 20 cm/year.

Tides in the Canal are identical to those predicted for Honolulu Harbor. Frequent oscillations of the Canal surface were observed, predominantly at periods of about sixteen minutes.

Over the sill and in the channel is found a circulation pattern common to most estuaries. It is made up of two components. The tidal flow is the first component; it is into the Canal on flood tide and out of the Canal on ebb at all depths. Superimposed on the tidal action is a surface flow of brackish water seaward, in a layer about 0.5 meters thick; this layer entrains sea water from below, causing a compensating landward drift at depth. This mechanism is most clearly seen at times of high and low water, when it is not obscured by the tidal flow (Figures 10 and 13, Station 1). The Canal is a partially mixed, moderately stratified estuary in Pritchard's (1967) classification scheme. This implies that the principal mechanism responsible for mixing sea water from the deep layer into the surface

layer is tide-generated turbulence and interfacial shear, and that fresh water runoff into the Canal is of sufficient magnitude to maintain large salinity gradients.

The average residence time of fresh water in the surface layer varies between two and thirty hours, depending on runoff and wind conditions. The average residence time of sea water in the deep layer is about four tidal cycles on the sill and about half a tidal cycle seaward of the sill.[1]

Renewal of water in the basin below sill depth occurs infrequently, and it is likely that this water has a minimum average residence time of at least four days, or eight tidal cycles. The principal mechanism by which this water is renewed involves an increase in its temperature by solar heating to a point where it is lighter than the relatively cool water on the sill. On the flood tide the sill water spills over into the basin, sinking to an appropriate depth.

The Manoa-Palolo Drainage Canal seems to be the principal source of bacterial pollution in the Canal. Bacterial counts are also high in the Ala Wai Yacht Harbor, although it is unlikely that these organisms are transported in any significant amounts into the Ala Wai Canal.

---

[1]Since tides are of the mixed type in Hawaii, the period between successive low water stands may vary between 12 and 24 hours. Therefore, when speaking of processes which are dependent on changes of sea level, rather than on time, *per se*, it is more accurate to speak in terms of tidal cycles rather than hours. Thus a tidal cycle in this study will refer to a period between successive high or low water stands, rather than the usual temporal definition associated with the lunar period.

METHODS AND DATA PRESENTATION

1. Bathymetry. A bathymetric survey was carried out on July 13, 1969, using a Raytheon Model DE-719 Fathometer Depth Recorder. The results were used to construct the map shown in Figure 2. All depths in this map are referred to Mean Lower Low Water; this is the "zero" found on tidal charts constructed from U. S. Coast and Geodetic Survey tide tables and published annually by the Dillingham Corporation. Information obtained from this survey is listed in Table 1. Explanations of terms such as "basin" or "sill" are given on page 13. Entries in the table are also referred to MLLW. Volumes for any particular sea level can be obtained by multiplying the surface area by the appropriate difference in depth and adding this volume to the MLLW volume.

The City and County of Honolulu carried out a survey in a portion of the Canal during May of 1965; this was done in order to draw up specifications for a dredging operation which was to begin the following year. These data were used to construct a map of the bottom topography as it must have looked then; it is presented in Figure 3 mainly as an item of historical interest.

2. Tides. Two Belfort Liquid Level Recorders, damped to filter out high frequency oscillations, were used to measure sea level in the Canal. One was placed at Station 1, the other at the extreme landward end of the Canal. Figure 1 shows the location of stations on the Canal. Thirteen days of records were obtained at Station 1, but due to instrument failure only two days were recorded at the

landward end. An example of a typical record is shown in Figure 4.

3. Fresh water runoff. Figure 5 shows the drainage area from which the Ala Wai Canal receives fresh water runoff; it covers about 1.06×10^4 acres (4.3×10^7 m^2) and includes Manoa, Palolo and Makiki Valleys. Half of the area is undeveloped, wooded terrain such as the valley slopes, and the other half consists of residential and business districts characterized by asphalt streets and other materials which are much less porous than the valley slopes.

Most of the water enters the Ala Wai by means of the Manoa-Palolo Drainage Canal; as the name implies, it is the confluence of the two streams which drain the Manoa and Palolo Valleys. A substantial amount of fresh water is introduced by Apukehau Stream, which receives the drainage from Makiki Valley, and lesser amounts are introduced by several drainage ditches and numerous storm sewers located along the banks of the Ala Wai.

Continuous recording gauging stations are operated in the area by the U. S. Geological Survey; they are located as shown in Figure 5. Gauge #2470 monitors the flow of Palolo Stream, which drains Palolo Valley; gauges #2385 and #2405 measure the runoff from the area above the confluence which marks the beginning of Manoa Stream. Note that no stream gauges measure the runoff from Manoa Valley below this confluence, nor the runoff from Makiki Valley.

In order to determine the total runoff into the Canal, it was necessary to estimate the runoff due to these parts of the drainage area not directly monitored by stream gauges. This was accomplished

by obtaining all available rainfall data for the area and dates of interest, and contouring isohyetal lines. The areas were then planimetered to obtain total precipitation for that day. Due to such things as evaporation and diversion of water, the amount of runoff finally reaching the Ala Wai can be expected to be somewhat less than that of the total rainfall, and the literature was, therefore, searched for appropriate percentages which could be applied to the areas under consideration.

Mink (1962) found that runoff on the leeward Koolau Mountains was about 25% of the rainfall; this relationship was assumed for the slopes of Makiki and Manoa Valleys.

Chinn (1965) found that an asphalt catchment on the island of Hawaii was still 78% efficient after three years of minimum maintenance. Something close to this figure might apply to business and residential districts where streets are paved with asphalt, but the net efficiency would be somewhat lower due to open, unpaved areas such as lawns and empty lots. The Honolulu Department of Public Works (1969) estimates that runoff is 55 to 70% of rainfall in residential areas. It was decided to assume that the runoff in such areas as Waikiki and residential portions of Manoa Valley was 65% of the rainfall. This decision to bias the estimate in the direction of higher runoff was based in part on the visual inspection of an aerial photograph which made it clear that only a small percentage of land in these districts is open and unpaved.

To get an idea of how runoff in 1969 compared with other years,

the mean monthly discharges recorded at the stream gauge stations in 1969 were compared with the 10-year period from 1959 to 1969. This comparison is shown in Figure 6. The rainy season is considered to extend roughly from December through April, and the mean discharge for this period was 70% higher during 1969 than the mean for the previous 10-year period. This proved fortunate, in that it enabled data to be collected over a very wide range of runoff conditions. Table 2 lists the estimated runoff into the Ala Wai for days on which data surveys were made. This runoff is separated into two components: the runoff monitored directly by stream gauges and the runoff estimated from rainfall data.

Several shortcomings in this table must be pointed out here. It was felt that an attempt to achieve an accuracy of $\pm$ 10% in all measurements made during this study represented a reasonable goal. The accuracy of the stream gauge data is within these limits; calibration of these gauges is routinely checked by the U. S. Geological Survey each month and is found accurate to within about 8%. However, a more serious source of error is found in the procedure used to determine the additional runoff from areas with ungauged streams. The procedure suffers from two failings. The first is the process of establishing isohyetals over an area; precipitation gradients in the valleys can be quite large, and a certain amount of error was inevitably introduced by linearly interpolating between the available rain gauge data. The second is the simplification of the rainfall-runoff relationship to a linear function; the amount of runoff for

a given rainfall depends not only on the type of terrain, but is also a complicated function of such things as intensity, evaporation, and the frequency of precipitation in the area.

Although it was not possible to objectively determine the probable percentage of error, it was felt that ± 50% of the ungauged runoff was a liberal estimate and these limits were, therefore, entered in the table.

4. Wind. Wind data were gathered on the Ala Wai on June 29th and 30th, and the results are shown in Figures 12 and 15. Mean speed was estimated by visually averaging the readings from a Sims Wind Anemometer. Direction was obtained by holding aloft a light strip of cloth and noting the angle it made with the longitudinal axis of the Canal.

It was felt desirable to have more general information on the wind regime, such as averages over an entire day. It seemed plausible that at least a good qualitative idea of conditions on the Canal, especially during strong trade wind weather, could be inferred from Honolulu International Airport records.[2] This airport is located about 5 miles northwest of the Ala Wai. The airport records for June 29th and 30th were examined in order to test this suggestion, and it was found that while the instantaneous Canal readings showed a somewhat stronger easterly component, the average wind speed agreed

---

[2]Personal communication, Dr. R. Taylor, Meteorologist, Hawaii Institute of Geophysics.

well with airport data if a vertical log profile was assumed. (Airport data are collected at a height of 30.5 meters above mean sea level, and the Canal data were taken about 1 meter above water level.)

It was, therefore, assumed that airport records were fairly good indications of wind speed and at least the quadrant from which the wind blows on the Canal. Wind speed and direction recorded at the airport and corrected to a height of 1 meter are given in Table 3 for the dates and times during which surveys were made on the Canal.

5. Salinity and temperature. Salinity and temperature profiles were made with a Beckman RS-53 Portable Salinometer along the length of the Canal during twelve surveys conducted in 1969. No measurable lateral variations were noted on the first survey, and all subsequent measurements were confined to the longitudinal axis of the Canal.

After calculation of sigma-t from the temperature and salinity data, a longitudinal section was prepared for each of these three parameters (Figures 21 through 31).

The data collections of June 29th and 30th were spread over half a tidal cycle, and it was felt that this lack of synopticity precluded the preparation of meaningful longitudinal sections. Instead, the individual profiles are presented in Figures 10, 11, 13 and 14 with current data which were collected at the same time.

6. Currents. Current profiles were obtained along the axis of the Canal using two Ekman-Merz current meters. These measurements were made on the flood tide of June 29th and the ebb tide of June 30th. Figure 16 indicates sea level at the time each station was occupied.

Temperature and salinity measurements were also made at this time, and they are presented in Figures 10, 11, 13 and 14 along with the velocity profiles.

It is regrettable that additional current data were not obtained. It would have been informative, for example, to determine volume transports during different tidal, wind, and runoff conditions. Such measurements were, in fact, planned; unfortunately, the author's personal work load was such that it was not possible to make this additional survey.

7. Dissolved oxygen. A Yellow Springs Model 54 Oxygen Meter was used to obtain oxygen profiles along the axis of the Canal, and longitudinal sections were prepared for the six surveys on which these measurements were made [Figures 23(d), 24(d), 28(d), 29(d), 30(d) and 31(d)].

8. Nutrients. Water samples were collected on the surveys of October 20th and December 9th. These were analyzed for phosphate, nitrate, and nitrite contents using the methods of Strickland and Parsons (1965). Longitudinal sections are presented in Figures 30(e), 30(f), 30(g), 31(e) and 31(f).

9. Suspended load. The water samples mentioned in the previous section were also analyzed for suspended load. The samples were first filtered through a pre-weighed Millipore filter; after oven-drying to drive off excess moisture the filters were weighed again to obtain the weight of the suspended material. Longitudinal sections were also prepared from this data [Figures 30(h) and 31(g)].

10. Bacteria. Water samples along the length of the Canal were obtained on the survey of December 9th for microbiological analysis. Filter techniques developed by the Millipore Corporation (1969) were used to test for total coliform, fecal coliform and fecal streptococci. Although pollution standards are written in terms of coliform bacteria, there is some evidence that streptococci may be more resistant to chlorination; it is for this reason that some authorities recommend the inclusion of these organisms as supportive data. Results are presented in Figures 32, 33 and 34.

RESULTS AND DISCUSSION

1. Bathymetry and silting. Topographically, the Canal can be divided into several distinct regions. To facilitate exposition, they are defined below and shown in Figure 20. All depths are referred to MLLW.

The BASIN extends from Station 13 to the extreme landward end of the Canal. It has a maximum depth of 3.5 meters.

The SILL occupies the area from Station 13 to the McCully Street bridge. It is an extensive shoal region, having an average depth of about 1 meter.

The SMALL BASIN occupies the curved portion of the Canal from the McCully Street bridge to the Kalakaua Street bridge, about midway between Stations 3 and 4. It has the same maximum depth as the larger basin, but its volume is smaller by a factor of 8.

The CHANNEL runs from the small basin to the mouth of the Canal at Station 1. The depth at the mouth is about 4 meters, but this decreases rapidly to about 2.5 meters at the Kalakaua Street bridge.

The STREAM refers to the Manoa-Palolo Drainage Canal. It has an average depth of about 0.5 meters and enters the Canal just seaward of Station 13.

These topographic features can be explained qualitatively in terms of the original depth at the time of construction and differing siltation rates along the Canal.

The Ala Wai was originally dredged in two sections joined approximately at the bend. The landward section was dredged to a depth of

3 to 6 meters and the section extending seaward was dredged to a depth of about 3 to 4 meters. A channel about 7.5 meters deep was also dredged from the Ala Moana bridge to about 150 meters seaward. Depths close to the original are found in the large and small basins, but heavy silting has significantly altered the bathymetry in other portions of the Canal.

In the basin, deposition is relatively slow, although some sediment is introduced by the large drainage ditch on the landward side of the basin at about Station 8, and more is carried in by storm sewers, located at the extreme landward end. The deposition at these two locations is evident in the bathymetry of Figure 2.

But the major source of silt is the stream, and it enters the Ala Wai at such an angle that a seaward flow out of the Canal is favored. Since the width of the Ala Wai at this junction is more than twice that of the stream, there is a sudden decrease in the mean velocity of the water as it enters the Canal. This decreased velocity is less than the critical velocity necessary to keep much of the silt in suspension; the result is a sudden dumping of the suspended load in the Canal, thereby creating the sill region.

Since the flow must curve at the stream entrance to the Canal, the characteristic bathymetry of a river meander is recognizable here. Heavy deposition is found on the inside of the curve, where velocities are relatively small; light deposition, perhaps scouring, are found on the outside of the curve, where velocities are higher.

An estimate of the silting rate in this region could be made if

the bathymetry at some previous time was known. A dredging operation was completed in the Canal in mid-1966. The region involved extended 250 feet landward and 1500 feet seaward of Station 13; in addition, the mouth of the stream was dredged to a distance 500 feet landward of its junction with the Ala Wai. Job specifications for this work were drawn up by the Engineering Department of the City and County of Honolulu, and they indicated the area was to be dredged to a depth of 6 feet below mean sea level. Figure 3 shows the area's bathymetry before dredging. If it is assumed that the contractor met the specifications, an estimate can be made of the amount of silt deposited since completion of the job. This assumption was made, and it was found that in a period of 40 months 2.1×10^4 m^3 of silt had been deposited in the dredged portion of the Ala Wai and 2.4×10^3 m^3 in the dredged portion of the stream. An area 3.2×10^4 m^2 was dredged in the Ala Wai, and 6.0×10^3 m^2 in the stream. Thus, the average silting rate on the sill and in the stream are about 20 and 12 cm/year, respectively. Average rates were also calculated for cross sections at intervals of 100 feet along the estuary. These values ranged from a maximum of 28 cm/year in a section 600 feet seaward of Station 13 to less than 10 cm/year in a section 1200 feet seaward of Station 13. The map of Figure 3 illustrates why the dredging was necessary; a tidal flat had been created just seaward of the stream entrance.

Further downstream, the constriction of the Canal at the McCully Street bridge causes an increase in the mean velocity of the water. This causes the re-suspension of some of the silt, and increases the

horizontal distance traveled by particles falling through the water column. Thus, for a short distance seaward of the constriction, a smaller amount of sediment actually reaches bottom; it is swept further down the Canal. This decreased deposition of silt has, in effect, created the small basin at the curve of the Canal.

The sloping bottom of the channel may be explained by the increase in average current speed towards the sea, and by a difference in flow velocities which are necessary to deposit or re-suspend sediment. (The reason for the increase in current speed seaward is given on page 25.) The flow velocity at which a suspended particle begins to fall is known as the "deposition velocity"; the "erosion velocity" necessary to re-suspend this material is usually about 50% larger than the deposition velocity (Postma, 1967). On the flood tide, some sediment is re-suspended from the bottom of the channel, and a quantity appropriate to the velocity of the water is carried landward. As it moves further into the Canal, the velocity of the water decreases and the suspended material begins to fall and finally settles on the bottom. On the ebb the currents in this location may be too weak to re-suspend and carry the silt away, or the critical velocity may be reached too late in the tidal cycle to transport the material all the way back to its original location. This process repeats itself every tide, causing the asymmetrical deposition of silt observed in the channel.

2. Tides. Tides in the Canal are of the same phase and amplitude as those predicted for Honolulu Harbor. The time resolutions of the instruments were such that, for a given measurement, there existed an

uncertainty of about $\pm$ 5 minutes. Within the limits of this resolution, no phase difference was observed between the two ends of the Canal.

Examination of the records revealed short period oscillations of the Canal surface. These oscillations had amplitudes of from 2 to 20 centimeters and periods ranging from about a minute to an hour and a half, but were conspicuously dominated by periods of about sixteen minutes. If this represents the natural period of oscillation of the Canal, the sea level records at each end of the Canal should be out of phase by 180° or about eight minutes. Unfortunately, the time resolution of the gauges was inadequate to detect any such lag in the records.

Proudman (1953) gives the following formula for the period of seiches in a narrow channel with vertical walls and flat bottom:

$$T = \frac{2L}{(gh)^{1/2}}$$

where L is the length of the channel,
h is the depth, and
g is the acceleration due to gravity.

This equation, when employed with the dimensions given in Table 1, yields a natural period of 24 minutes for the Canal. This value, although of the correct order of magnitude, is unsatisfactorily high. It may be that the bend in the Ala Wai or the significantly different mean depth in each of the separate topographical regions causes the Canal to respond in the manner of a two- or three-element coupled oscillator. The existence of the yacht harbor at the mouth of the Canal introduces the possibility of still another co-oscillating basin.

The increased complexity of such a system would render the formula inadequate.

3. Water properties in the Canal.

A. Water masses. Large spatial and temporal variations characterize the distribution of temperature and salinity in the upper layer of the Ala Wai. In some estuaries, these changes in surface waters might not measurably affect the properties of deeper water masses. But the Ala Wai is shallow, and the volumes involved are relatively small; surface conditions do have a significant influence on the salinity and temperature of the underlying layer. Thus, large changes in the properties of the upper layer may change the average salinity and temperature of the underlying layer by 1 °/oo and 3°C, respectively. This inconstancy makes it difficult to define water masses other than by a characteristic range of temperature and salinity values.

Another problem is encountered in attempting to fix the physical extent of a water mass. This implies a delineation of boundaries, and although very large gradients may have existed in, say, a vertical direction, the methods of data collection used in this study may have been inadequate to accurately determine this gradient. Rapid changes in salinity and temperature were common over a typical distance of half a meter, and the salinometer which was employed had the effect of reading the average salinity of a sphere of water about 20 centimeters in diameter. Furthermore, in some cases an inadequate number of readings may have been taken. Thus, in some instances, linear interpolation between a surface value and readings at 0.5 and 1 meter may

have blurred a sharp gradient which would have otherwise served as a natural boundary between the two layers of water. Despite these imprecisions, it is convenient to describe three water masses in general terms and to label them, if only for ease of exposition.

The SURFACE WATER is that mass of brackish water found at the surface of the Canal. It is usually found seaward of Station 13, but during large runoffs may extend over the basin. Its thickness varies, but seldom exceeds 1 meter except during heavy runoffs or rainstorms, when its bottom limit may extend to 2 meters or more. Its salinity may vary from 0 to 32 °/oo, and its temperature may range between 20 and 30°C; both these parameters are strong functions of runoff. Vertical gradients in this water may vary from 1 °/oo/m for periods of low runoff to 30 °/oo/m during storms.

CHANNEL WATER is water from the Ala Wai Yacht Harbor which flows into the channel, fills the small basin and continues onto the sill. It is diluted slightly by fresh water, and its salinity slowly increases with depth and with distance from the stream entrance at Station 13. If this were undiluted offshore sea water, its salinity would be about 34.7 °/oo (Wyrtki et al., 1967). The bottom salinity at Station 1 does, in fact, approach this value during periods of low runoff, but may decrease to 33 °/oo or less during high runoff.

BASIN WATER refers to that water found below the sill depth (about 1 meter at MLLW) in the basin at the landward end of the Canal. It is essentially channel water which has flowed over the sill and has sunk into the basin, but its temperature is increased by solar heating.

The temperature of this water was sometimes as much as a degree higher than that in the channel. This is discussed further on page 23. At any rate, this water merits special consideration because of its isolation and relatively infrequent renewal.

Tully (1958) recognizes three distinct zones which are usually present in an estuary: an upper and lower zone characterized by small vertical gradients, and a boundary zone in which the gradient of a property is quite large. However, in the Ala Wai the boundary between the surface layer and channel water will be taken as that point at which the salinity or density gradient shows an abrupt decrease. This division may be incomplete, since it is possible that a top layer of nearly homogeneous water may overlie a very strong halocline. If this is the case, the spacing between measurements is usually not small enough to accurately define the two layers. Thus, if widely differing salinity values are found at 0 and 0.5 meters, a linear interpolation is made between the points; if a relatively homogeneous upper zone overlies a halocline, they are rendered indistinguishable by this technique.

B. Short-term variations of water properties.

a. Salinity. The distribution of salt in the Canal is strongly dependent on runoff, tidal stage and wind conditions. In order to isolate the effects of any one of these three parameters, data were examined for days on which the remaining two parameters were comparable.

(i) The effect of runoff. April 1st, July 12th and

December 9th [Figures 24(a), 28(a) and 31(a)] had comparable tide and wind conditions, but the runoff varied by a factor of 20. The lowest runoff (0.29 m^3/sec) occurred on July 12th and the highest (5.4 m^3/sec) on April 1st.

Increased runoff naturally lowered the mean salinity of the surface layer. However, the thickness of the top layer was not significantly increased; therefore, the mean velocity must have risen to accommodate the increased amount of water flowing out of the Canal. This, in turn, produced greater shear at the interface, overcoming the larger salinity gradient and mixing relatively fresh water down into the bottom layer. Note that the salinity in the bottom layer on April 1st is a full 1 °/oo lower than on July 12th; the situation on December 9th is intermediate between these two extremes.

(ii) The effect of tides. Compare the salinity distributions in the sections obtained at high and low tide on July 12th [Figures 28(a) and 29(a)]. Average runoff and wind conditions were the same during both surveys.

At low tide the vertical salinity gradient at Station 4 is about 0.2 °/oo/cm; at high tide this gradient is reduced to 0.016 °/oo/cm. Fresh water is being continually discharged into the Ala Wai; although surface currents are reduced on the flood, a fresh water head is built up which continues to drive fresh water out of the Canal. Thus, the incoming tide increases shear at the interface, causing an increase in entrainment and turbulent mixing of channel water into the top layer. This weakens the halocline and increases the mean salinity

of the top layer.

A method described by Tully (1953) was used to delineate the halocline on the surveys of July 12th. He found that plotting a property as a function of depth on semi-logarithmic paper greatly facilitated delineation of these zones. The technique usually produced three straight lines, the intersections of which marked the boundaries of the zones. Although the data taken were not wholly adequate to precisely fix the limits at each station, it was possible to obtain estimates of these limits. The resulting sections are shown in Figures 28(e) and 29(e). The vertical lines indicate the uncertainty involved in each determination. The halocline is the zone in which turbulent mixing and entrainment are greatest, and these figures suggest intensification of these processes on the flood tide.

(iii) The effects of the wind. Stratification in a relatively shallow estuary such as the Ala Wai is strongly influenced by the wind. During normal trade wind weather, the wind on the Canal blows from the NE quadrant, driving surface water seaward. This increases shear at the interface between upper and lower layers, reducing the salinity gradient by entrainment and vertical mixing.

Comparable runoff and tidal conditions occurred on May 9th and December 9th [Figures 25(a) and 31(a)]. However, the wind speed on December 9th was double that of May 9th, and this is reflected in the salinity distributions. The decrease in wind speeds, and thus in the outward flow of the surface layer, resulted in greater stratification and a pile-up of fresh water in the Canal on May 9th. Indeed, the

drop in wind velocity had an effect on the salinity distribution comparable to increasing the runoff by about a factor of eight. This can be seen by comparing the salinity sections of May 9th and April 1st.

b. Temperature. The temperature structure in the Ala Wai is the result of overlaying a body of fresh water which has large temperature variations upon a relatively stable bottom layer. The distribution is further modified by the intensity of solar radiation and by the magnitude of the fresh water runoff into the Canal. Thus, the large diurnal temperature variations in the Manoa and Palolo streams are reflected in the morning and afternoon surface temperatures of July 12th [Figures 28(b) and 29(b)], and large vertical gradients of about 6°C/m occurred during the heavy runoff on March 16th [Figures 21(b) and 22(b)].

Water in the basin is frequently warmer than the channel water, sometimes by as much as 1°C. The reason for this is that surface water flows rapidly seaward from Station 13, carrying much of the incoming heat from solar radiation with it, while no such seaward transport of heat occurs in the basin. This is a major factor in the renewal of water in the basin. If the basin water is warmed sufficiently, it becomes lighter than channel water which flows over the sill on the flood; the result is that this channel water will sink either to the basin bottom or to some other appropriate depth, displacing the lighter water which resides there. This is discussed further in the section on circulation, page 36.

C. Seasonal variations of water properties.

a. Salinity. Monthly averages of salinity over the surface should show strong seasonal variations, with a minimum during the rainy season and a maximum during the dry season. The same might be expected of subsurface water in the Canal, but not enough data were collected to present meaningful monthly averages for either surface or deep water; large short-term variations tended to mask the smaller seasonal variations.

b. Temperature. All the data collected were used to calculate monthly temperature averages for water in the harbor, in the channel, and in the basin; isopleths were then constructed (Figures 7, 8 and 9). No attempt was made to correct the depths for tidal variations, thus the time averages presented are smeared over a depth of about half a meter. It should be noted that the more reliable portions of these diagrams are the sections below about 1 meter depth; this is because short-term variations are smaller below the surface. Seasonal changes are immediately evident; the average summer increase in temperature is about 2°C in the lower layer. The largest vertical differences are observed during the dry season, when the increased solar radiation and decreased stream flow raise surface temperatures to their yearly highs.

4. Circulation.

A. A general classification scheme for circulation in estuaries. Pritchard (1967) has described three circulation patterns which are distinct points in a continuous sequence of estuarine types. He

classifies estuaries by the type and degree of mixing that takes place.

The first is a highly stratified salt wedge; this is a non-tidal model with frictional forces. The dominant mixing agent in this case is velocity shear created by the seaward flow of fresh river water over a wedge of sea water. This flow causes interfacial waves which become unstable and break, transporting volume into the upper layer. The transport in the top layer increases downstream by an amount equal to the sea water entrained, and the surface inclines seaward, creating a pressure gradient to compensate the upstream force originated by friction at the interface. When the influence of river flow is strongly dominant over that of the tides, such as in the Mississippi River, this salt wedge model is approximated most closely.

The second case is that of a moderately stratified estuary, in which the principal mixing agent is turbulence generated by tidal action. Turbulent eddies carry fresh water down and sea water up; the result is a seaward salinity increase in both layers and a salinity increase with depth at any given point. Since this turbulent transport of sea water is greater than in a salt wedge type of estuary, the downstream increase in volume transport is correspondingly larger. (Note that if the cross-sectional area remains constant, as in the Ala Wai Canal, then the average current speed must increase seaward at any given instant of time.) This type of estuary is by far the most common.

The third model is the vertically homogenous estuary, which occurs when tidal mixing is sufficiently vigorous to break down all vertical

stratification. It is a theoretical end point of this classification scheme, and may not exist in nature.

The most important parameter determining the position of any given estuary in the sequence described above is the ratio V_f/R, where V_f is the volume of water flowing up the estuary through a given section during the flood tide, and R is the volume of fresh water flowing into the estuary above the section during a complete tidal cycle. The significance of the ratio is this: in a salt wedge, V_f/R is on the order of unity; in a partially mixed estuary the ratio is characteristically on the order of 10 to 100; in an estuary approaching vertical homogeneity, V_f/R is on the order of 1000. (On a typical day, the Ala Wai was found to have a ratio of about 8. See page 29.)

B. Circulation in the Ala Wai.

a. General patterns. Current measurements were obtained in the Ala Wai on June 29th and 30th. Although the tidal range on these days could be considered typical, wind speed and runoff were slightly higher than the average values found on the other surveys (excluding the storms of March 16th, April 1st and June 10th). This would tend to increase somewhat such things as current speed and volume transports, and this fact should be kept in mind throughout the following discussion.

The data revealed alternating periods of two-layer and one-layer flow. In the two-layer system, brackish water at the surface flows seaward and out of the Canal, entraining saline water from below and causing a compensating flow into the Canal at depth. Added to this

pattern is the tidal flow. This tidal component is approximately sinusoidal, leads sea level by 90°, is into the Canal on flood and out of the Canal at ebb tide. The current measurements made at Station 1 (Figures 10 and 13) show the compensating landward drift in the deep layer; these velocity profiles were obtained at high and low tide, when the tidal flow has vanished.

Tidal flow in the deep layer is influenced by the landward drift, which decreases the flow on the ebb and intensifies it on the flood. The surface current speed is determined mainly by the magnitude of the fresh water runoff and by the size of the tidal range. On the flood, slack water at the surface will occur earlier during periods of low runoff and large tidal range than during periods of high runoff and small tidal range; the duration of any current reversal at the surface (i.e. currents directed into the Canal) also depends on these two factors, being longer for the former case than for the latter. Fresh water is being continually discharged into the Canal, and during a current reversal on the flood it begins to pile up, creating a head. If the discharge is large, or the tidal range is small, or both, the critical point is quickly reached when the head of fresh water overcomes the tidal forces and seaward surface flow is resumed. If the runoff is too small, or tidal range very large, or both, surface flow into the Canal could conceivably continue until high tide. On the ebb, both components are in the same direction and the surface flow out of the Canal is intensified.

The tide of June 29th had a range of 0.8 meters and the runoff

for that day was about 0.9 m^3/sec. Current reversal at the surface occurred at peak flood tide, and persisted for about an hour. This is shown in the graphs of volume transports with time in Figure 17.

b. Volume transports. Over a complete tidal cycle, continuity requires that

$$T_{in} - T_{out} + F - E = \Delta V$$

where T_{in}, T_{out} are volumes transported into and out of the Canal,
F is the volume of water introduced into the Canal by runoff and precipitation,
E is the volume of water evaporated, and
ΔV is the change in volume of the Canal during the tidal cycle.

Figure 17 shows volume transports with time in each layer at the mouth of the Canal. The net transport is also shown. These curves were constructed from the current meter data of June 29th and 30th; consequently, each complete tidal cycle shown is really a composite of parts of two different tidal cycles. The flood portion of the curves were constructed using data of the 29th, and the ebb employed data of the 30th.

Net transport on the flood tide was 2.31 x 10^5 m^3 into the Canal, and net transport on the ebb tide was 2.17 x 10^5 m^3 out of the Canal. From Table 2, the runoff on the 29th of June was 0.90 m^3/sec., and that of June 30th was 0.42 m^3/sec. Then the volume of fresh water introduced during the tidal cycle was 0.37 x 10^5 m^3. (The period of this particular tidal cycle was 15.5 hours. See footnote, page 4.) Low tide on June 30th was 0.3 meters higher than low tide on June 29th.

From Table 1, the surface area of the Canal is 2.0×10^5 m^2, so that the change in volume of the Canal, ΔV, was 0.60×10^5 m^3. If evaporation is assumed to have been twice the yearly average of open ocean values in this latitude (200 cm/year), then E is about 10^3 m^3; this amount is negligible compared to the other terms in equation (1).

Using these values in equation (1), we find it balances to within 9.0×10^3 m^3. This amount is about 4% of the net volume which flowed into or out of the Canal, and is within the accuracy of the current measurements made.

c. The ratio V_f/R. On June 29th, the total volume of water transported into the Canal during flood tide was 4.0×10^5 m^3. During the complete tidal cycle of June 29th, the amount of fresh water discharged into the Canal was about 0.5×10^5 m^3. Consequently, the ratio V_f/R is about 8, which indicates that the Ala Wai is a partially mixed estuary according to Pritchard's scheme of classification (page 26). Can this description be applied to the Canal during the rest of the year? Only the runoff on the three days of storms listed in Table 2 exceeded that of June 29th. Since decreased runoff would increase the ratio V_f/R, the Ala Wai should be partially mixed during most of the year. However, the relatively low value of V_f/R suggests that during periods of high runoff, the Canal may temporarily assume the characteristics of a salt wedge estuary. The storm of March 16th, for example, resulted in a typical salt wedge structure [Figure 21(a)]. But these instances must be infrequent, since examination of stream gauge data for 1969 revealed only two other cases of comparable flow.

d. Residence times. The residence time, t, of a substance which occupies a given volume, V, and which is renewed at a given rate, R, can be defined as the ratio of the volume to the renewal rate, i.e. $t = V/R$. This is the average time any particle of the substance will reside in that volume. In the following discussion, the residence time of sea water in the channel and basin and the residence time of fresh water in the surface layer will be considered.

(i) Surface layer. A standard method for computing the rate at which river water is flushed out of an estuary, and thereby estimating the rate of removal of a pollutant introduced by the river, is to use the fresh river water as a tracer (Bowden, 1967). The fresh water, F, accumulated at any given time in a volume, V, is given by

$$F = \int_V \frac{s_o - s}{s_o} \, dV$$

where s is the salinity at any point in the volume, and s_o is the salinity of water which is available for mixing. If R represents the rate at which fresh water is removed from the volume, then the residence time, t, is given by $t = F/R$.

This expression was used to determine the average residence time of fresh water between Stations 1 and 13 for the twelve different surveys which were made during the study; the basin was excluded from these computations. The results should apply mainly to the top layer, since the bulk of fresh water is found there. A steady state was assumed, so that R, the removal rate of fresh water, was the same as

the runoff rate into the Canal. The results are given in Table 4 and are shown in the plot of residence time vs. runoff in Figure 19. The rather large error limits are due mainly to uncertainties in the amount of runoff, R, listed in Table 2. Reasons for this uncertainty are explained on page 8. Also, some error may have been introduced in the calculation of F because of imprecise determination of the salinity curve in the top layer. This is discussed on page 20. In addition, scatter could be expected for the reasons discussed in the following two paragraphs.

Wind conditions during each survey influenced the upper layer flow and residence time. Thus, July 12th and June 30th showed shorter residence times than June 25th and March 29th in spite of smaller runoffs, evidently because average wind speeds were 50 to 60% higher during the former. On the other hand, the low residence time of December 9th as compared to May 9th (both had comparable runoffs) was apparently caused by the relatively weak winds of the latter.

Tidal stages varied during each survey, and since the salinity structure is partially dependent on the tides, different values for F could be expected at different tidal stages. This error is probably not very large; for example, the residence times at high and low tides of July 12th differed by only two hours.

In spite of such uncertainties, some interesting features of Figure 19 are evident. There are two distinct portions of the residence time curve. Below about 1 m^3/sec runoff the residence time is a very strong function of runoff; above this value the relationship

is very weak, and residence time is essentially constant at about 3 hours. For values of 0.5 to 1 m^3/sec, a residence time of 6 to 10 hours seems typical; for runoff below this range, residence times could increase up to 30 hours, depending on such things as wind speed and direction.

Such a curve might be expected from physical considerations. During very low runoff the mean surface current is decreased, so that it takes a particle of water longer to travel from the mouth of the stream to the mouth of the Ala Wai. Vertical stratification is also decreased, and turbulent processes can then mix the fresh water down into the water column more efficiently, thereby detaining a greater percentage of the fresh water in the deep layer, which oscillates back and forth in the Canal with the tides. As the runoff increases, so do the mean surface current and the vertical stratification; both of these circumstances tend to reduce the residence time. Finally, the runoff becomes so great that the surface layer is essentially a river which flows unimpeded through the Canal. Evidently at this point the depth of the surface layer begins to increase, accommodating itself to the higher flow. This tends to maintain a more or less constant current speed at the surface, and the residence time of a water particle is thus limited only by the distance it must travel through the Canal.

(ii) Channel water. It was not possible to determine the variation of residence time with depth in this lower layer with the data available, although it seems intuitively obvious that it must increase with distance from the interface with the upper layer.

However, the longitudinal variation of residence time was examined by using the following method.

Assume all the water in the estuary is a mixture of sea water of salinity s_o and fresh water in varying proportions. Then the sea water content of an upper layer (by volume) is given by $\int_V (s/s_o)\, dV$, where s is the salinity at any point, and V is the volume. The sea water transport, S_i, during a tidal cycle in a layer at station i is

$$S_i = Y_i \int_0^T \int_0^{z_i} (s_i/s_o) v_i \, dz \, dt \qquad (2)$$

where Y_i is the width of the Canal at station i,
z_i is the depth of the interface of the bottom and top layer,
$v_i = v_i(z)$ is the velocity in the layer,
$s_i = s_i(z)$ is the salinity in that layer, and
T is the time of a tidal cycle.

Then continuity requires that

$$W_i = S_{i+1} - S_i \qquad (3)$$

where W_i is the vertical transport of salt water from the bottom layer to the top layer.

W_i must also be the renewal rate of sea water in the lower layer; it is replaced by water from an adjoining section. If the volume of this part of the lower layer is known, a residence time can be calculated.

The velocity and salinity measurements obtained on June 29th and 30th were used in equations (2) and (3) to calculate the amount of sea water entrained out of the lower layer and transported out of the

Canal by the upper layer. Since these measurements were obtained at different stages of the tidal cycle and at different stations along the axis of the Canal, it was possible to construct Figure 18. The surface in Figure 18 defines the sea-water transport in the surface layer with distance along the Canal and time in the tidal cycle. If a curve is generated in the time-transport plane, the area under that curve gives the total volume of sea water transported seaward in the upper layer during a complete tidal cycle. The difference in the volume transported between two points, e.g. two stations on the Canal, represents the vertical transport of salt water from the bottom layer to the top layer in the volume bounded by the two stations. This is the term W_i of equation (3). It is also the renewal rate for the sea water in the bottom layer. These rates, W_i, were calculated for the volumes between stations listed in Table 5. The volume, V, of the lower layer bracketed by the two stations is also listed, as is the average residence time, $t = V/W$, for the water in that volume. The mean age, A, of water in the lower layer is simply the cumulative residence time up to that point; the age varies from about half a tidal cycle at the mouth of the estuary to about six tidal cycles at the stream entrance.

The residence times in Table 5 tend to be high because no account was taken of renewal in the bottom layer by mixing with harbor water on the ebb tide. Thus, if the bottom layer water is thought of as a piston which protrudes into the harbor on the ebb tide, the possibility exists that all or part of the water which protrudes will be exchanged

for harbor water. The effect on residence time would be greatest in the volume closest to the mouth of the Canal, i.e. between Stations 1 and 3. An estimate of this effect can be made in the following manner.

During the ebb tide of June 30th, approximately 0.8×10^5 m^3 of deep layer water flowed out of the Canal and into the harbor. If we consider this entire volume to have been exchanged for "new" water from the harbor, it follows that in the volume between Stations 1 and 3 approximately 1.58×10^5 m^3 of water would have been renewed during one tidal cycle. This would yield a residence time of 0.37 tidal cycles as opposed to the 0.46 tidal cycles listed in Table 5. These two residence times can be considered a minimum and maximum estimate, respectively. The influence of this exchange with harbor water will decrease with distance from the Canal mouth.

Table 5 suggests that less intensive vertical mixing takes place over the sill region than in the channel. The residence time is smaller in the channel by a factor of 7 or 8. Two possible explanations are the abrupt change in width at the Canal bend from 75 to 50 meters, and the prominent hump evident in the bottom topography between Stations 1 and 4. The reduction in width increases the mean flow of the top layer, causing larger shear stresses to develop, and the tidal flow back and forth over the relatively more irregular topography may generate more turbulence in the bottom layer.

It must be emphasized that Table 5 is the result of measurements taken over only one tidal cycle, and strictly speaking, are represent-

ative of only those days with the same runoff and tidal range. Increased runoff would increase the entrainment of sea water from the lower to the upper layer and a larger tidal range would have the same effect by producing more vigorous turbulent mixing; thus, an increase in either runoff or tidal range should decrease residence time. This dependence of channel water residence time on runoff and tidal range cannot be further defined for lack of data. But the tidal range for June 29th and 30th of 0.8 meters could be considered as average for the Ala Wai during any part of the year, and the runoff was of the same order as the other surveys except for those days on which storms occurred. This suggests that the values which were calculated might at least be of the order of magnitude of residence times found during most of the year.

(iii) Basin water. Renewal of basin water can take place only if water of a higher density flows over the sill. The required density difference can be brought about if the temperature of the water in the basin is increased sufficiently over the temperature of the water on the sill; this, of course, requires unequal heating of the two water masses. Such a process seems to occur in the following manner.

On the sill, the continuous flow of stream water seaward in the surface layer inhibits the solar heating of the underlying water; that is, heat is advected away from the sill region. On the other hand, heat continues to be stored in the basin. The result is a larger increase in the temperature of basin water than in the temperature of

subsurface water on the sill. This temperature differential is increased if the stream water is relatively cool and the runoff is large, since vertical mixing would tend to lower the temperature of the sill water still further. Good examples of the results of this differential heating are shown in the temperature distributions of March 29th, April 1st, July 12th and October 20th [Figures 23(b), 24(b), 28(b), 29(b) and 30(b)].

The salinities of the two waters, though less important, will also affect the relative densities. The difference in salinity between basin and sill water depends on such things as runoff, wind speed, and the amount of evaporation in the basin. High runoff lowers the salinity of water on the sill, but the effect of this on the density is overridden by a temperature reduction if the stream is cool enough. This is frequently the case. High evaporation in the basin hampers renewal by sill water in that it increases the density of the basin water and decreases the effects of the unequal heating process described above.

Evidence of at least partial renewal was found in six of the eleven surveys made; by partial renewal is meant the sinking of water from the sill to intermediate depths in the basin, rather than completely to the bottom. Renewal of the bottom water in the basin was indicated in three surveys.

The most clear-cut indication of sill water sinking to the bottom of the basin is given in the sigma-t section for October 20th [Figure 30(c)]. An increase in dissolved oxygen at the basin bottom supports

this observation [Figure 30(d)]. Note that in this case there is not much difference in the salinities of basin and sill water [Figure 30(a)]. A salinity difference does exist in the cases of March 29th and July 12th, and as the less saline water spills over the sill, it depresses the isohalines as shown in Figures 23(a) and 28(a). The oxygen isopleths slope this way for the same reason [Figures 23(d) and 28(d)]. It is also possible that high evaporation on the tidal flats at the extreme landward end of the basin may contribute to the slope of these isohalines. At any rate, in the absence of dynamic forces to maintain these slopes, they must eventually level out.

Note that renewal of basin water to the bottom does not always occur. The depth to which sill water sinks depends on how large a density difference is generated by the differences in temperature between sill water and basin water. As an example, anoxic conditions persisted at the basin bottom on March 29th and April 1st [Figures 23(d) and 24(d)], indicating that the sill water did not reach bottom. July 12th and December 9th show an increase in dissolved oxygen at the bottom, but the latter is suspect because of a region near the surface with unusually high oxygen values, raising the possibility of oxygen enrichment by diffusion rather than advection. However, the curve of the oxygen isopleths of July 12th suggest a definite flow of oxygen-carrying water along the bottom [Figure 29(d)].

An oxygen section was not obtained on March 16th, but the temperature and salinity characteristics of the water at the bottom of the basin suggest it is channel water which flowed over the sill during

the flood tide on which the measurements were made [Figures 21(a) and 21(b)]. Note that in this case the runoff was large and the surface layer was 3 to 4°C cooler than the deeper channel and sill water.

Three very different patterns of heat distribution are shown for May 9th, June 10th and June 25th [Figures 25(b), 26(b) and 27(b)]. All are characterized by higher temperatures at Stations 6 and 13, where the stream enters the Canal. The times of day during which these surveys were made suggest that stream water which is much warmer than Canal water flows into the Ala Wai during periods of high solar heating, but the decrease in solar heating as evening approaches reduces the stream temperature to a point below that of the Canal. This generates a surface layer of relatively cool water, and forms the apparent "core" of warm sea water at the stream entrance. Under these conditions, water at the sill is lighter than the basin water and, consequently, there is no renewal on the flood tide.

It is not possible to make an estimate of the average residence time of the basin water using the data collected. The intermittent character of the renewal process suggests the necessity of collecting data at least daily for a length of time at least of the same order as the residence time itself. However, a very rough estimate of some minimum residence time can be made.

Since two rapid surveys were carried out on July 12th, one at low tide and the other at high tide, it is possible in this case to make a rough estimate of the amount of water which sank to the bottom of the basin. If all the water which sank had a sigma-t equal to or

greater than 22.0 gm/cm^3, then the amount is simply the volume of this water present at high tide less the volume present at low tide. This quantity was estimated to be about 3.0×10^4 m^3. The volume of the basin below sill depth is approximately 1.1×10^5 m^3. Even if renewal occurred every day, which is unlikely, then the average residence time would be on the order of four days. From the crude approximations made in this calculation, it is obvious that it should be viewed merely as an indication that the magnitude of the residence time in the basin is on the order of days or weeks, rather than hours.

e. Possible three-layer flow pattern in the stream. Station 10 is located in the Manoa-Palolo Drainage Canal (the stream); this stream can be thought of as a smaller estuarine system itself, with the typical circulation pattern so implied. That is, fresh water flows seaward at the surface, entraining saline water from below and causing a compensating upstream drift at depth.

On June 29th a peculiar flow pattern was observed at Station 10 which warrants a short discussion. The flow appeared to be three-layered, with transport into the Canal at the surface and bottom and out of the Canal at intermediate depths (Figure 11). It is possible that this pattern did not actually occur, but was recorded as such because of the lack of synopticity in the current measurements. Measurements were made at three depths: 0, 0.5 and 1 meter, in that order. The complete set of measurements took 35 minutes; they were begun at high tide, but were not completed until after the tide had begun to ebb (Figure 16). It is entirely possible that at the time

the second measurement was made the entire bottom layer was moving upstream, but later, when the third measurement was made, the entire lower layer was moving downstream under the influence of the ebbing tide.

An alternative explanation is that the three-layer pattern was real and that the bottom layer was being driven downstream by a pressure gradient. If vigorous downward mixing of warm surface water, perhaps by the wind, were to increase the temperature and lower the salinity of the bottom water at Stations 13 and 6, this would decrease its density and give rise to the required pressure gradient. The relatively cool, saline water at the stream bottom would then flow into the Canal, intensifying the compensatory upstream flow at intermediate depths. It is apparent that this three-layer flow would be a transitory phenomena, for the flow would act to eliminate the pressure gradient which drives the bottom layer. Once the source of relatively dense water on the stream bottom had been depleted, the flow would revert to the more familiar one- or two-layer structure.

5. Dissolved oxygen. All longitudinal sections of the oxygen distribution exhibit essentially the same features: a high concentration of oxygen at the stream entrance, very low concentration at the bottom of the basin and relatively uniform intermediate values in the channel. The near-anoxic conditions below sill depth in the basin are indicative of the relatively infrequent renewal of the bottom water [Figures 23(d), 24(d), 28(d), 29(d), 30(d) and 31(d)].

6. Nutrients. The highest phosphate and nitrate values were

found in the surface layer of the Ala Wai [Figures 30(e), 30(f), 39(g), 31(e) and 31(f)]. There appear to be three major sources: the Manoa-Palolo Drainage Canal, the Apukehau Stream and the large storm sewer at the extreme landward end of the Canal. The Ala Wai Golf Course, which adjoins the Canal, must be fertilized periodically; it is likely that runoff from this land is also a major source of nutrients in the Canal.

7. Bacteria. Previous investigations have found that the Ala Wai Canal and Yacht Harbor did not meet state water quality standards. Cox (1969) summarizes the data. The purpose of the bacterial analysis done in this study was to try to identify the sources of bacterial pollution. Thus, it was hoped that bacterial counts at a number of stations along the axis of the Canal would show gradients which might indicate the sources. Since only one survey was made, the individual values obtained cannot be considered representative; individual readings may easily vary by an order of magnitude from day to day, and meaningful averages can be obtained only after extended periods of data collection. This study was concerned with relative values, which might be expected to be comparable on any one day. Thus, a sample taken near a source should always have a greater number of organisms than one further removed from that source.

Figures 33 and 34 show that relatively high values of fecal bacteria are associated with the Manoa-Palolo Drainage Canal, and that high values of fecal coliform are also found in the yacht harbor. Relatively low values are found in the basin, and intermediate values are

found on the sill and in the channel. Subsurface samples were taken at a depth of 1 meter at Stations 12, 4 and 10, i.e. in the yacht harbor, by Apukehau Stream and in the Manoa-Palolo Drainage Canal, respectively. Most of the data indicate a marked decrease with depth in the number of organisms. This is probably due to two reasons: the source is at the surface, and the salinity increases with depth. Only Station 4 showed coliform counts at depth comparable to counts found at the surface. This may be due to increased vertical mixing at this station, discussed on page 15.

All the data are consistent with the assumption of a source located at the stream, the flow of stream water mainly in a direction seaward of Station 13 and a die-off of organisms due to increased salinity. Circulation patterns make it unlikely that the Canal receives significant bacterial pollution from the harbor; the organisms seem to be concentrated at the surface and although surface currents flow into the Canal for short periods during flood tide, there is no net transport of surface water into the Canal from the harbor.

SUMMARY

1. The Ala Wai Canal is a partially mixed, moderately stratified estuary, as defined by Pritchard (1967).

2. The degree of stratification in the Canal is strongly dependent on runoff, tidal stage, and wind conditions.

3. Seasonal variations occur in the temperature structure. Temperatures in the deeper layers range from a high of about 27°C during the summer months to about 25°C during the winter. Insufficient data were obtained to determine seasonal changes in the distribution of salinity.

4. Different rates of silting at different locations in the Canal have, in effect, created a deep basin at the extreme landward end of the Canal.

5. Renewal of water in the basin is infrequent, and anoxic conditions prevail in the bottom meter of the water column.

6. The average silting rate on the sill is 20 cm/year, but parts of the sill exhibit rates as high as 28 cm/year.

7. The average residence time of fresh water in the surface layer of the Canal changes rapidly with runoff values less than about 1 m^3/sec; in this range, residence time is strongly influenced by wind conditions on the Canal and may exceed 30 hours. For runoff values greater than about 1 m^3/sec, the residence time remains essentially constant at about 3 hours.

8. The residence time of sea water underlying the surface layer is about half a tidal cycle in the channel and almost four tidal

cycles on the sill.

9. Fecal coliform and fecal streptococci are introduced into the Canal by the Manoa-Palolo Drainage Canal. High coliform counts are also found in the Ala Wai Yacht Harbor, but it is unlikely that there is a transport of these organisms from the harbor into the Canal.

APPENDIX A

TABLES 1 to 5

TABLE 1

AREA, VOLUME, MEAN DEPTH, AND DIMENSIONS OF THE ALA WAI CANAL

Ala Wai Canal:	
Length:	3.1×10^3 m
Volume:	3.6×10^5 m^3
Surface area:	2.0×10^5 m^2
Mean depth:	1.8 m
Basin:	
Length:	1.3×10^3 m
Width:	76 m
Volume:	1.9×10^5 m^3
Surface area:	8.4×10^4 m^2
Mean depth:	2.3 m
Sill:	
Length:	9.7×10^2 m
Width:	76 m
Volume:	7.3×10^4 m^3
Surface area:	7.4×10^4 m^2
Mean depth:	1.0 m
Small Basin:	
Length:	2.5×10^2 m
Width:	50 m
Volume:	2.3×10^4 m^3
Surface area:	1.2×10^4 m^2
Mean depth:	1.9 m

TABLE 1. (Continued) AREA, VOLUME, MEAN DEPTH, AND DIMENSIONS OF THE ALA WAI CANAL

Channel:

Length:	6.4×10^2 m
Width:	50 m
Volume:	7.8×10^4 m^3
Surface area:	3.2×10^4 m^2
Mean depth:	2.5 m

TABLE 2

ESTIMATED MEAN FRESH WATER RUNOFF
INTO THE ALA WAI CANAL DURING SURVEYS

DATE OF SURVEY	RUNOFF RECORDED BY STREAM GAUGES (m^3/sec)	RUNOFF ESTIMATED FROM RAIN DATA (m^3/sec)	TOTAL ESTIMATED RUNOFF (m^3/sec)
16 March	11.30	3.70	15.00 $\pm$ 1.85
29 March	0.45	0.04	0.49 $\pm$ 0.02
01 April	1.80	3.60	5.40 $\pm$ 1.80
09 May	0.50	0.19	0.69 $\pm$ 0.09
10 June	0.86	2.48	3.34 $\pm$ 1.24
25 June	0.22	0.33	0.55 $\pm$ 0.16
29 June	0.22	0.68	0.90 $\pm$ 0.34
30 June	0.25	0.17	0.42 $\pm$ 0.08
12 July	0.25	0.04	0.29 $\pm$ 0.02
20 October	0.23	0.17	0.40 $\pm$ 0.08
09 December	0.22	0.47	0.69 $\pm$ 0.23

TABLE 3

MEAN WIND SPEED AND DIRECTION RECORDED AT HONOLULU AIRPORT DURING SURVEYS. (WIND SPEED IS CORRECTED TO A HEIGHT OF 1 METER ABOVE MEAN SEA LEVEL)

DATE OF SURVEY	SPEED (m/sec)	DIRECTION (° true north)
16 March	2.6	30
29 March	3.1	30
01 April	4.6	60
09 May	2.1	110
10 June	3.1	20
25 June	3.4	60
29 June	4.5	60
30 June	4.8	50
12 July	5.0	60
20 October	3.1	50
09 December	4.3	60

TABLE 4

MEAN RESIDENCE TIME, t, OF FRESH WATER IN THE SURFACE LAYER OF THE ALA WAI CANAL

DATE OF SURVEY	t (hours)
16 March	2.3
29 March	18.6
1 April	2.6
9 May	14.4
10 June	2.5
25 June	18.7
29 June	4.9
30 June	10.8
12 July (low tide)	15.4
12 July (high tide)	13.6
20 October	11.1
9 December	4.2

TABLE 5

MEAN RESIDENCE TIME, t, OF DEEP LAYER CHANNEL WATER

STATIONS	W x 10^{-4} (m^3/tidal cycle)	V x 10^{-4} (m^3)	t (tidal cycles)	A (tidal cycles)
1 to 3	10.0	5.8	0.58	0.58
3 to 4	4.7	2.6	0.55	1.13
4 to 5	8.5	2.8	0.33	1.46
5 to 6	1.3	4.8	3.70	5.16
6 to 10	1.9	1.0	0.52	5.68

APPENDIX B

FIGURES 1 to 34

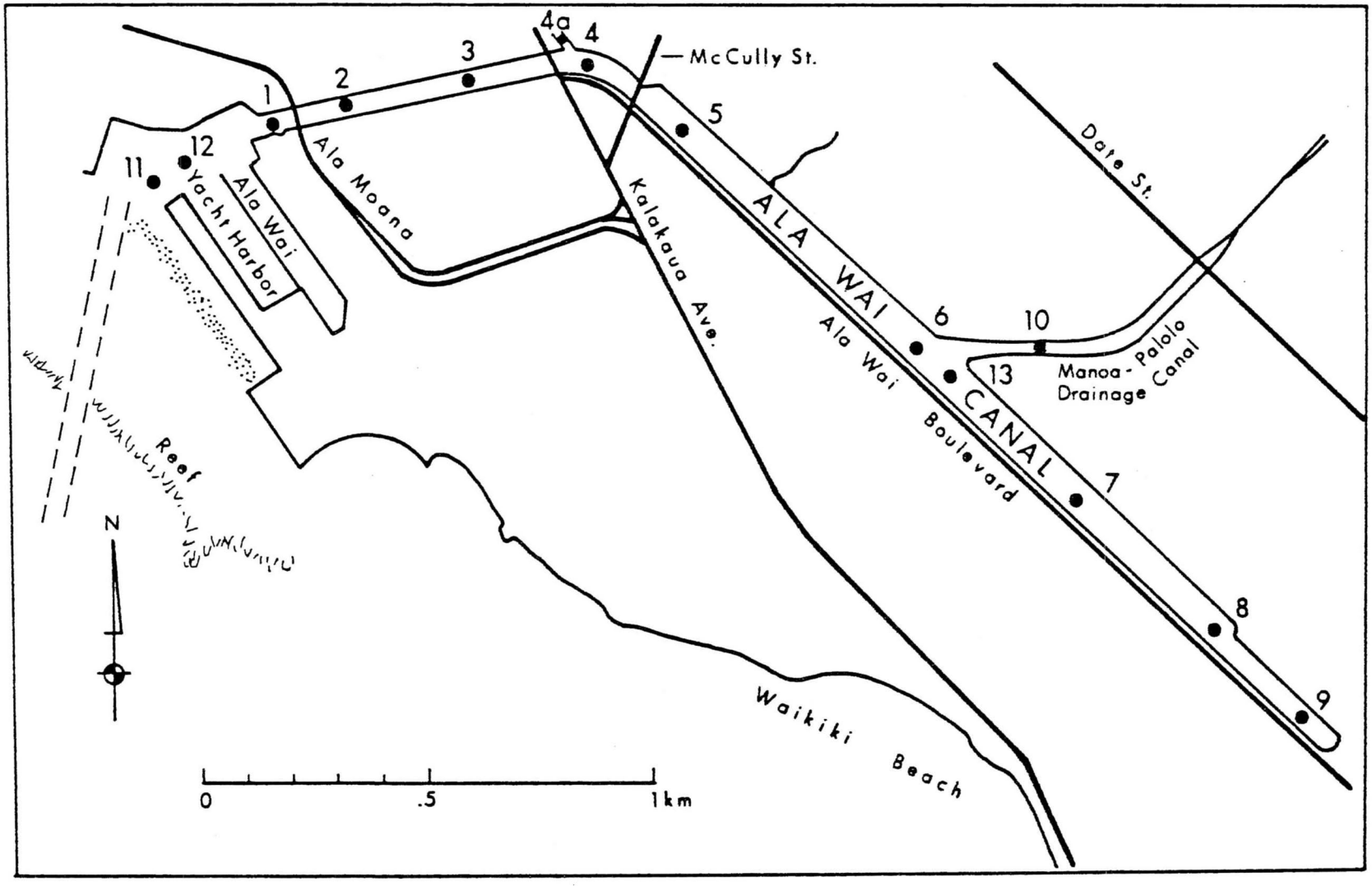

Figure 1. Chart showing the location of stations on the Ala Wai Canal.

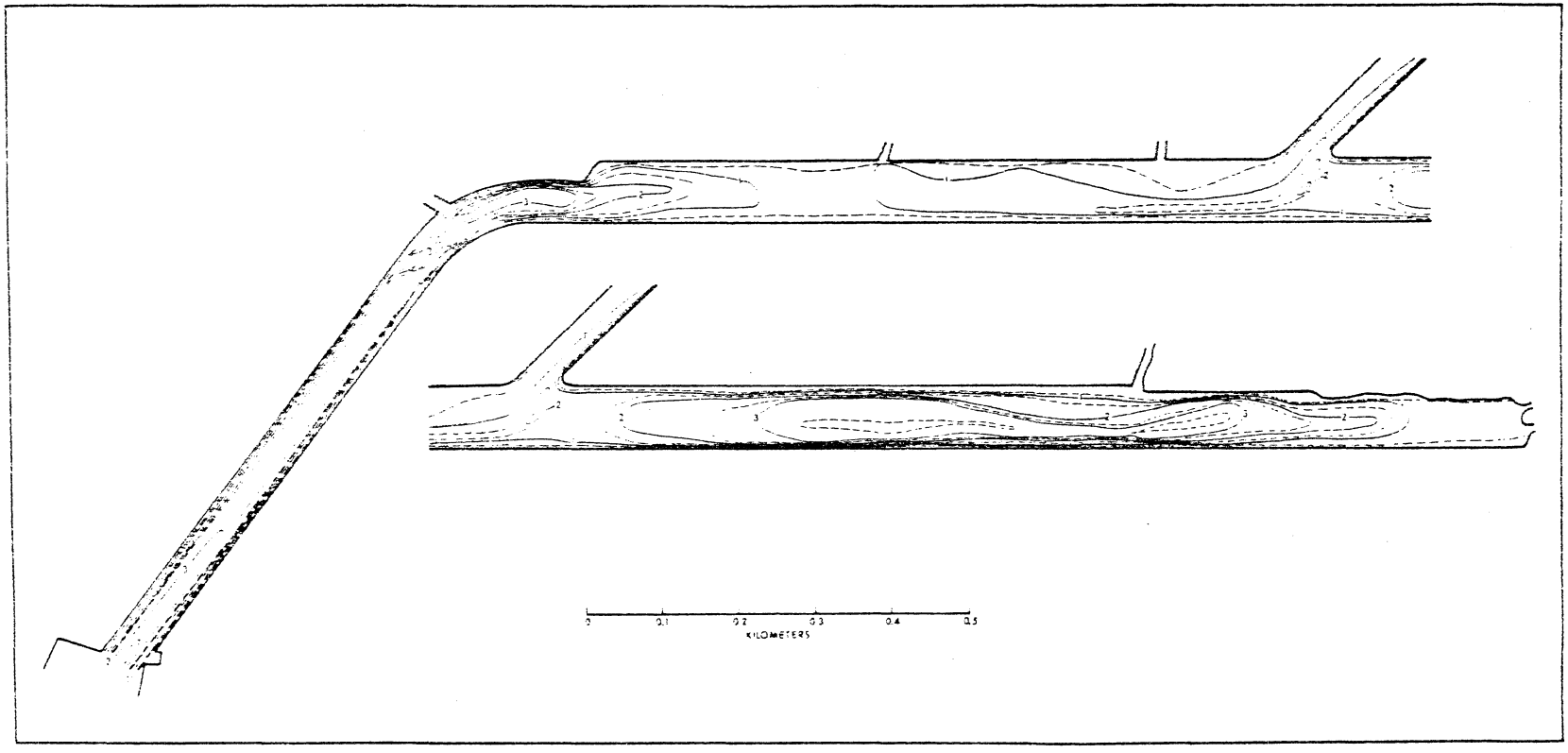

Figure 2. Bathymetry of the Ala Wai Canal. July 13, 1969. Contours are in meters, and are referred to MLLW.

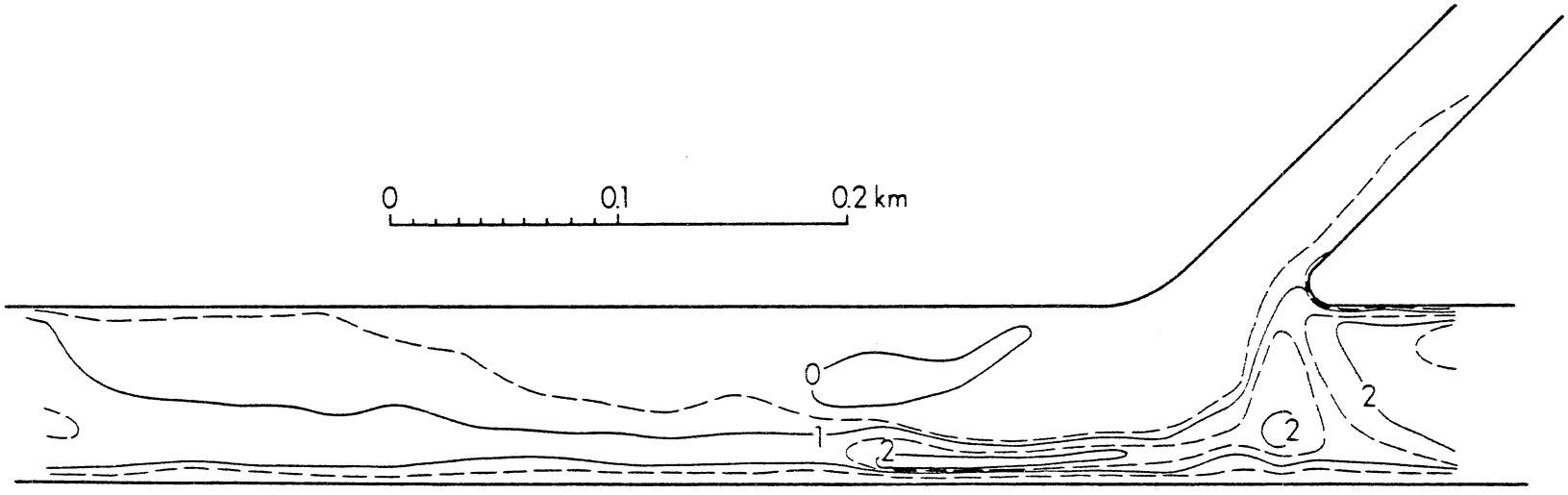

Figure 3. Bathymetry of a portion of the Ala Wai Canal. May 1965. Contours are in meters, and are referred to MLLW.

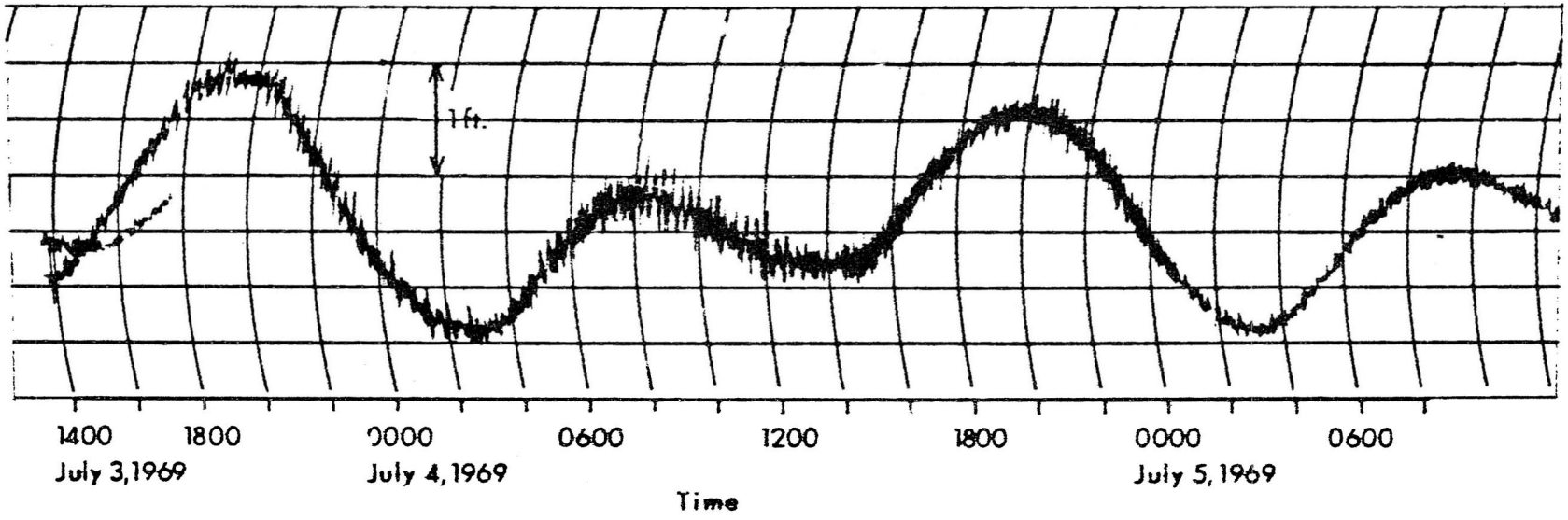

Figure 4. Tidal curve recorded at Station 1.

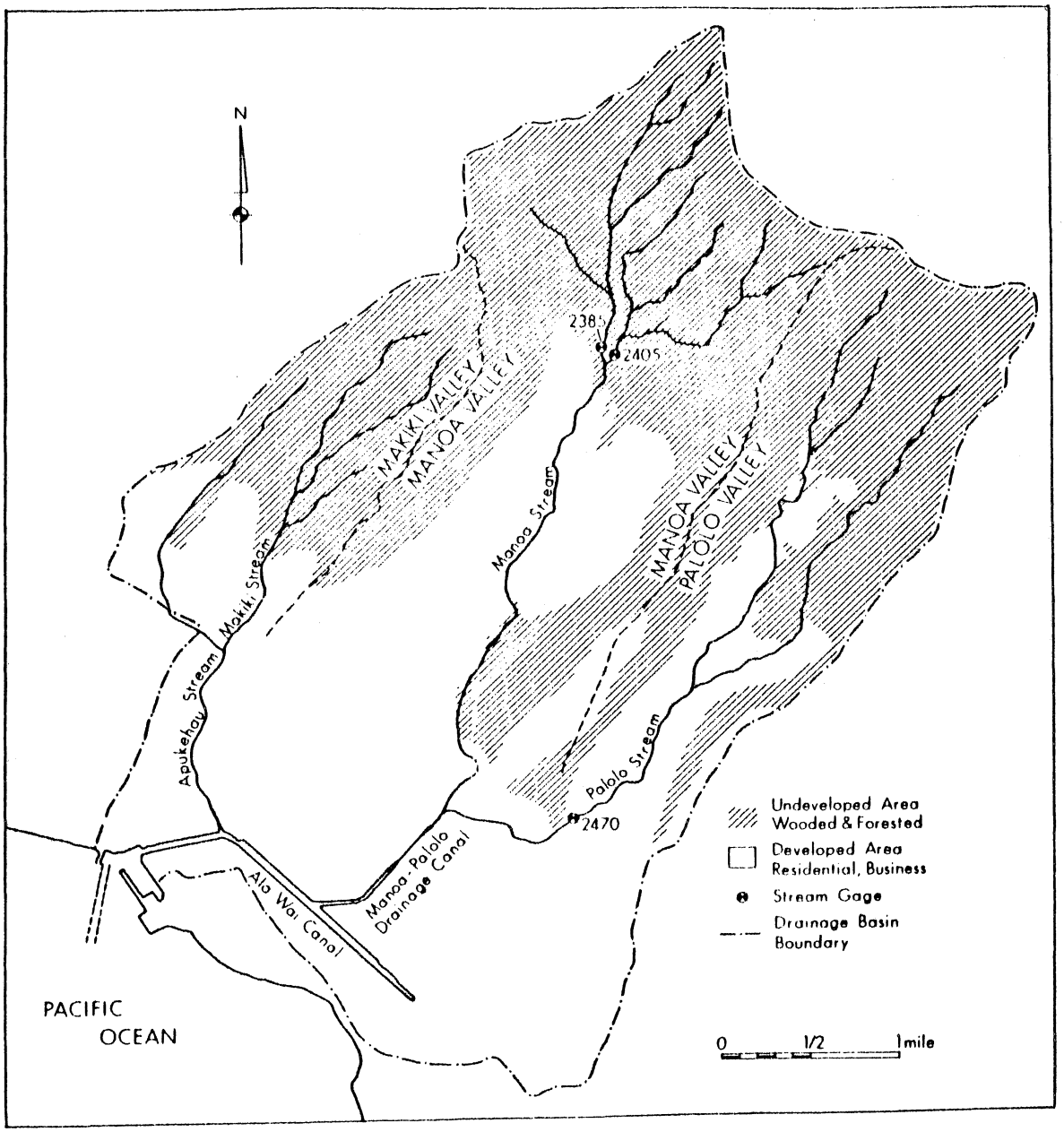

Figure 5. Chart of drainage basin, showing streams which discharge into the Ala Wai Canal and the locations of stream gauges.

Figure 6. Mean monthly discharges recorded at stream gauges 2385, 2405 and 2470.

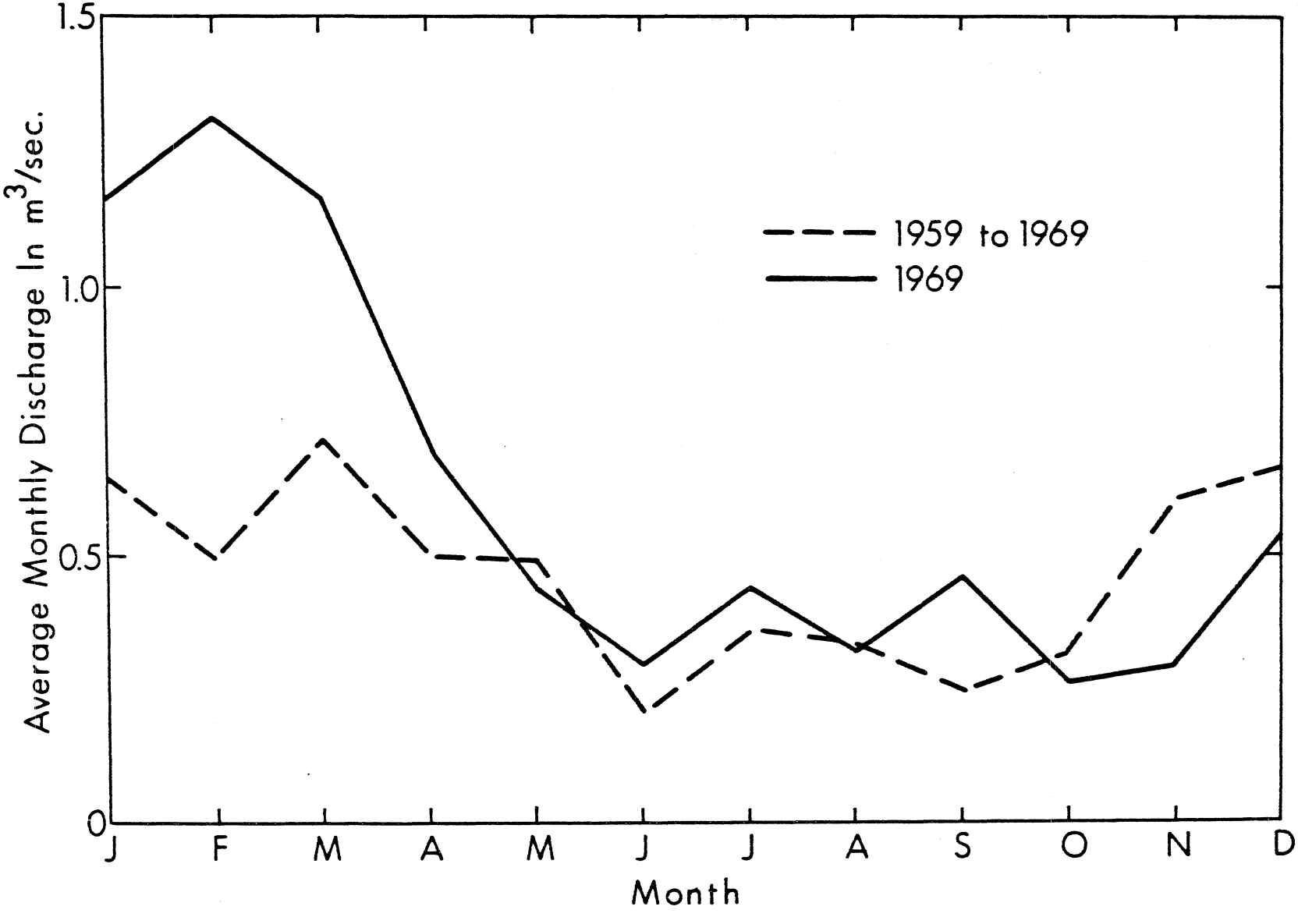
1.5
1.0
0.5
0
Average Monthly Discharge In m3/sec.
1959 to 1969
1969
J
F
M
A
M
J
J
A
S
O
N
D
Month

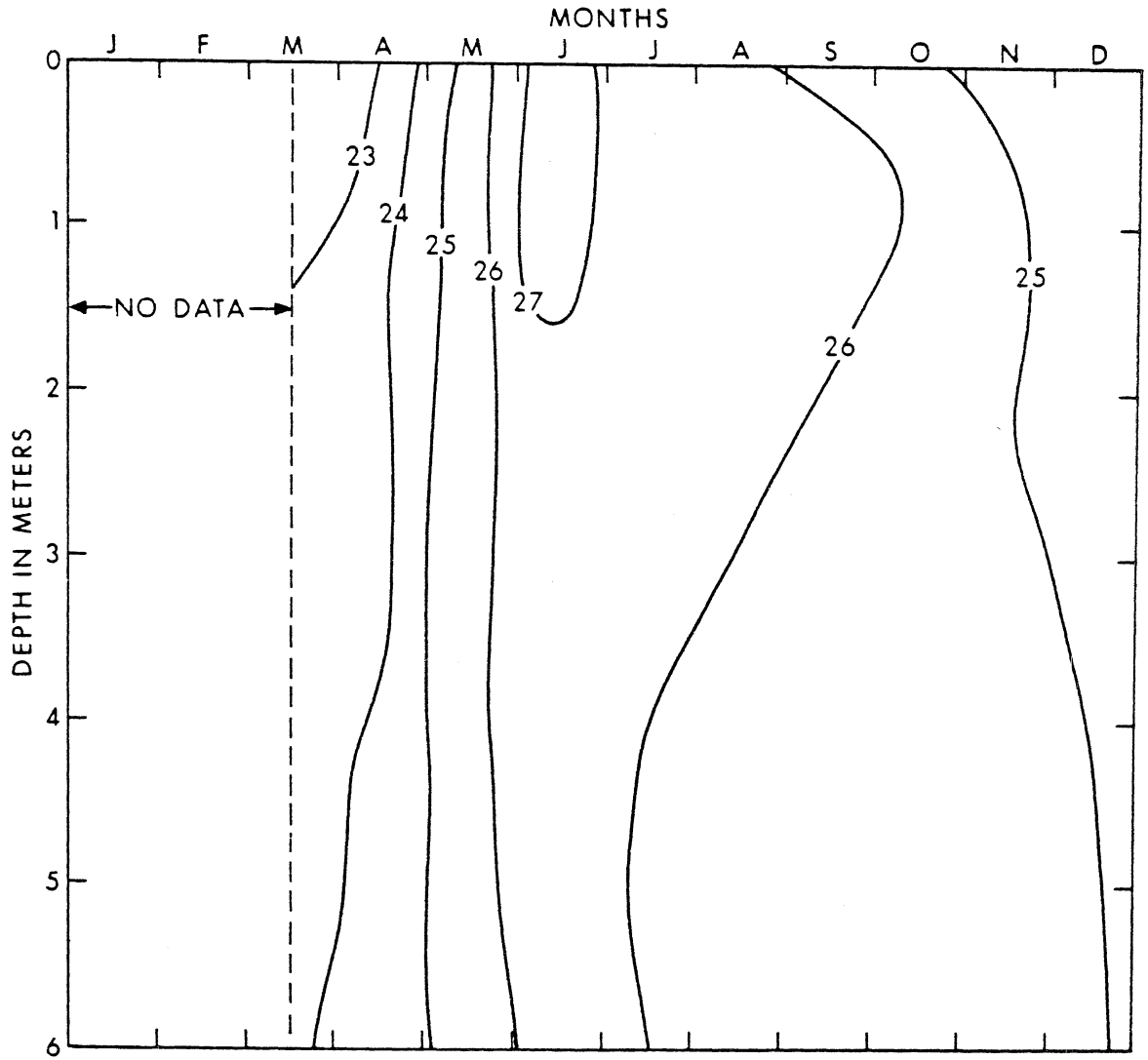

Figure 7. Temperature isopleths for Stations 11 and 12 in the Ala Wai Yacht Harbor. 1969.

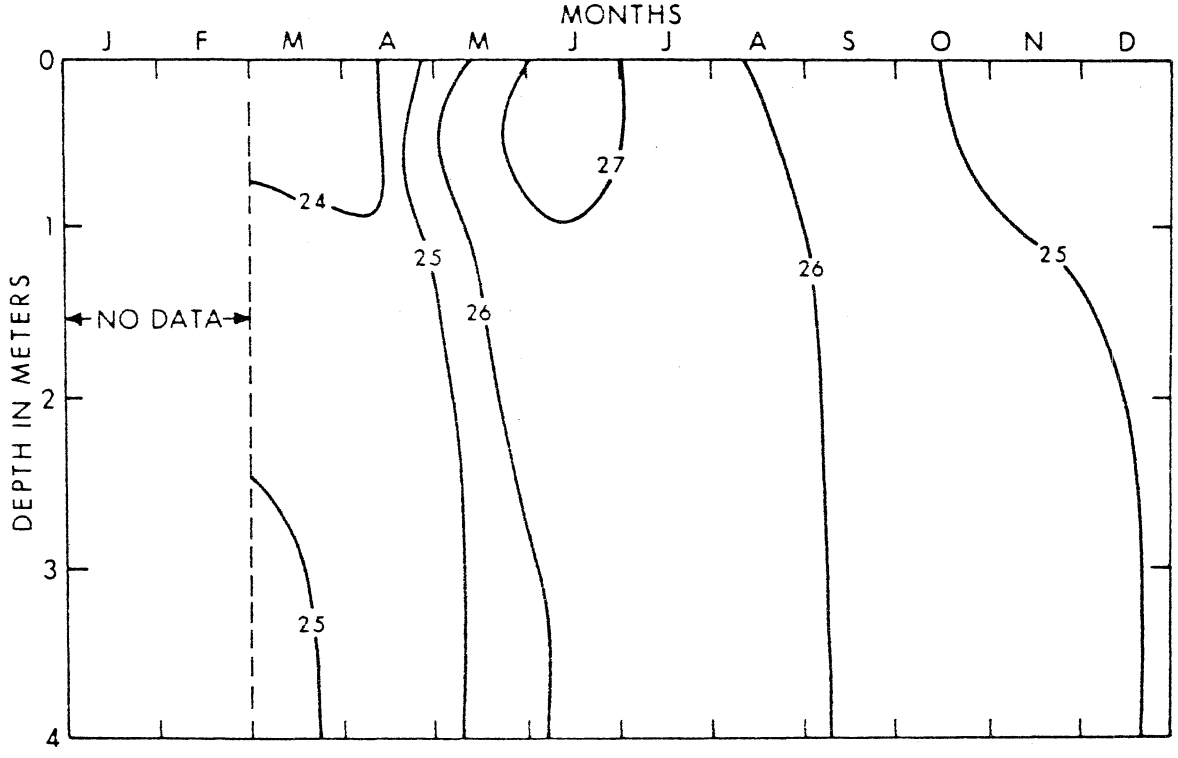

Figure 8. Temperature isopleths for Stations 1, 2 and 3 in the channel of the Ala Wai Canal. 1969.

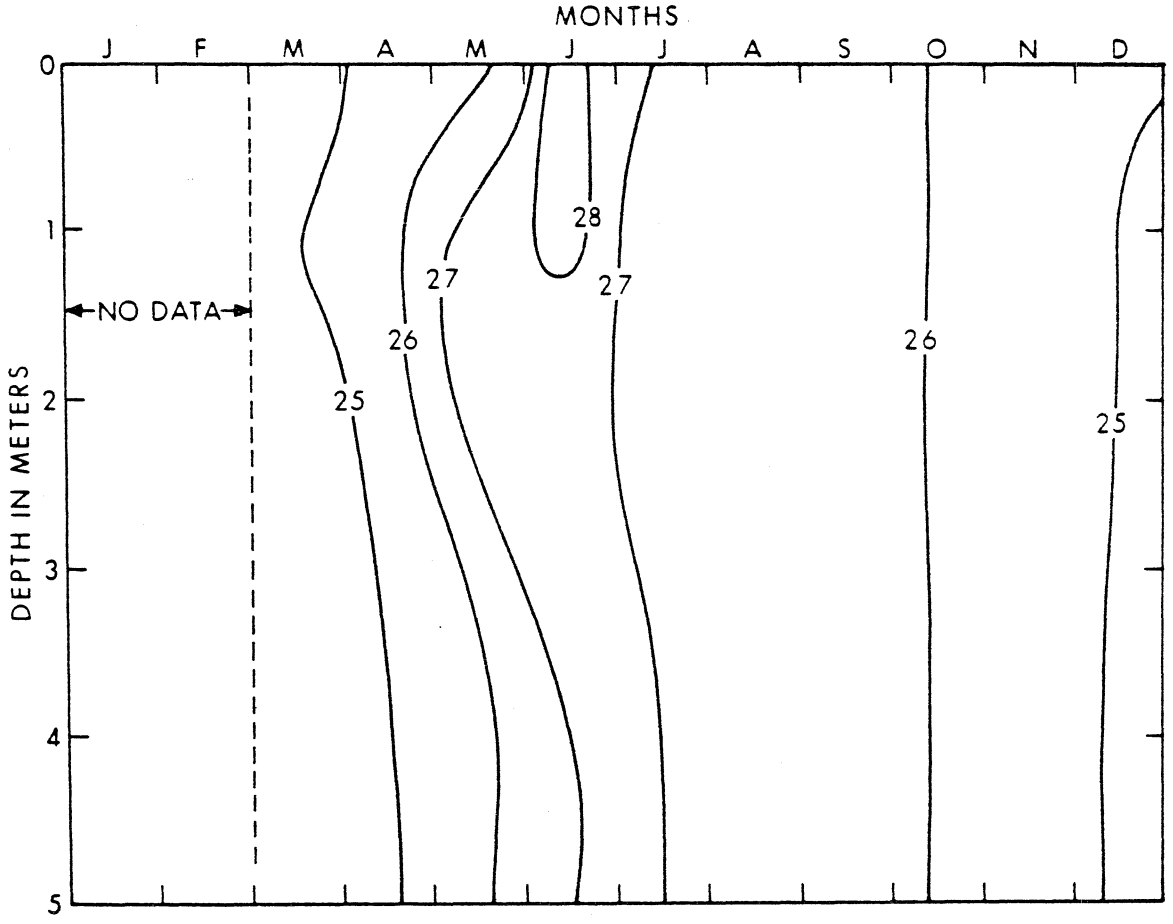

Figure 9. Temperature isopleths for Stations 7, 8 and 9 in the basin of the Ala Wai Canal.

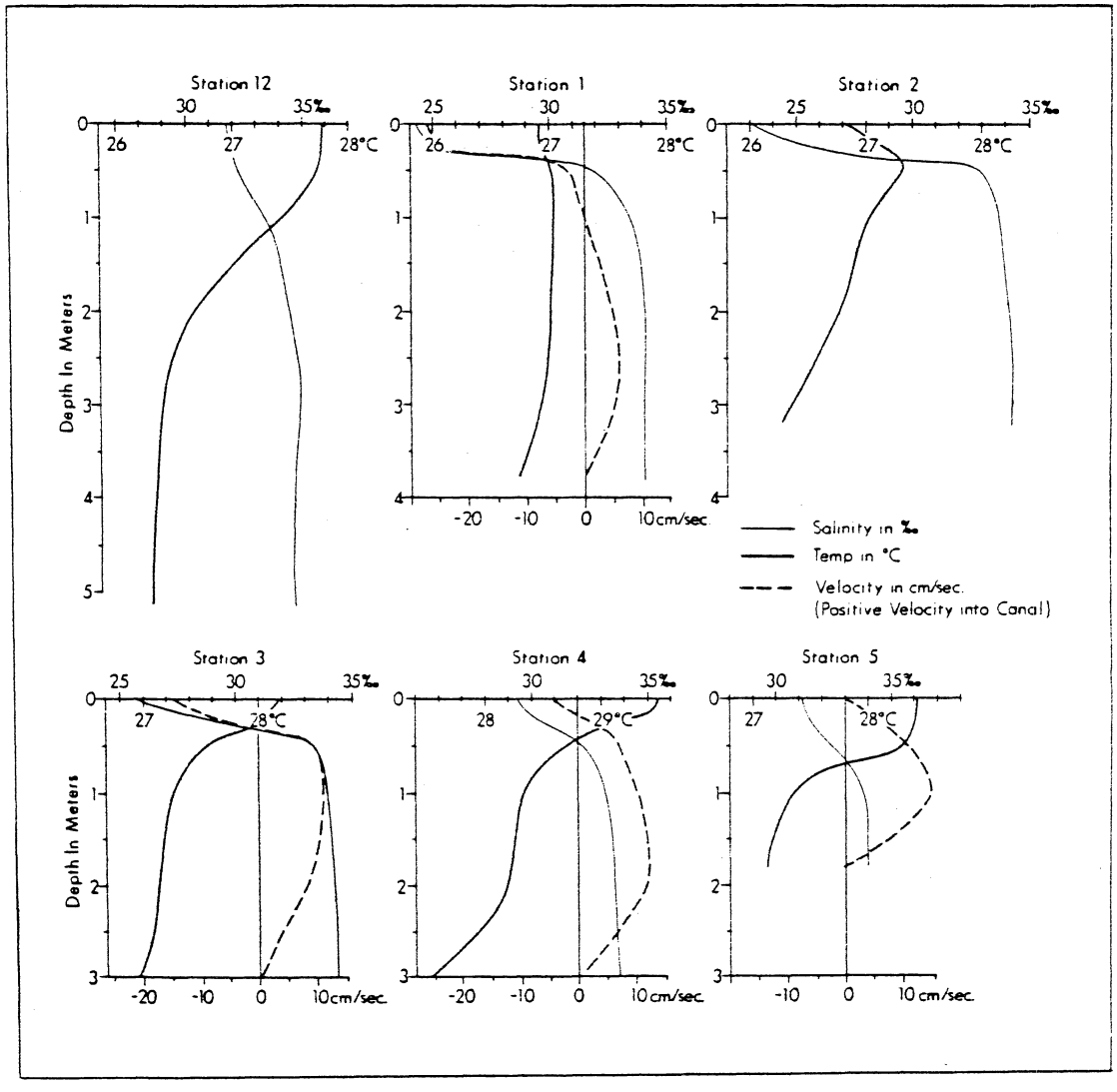

Figure 10. Current, salinity, and temperature profiles. June 29, 1969.

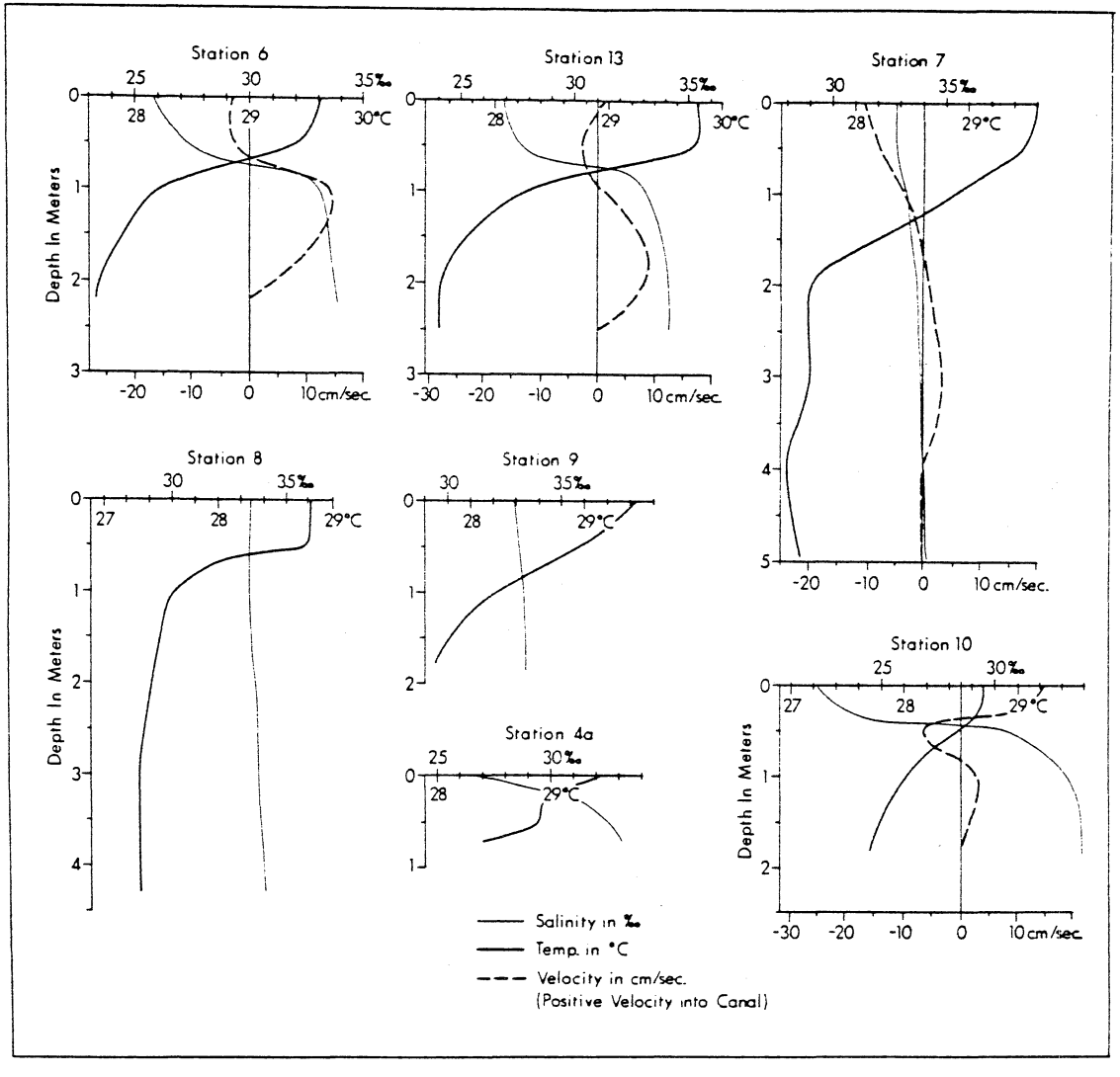

Figure 11. Current, salinity, and temperature profiles. June 29, 1969.

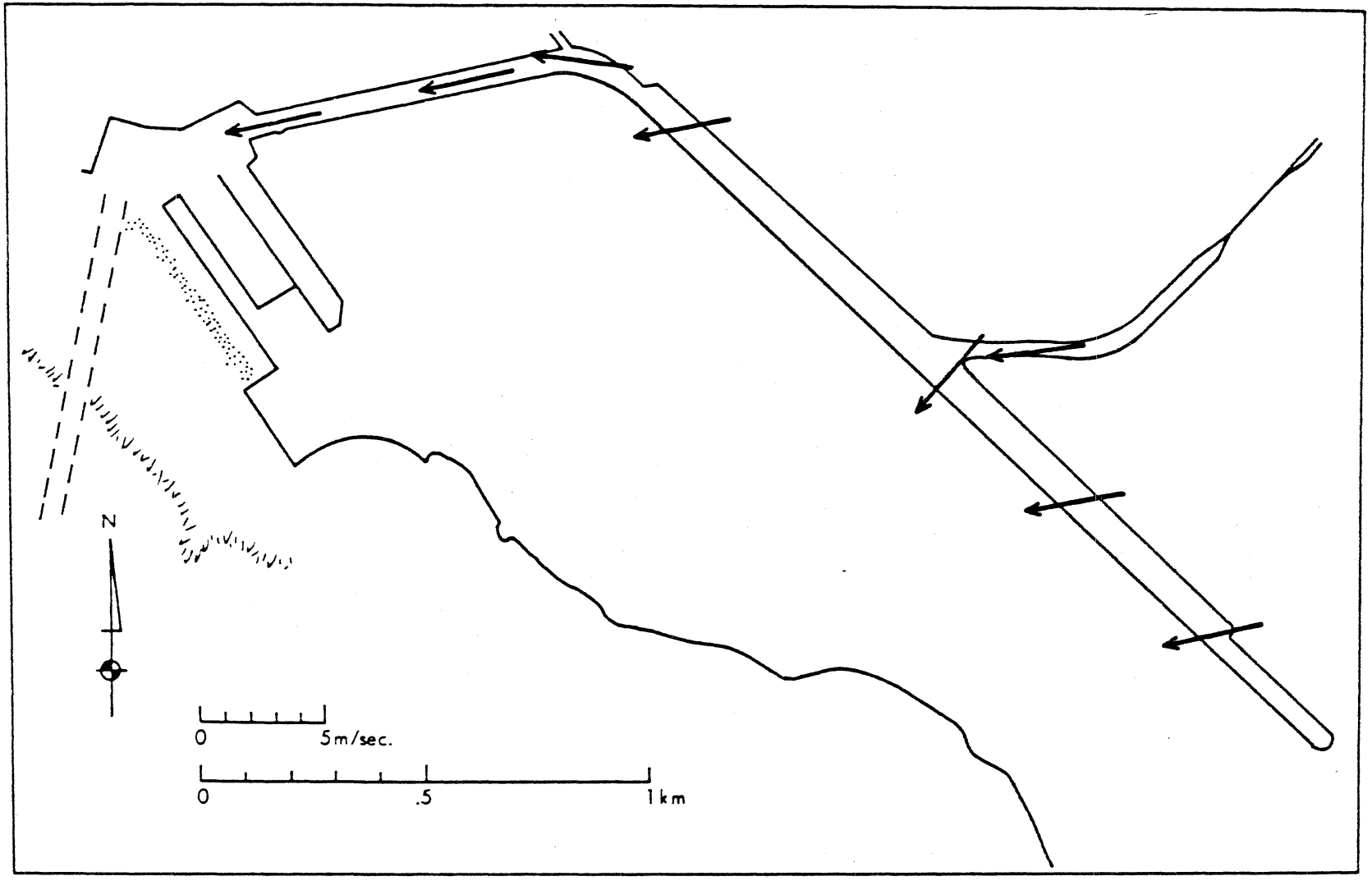

Figure 12. Wind speed and direction on the Ala Wai Canal. June 29, 1969.

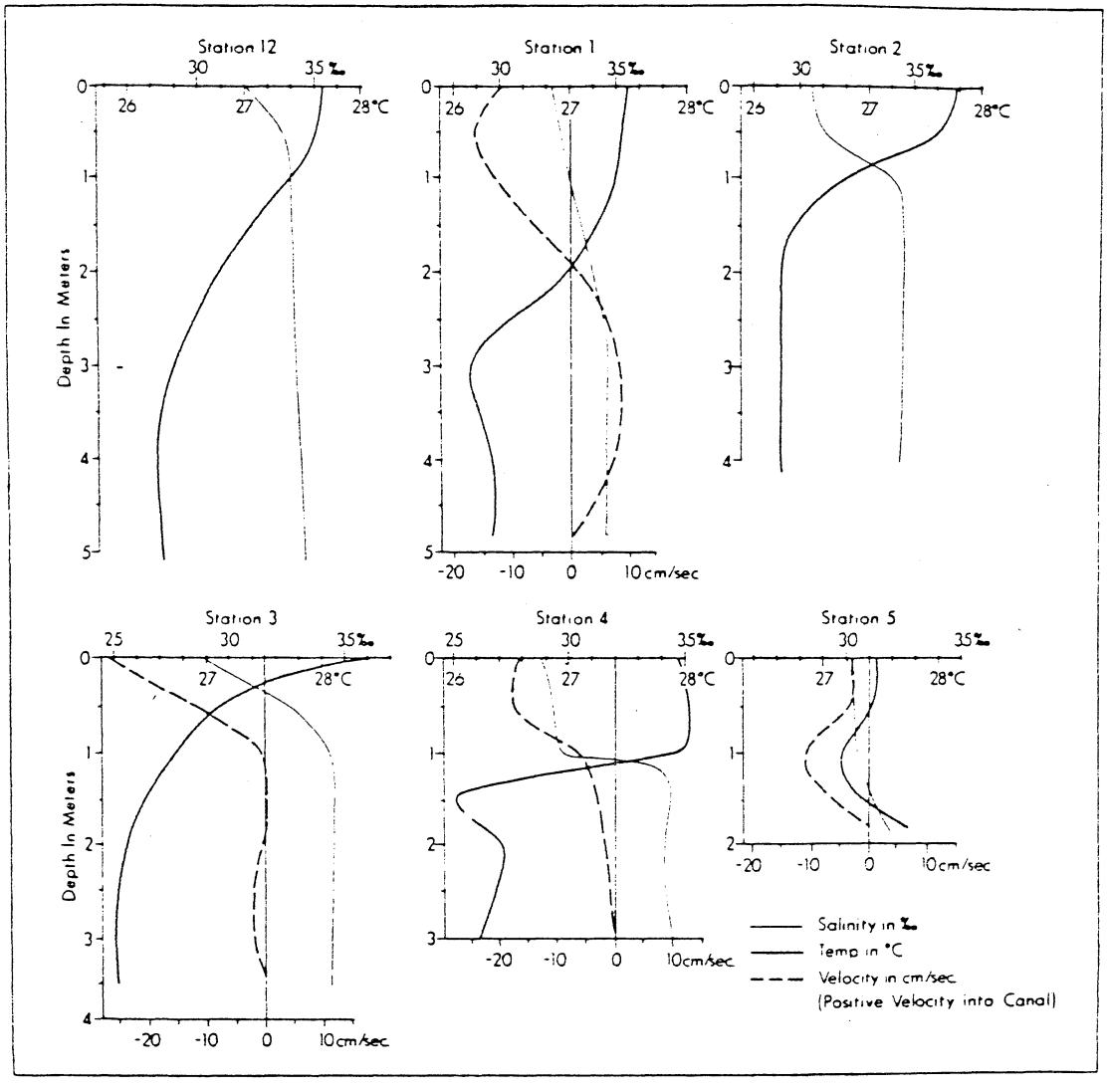

Figure 13. Current, salinity, and temperature profiles. June 30, 1969.

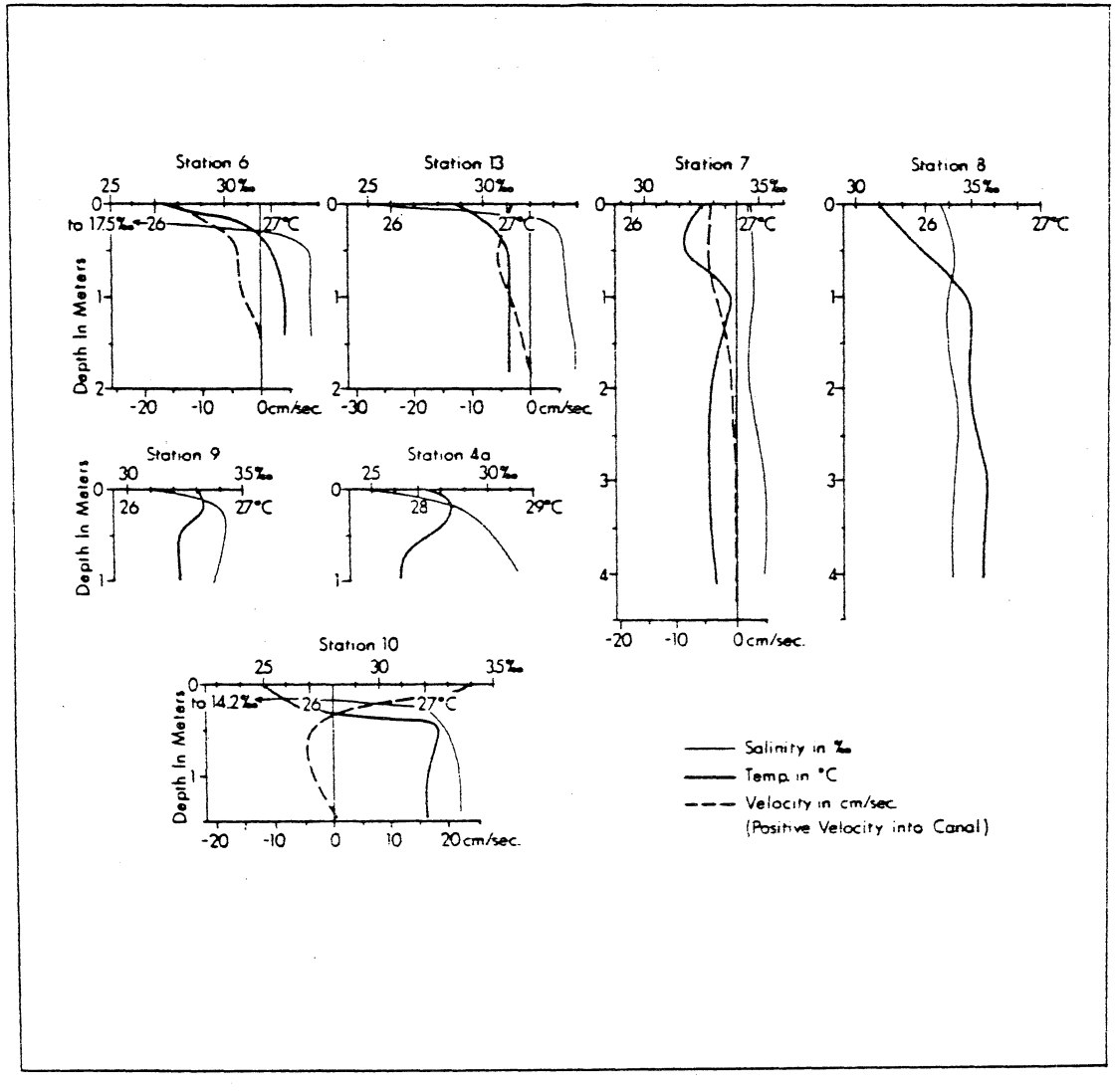

Figure 14. Current, salinity, and temperature profiles. June 30, 1969.

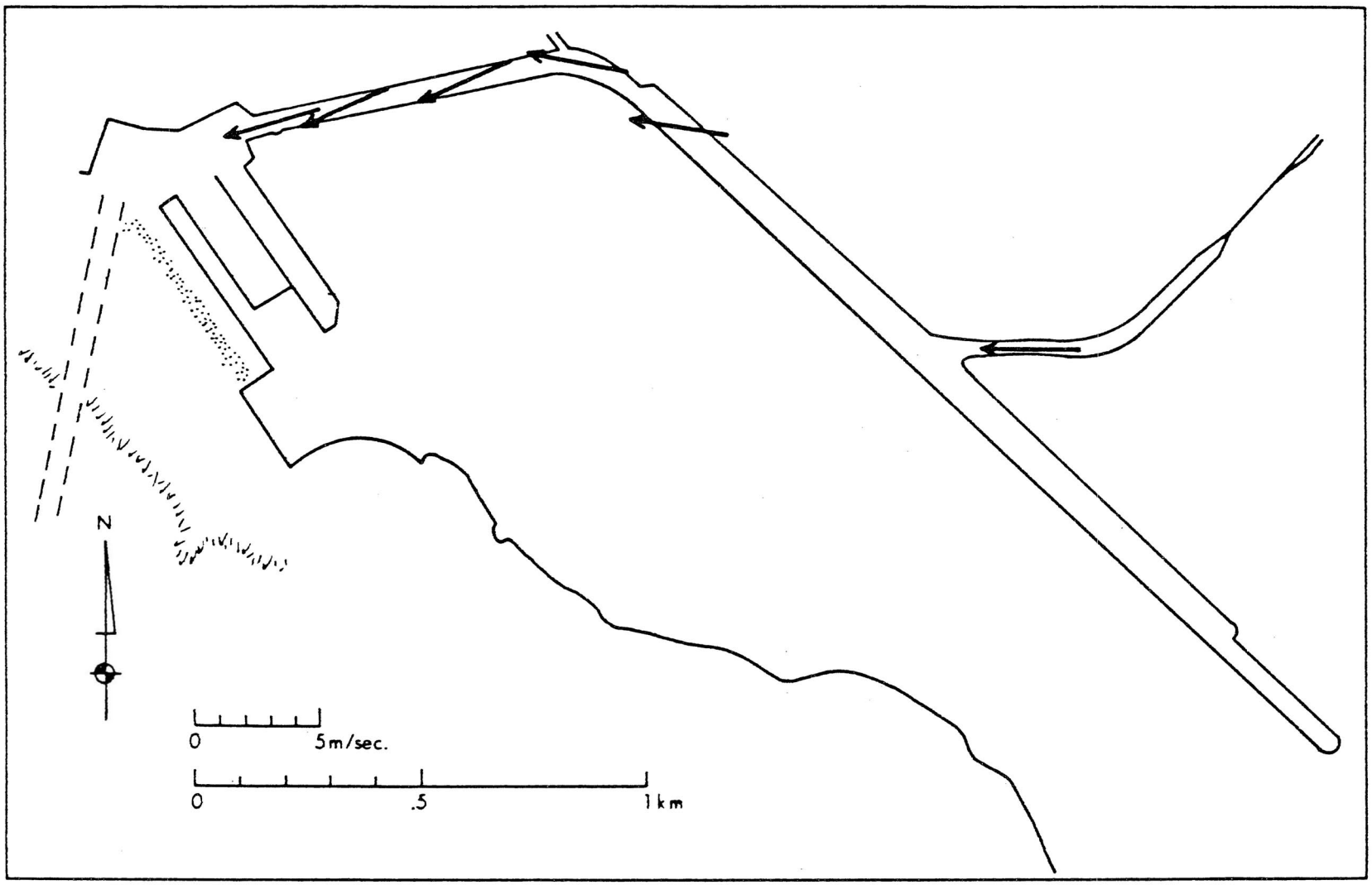

Figure 15. Wind speed and direction on the Ala Wai Canal. June 30, 1969.

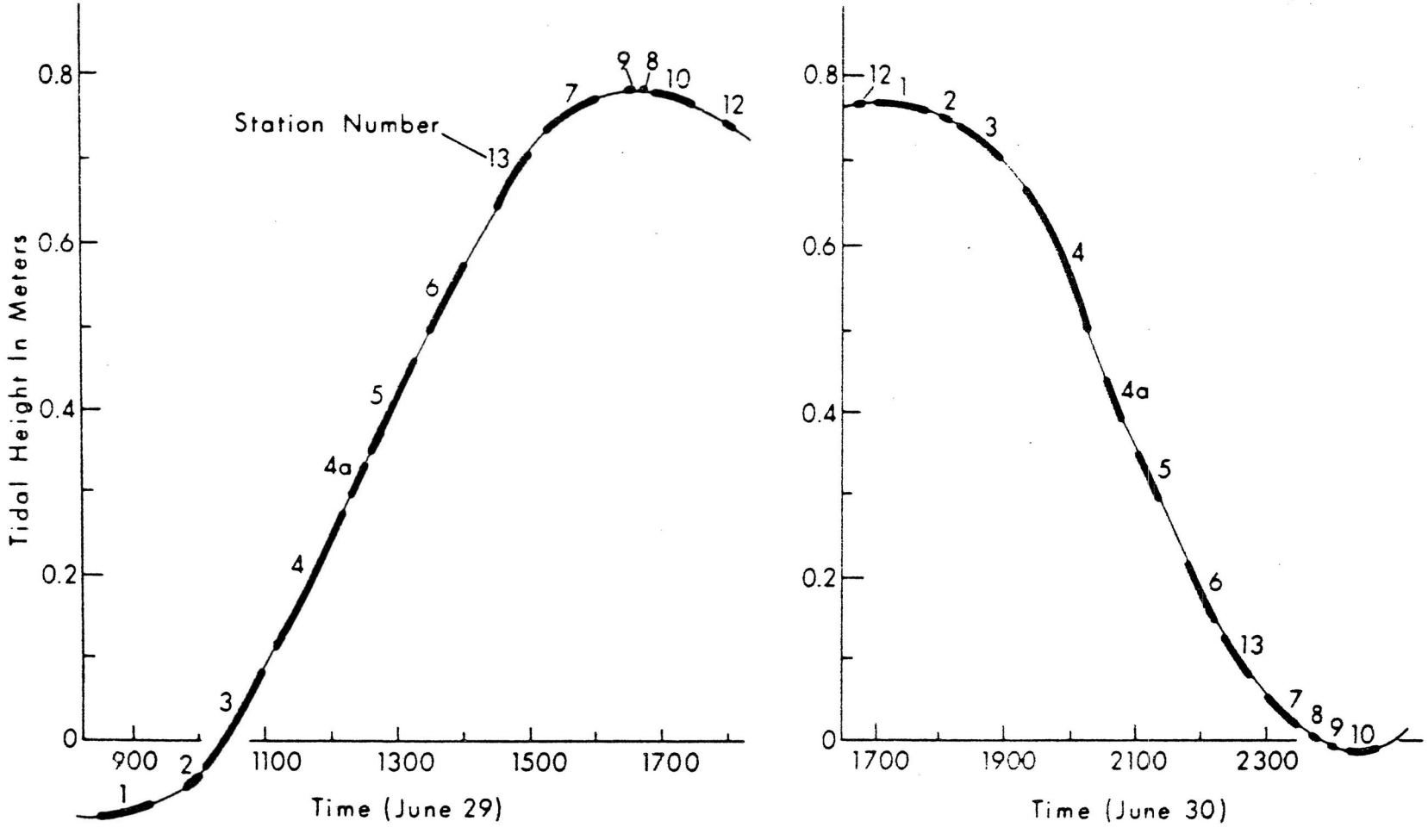

Figure 16. Sea level during occupation of individual stations on June 29 and 30, 1969.

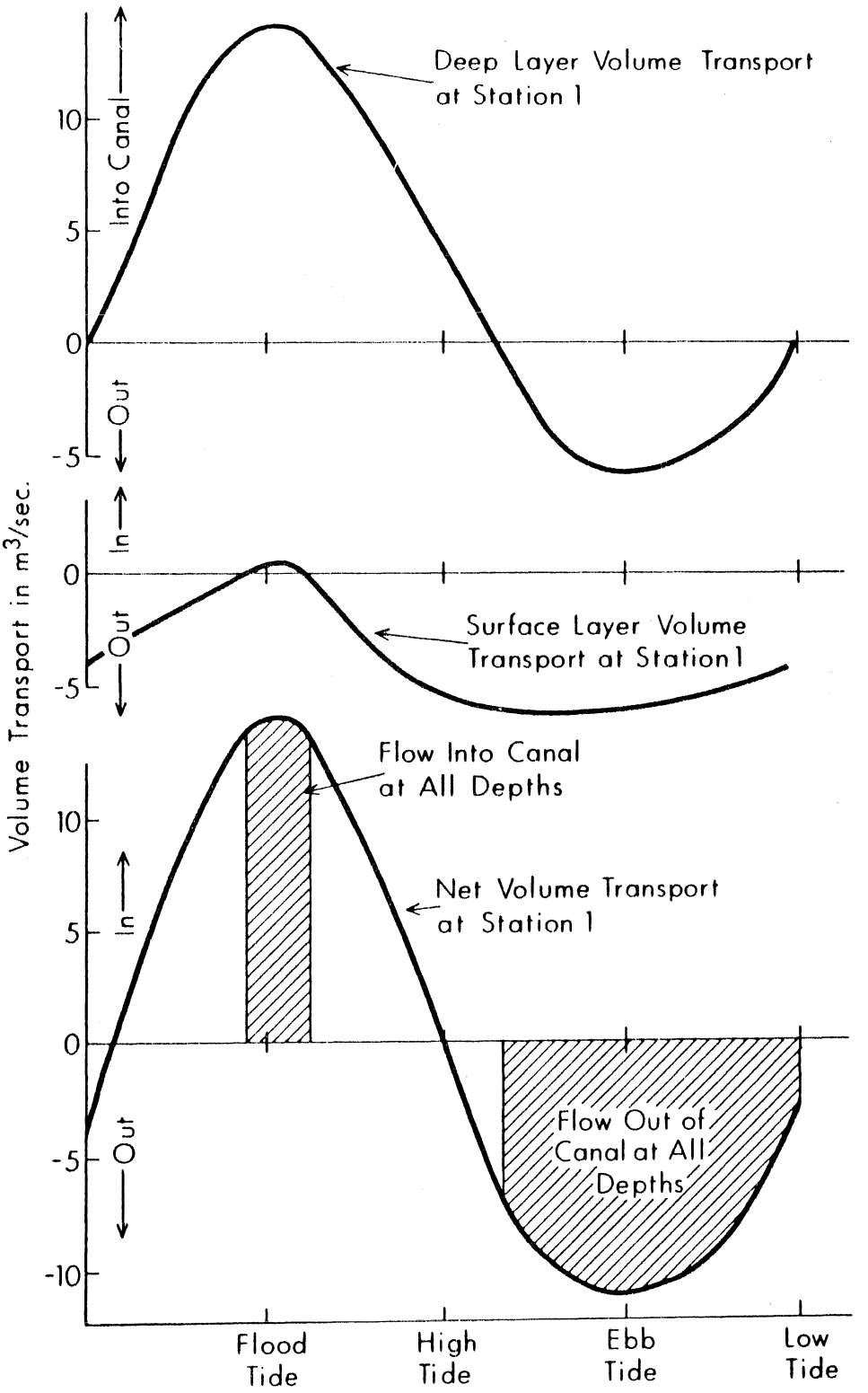

Figure 17. Volume transports at Station 1 over the composite tidal cycle of June 29 and 30, 1969.

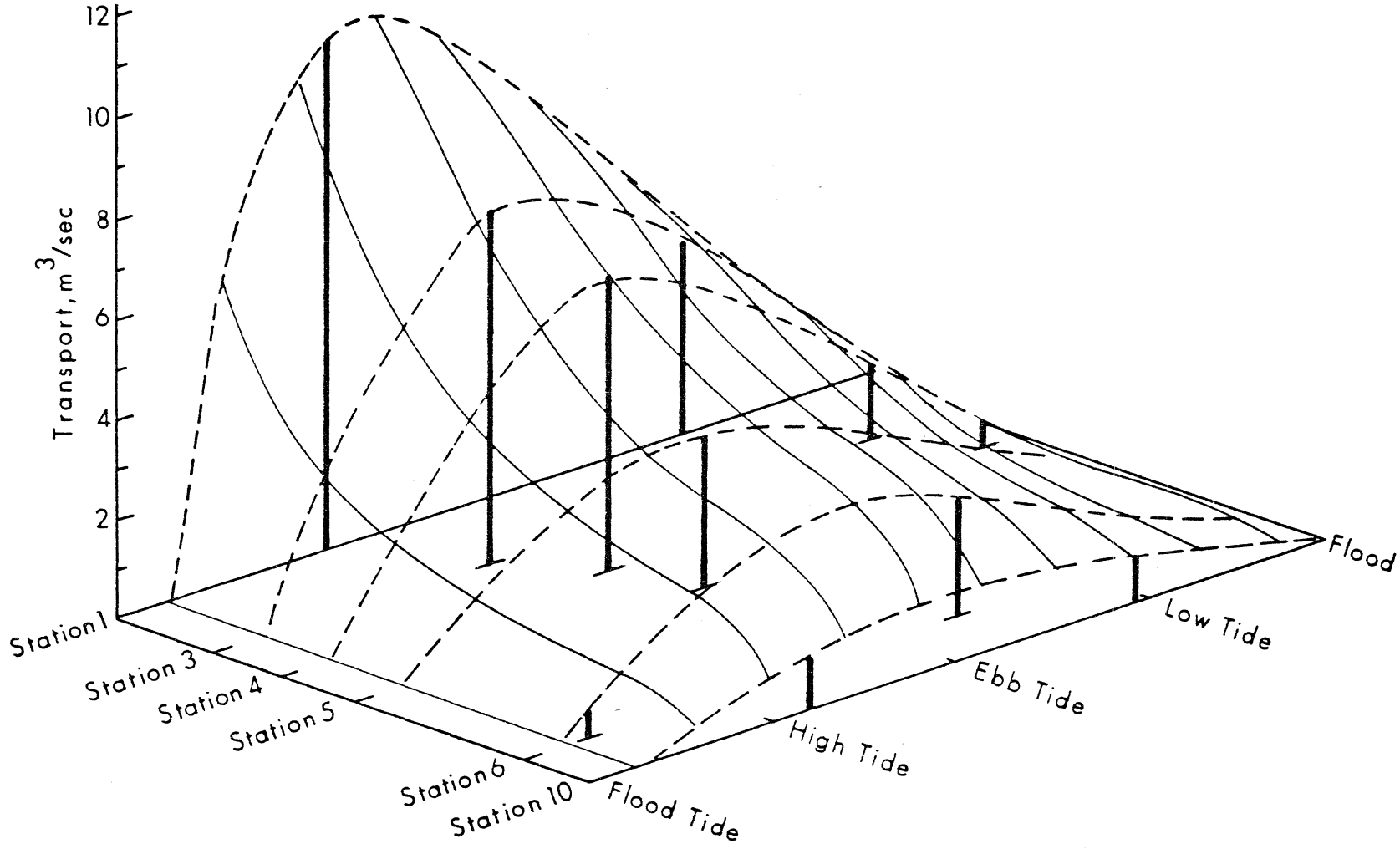

Figure 18. Transport of sea water out of the Canal in the surface layer as a function of location in the Canal and sea level. June 29 and 30, 1969.

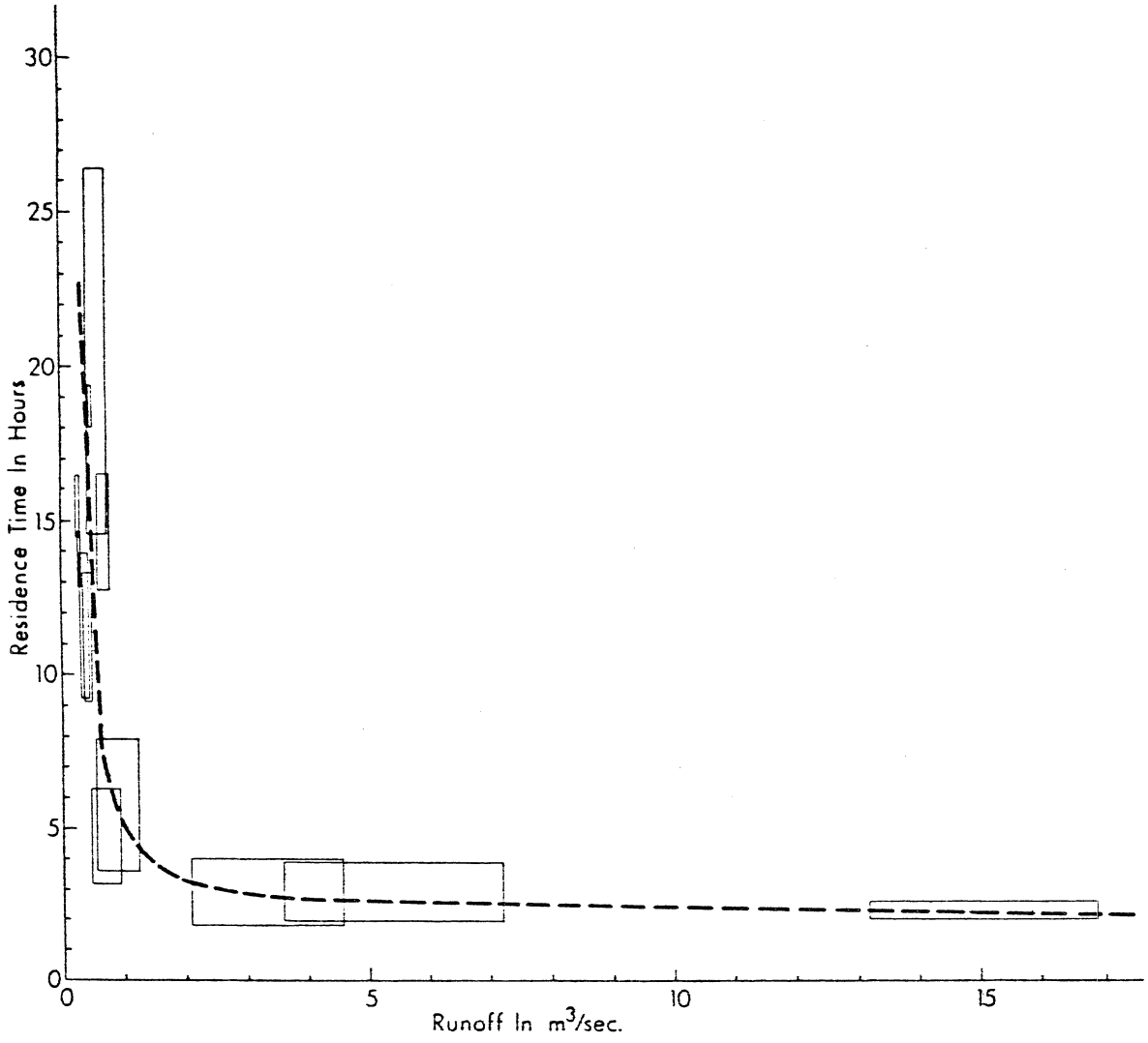

Figure 19. Residence time of fresh water in the surface layer as a function of fresh water runoff. Boxes indicate the uncertainty involved in determining individual points. This is discussed on page 31.

Figure 20. Longitudinal section of the Ala Wai Canal at mean lower low water, showing the stream and drainage ditch entrances to the Canal and the various topographic regions.

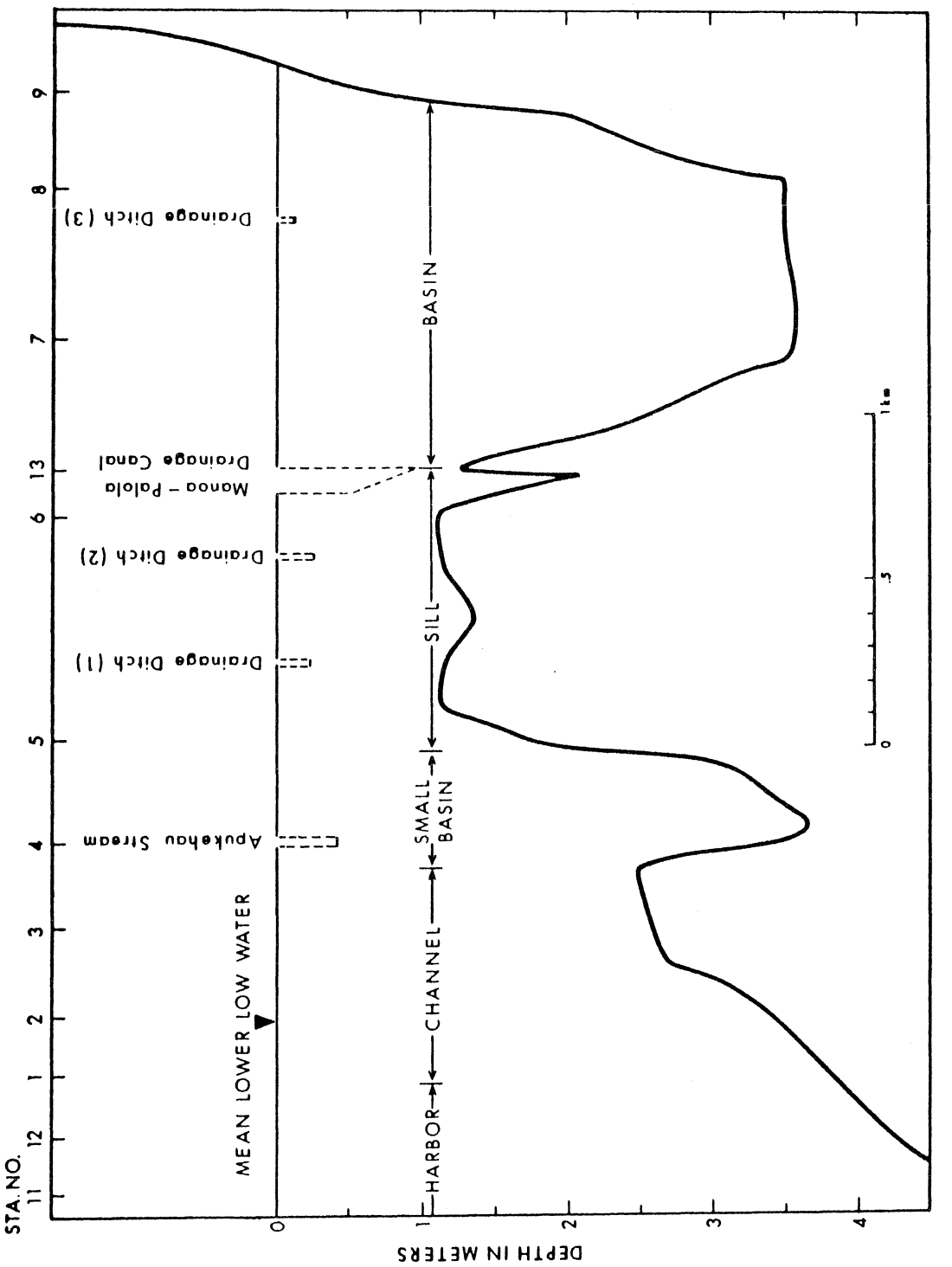
STA. NO.
11
12
1
2
3
4
5
6
13
7
8
9
MEAN LOWER LOW WATER
Aukahau Stream
Drainage Ditch (1)
Drainage Ditch (2)
Manoa – Palola Drainage Canal
Drainage Ditch (3)
HARBOR
CHANNEL
SMALL BASIN
SILL
BASIN
0
1
2
3
4
DEPTH IN METERS
0
.5
1 ft.

Figure 21(a). Longitudinal section of salinity in $^{o}/oo$. March 16, 1969.


STA. NO.
11 12 1 2 3 4 5 6 13 7 8 9
DEPTH IN METERS
0 1 2 3 4 5
4 6 8 10 12 22 24 26 28 30 32
2 4 6 8 10 12 14 16 18 20 22 24 26 28 30 32
.5m
0 12 24h
Data Period (Hatched Area)
0 .5 1km

Figure 21(b). Longitudinal section of temperature in °C. March 16, 1969.

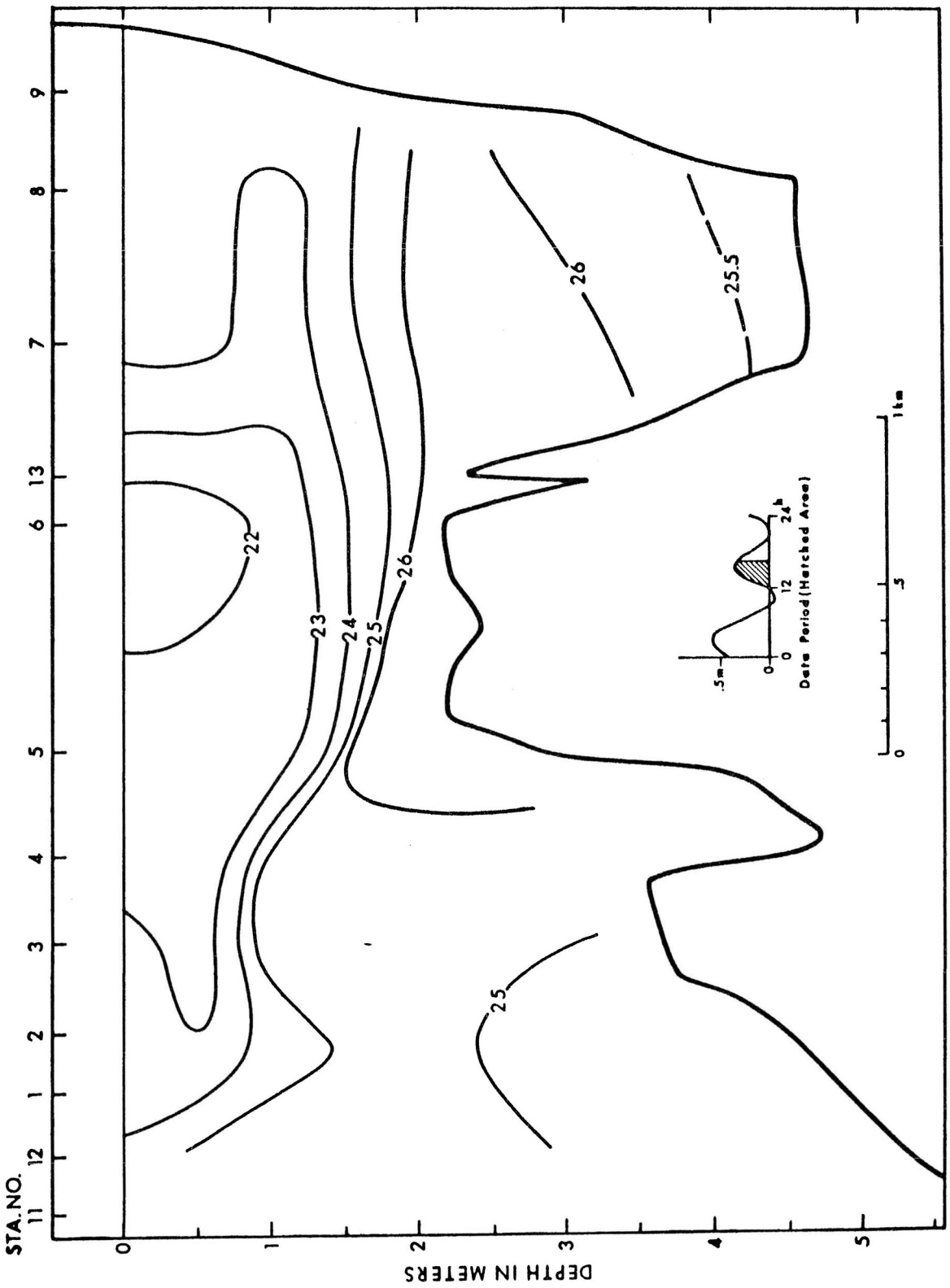
STA. NO.
11 12 1 2 3 4 5 6 13 7 8 9
DEPTH IN METERS
0 1 2 3 4 5
22
23
24
25
26
25
26
25.5
.5m
0
12
24h
Data Period (Hatched Area)
0
.5
1km

Figure 21(c). Longitudinal section of sigma-t in gm/cm^3. March 16, 1969.

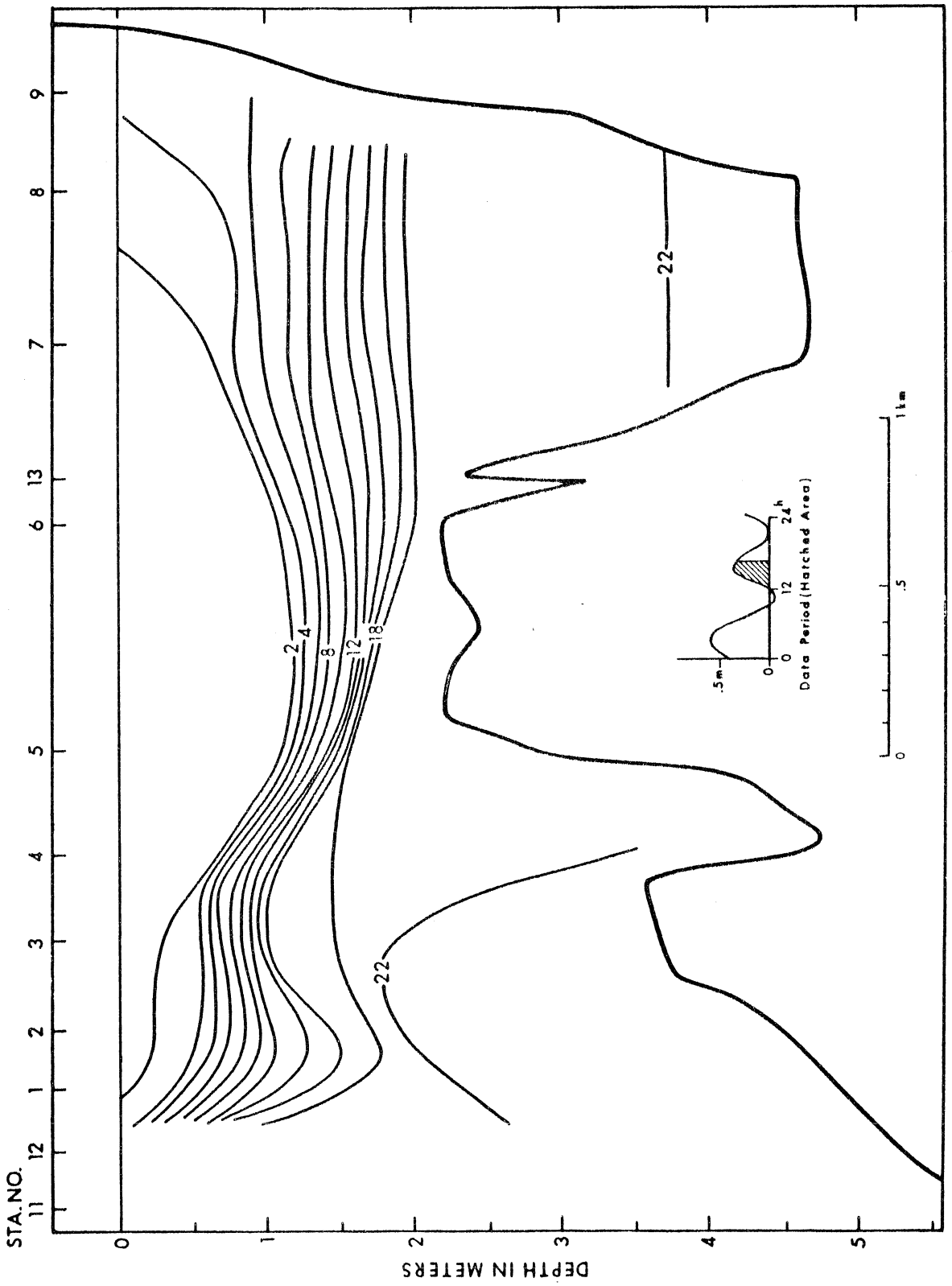
STA. NO.
11 12 1 2 3 4 5 6 13 7 8 9
DEPTH IN METERS
0 1 2 3 4 5
2 4 8 12 18
22
22
.5m
0
12
24h
Data Period (Hatched Area)
1km
.5
0

Figure 22(a). Longitudinal section of salinity in °/oo. March 16, 1969.

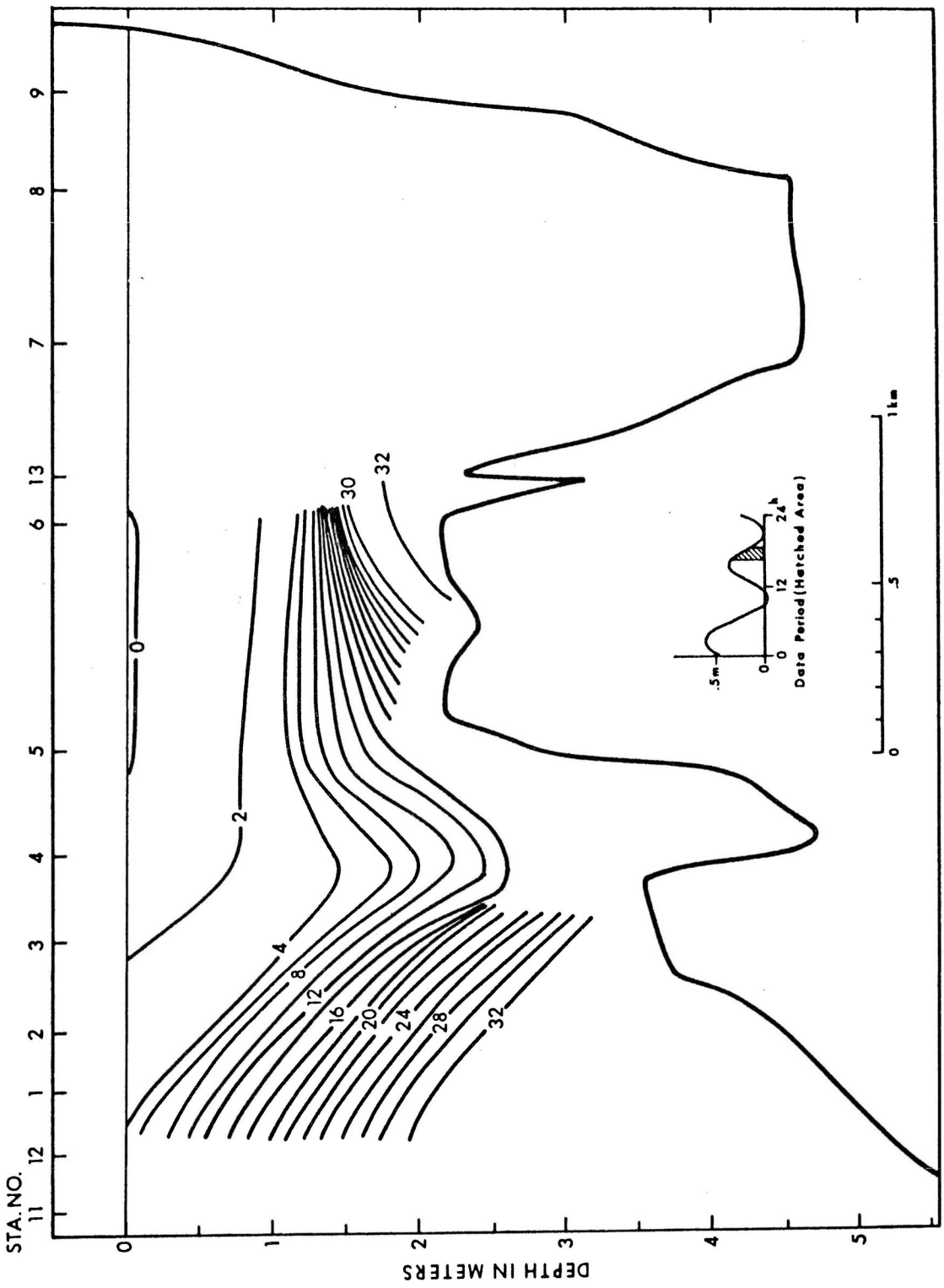
STA. NO.
11 12 1 2 3 4 5 6 13 7 8 9
DEPTH IN METERS
0 1 2 3 4 5
0
2
4
8
12
16
20
24
28
32
30
32
.5m
0
12
24h
Data Period (Hatched Area)
0
.5
1km

Figure 22(b). Longitudinal section of temperature in °C. March 16, 1969.

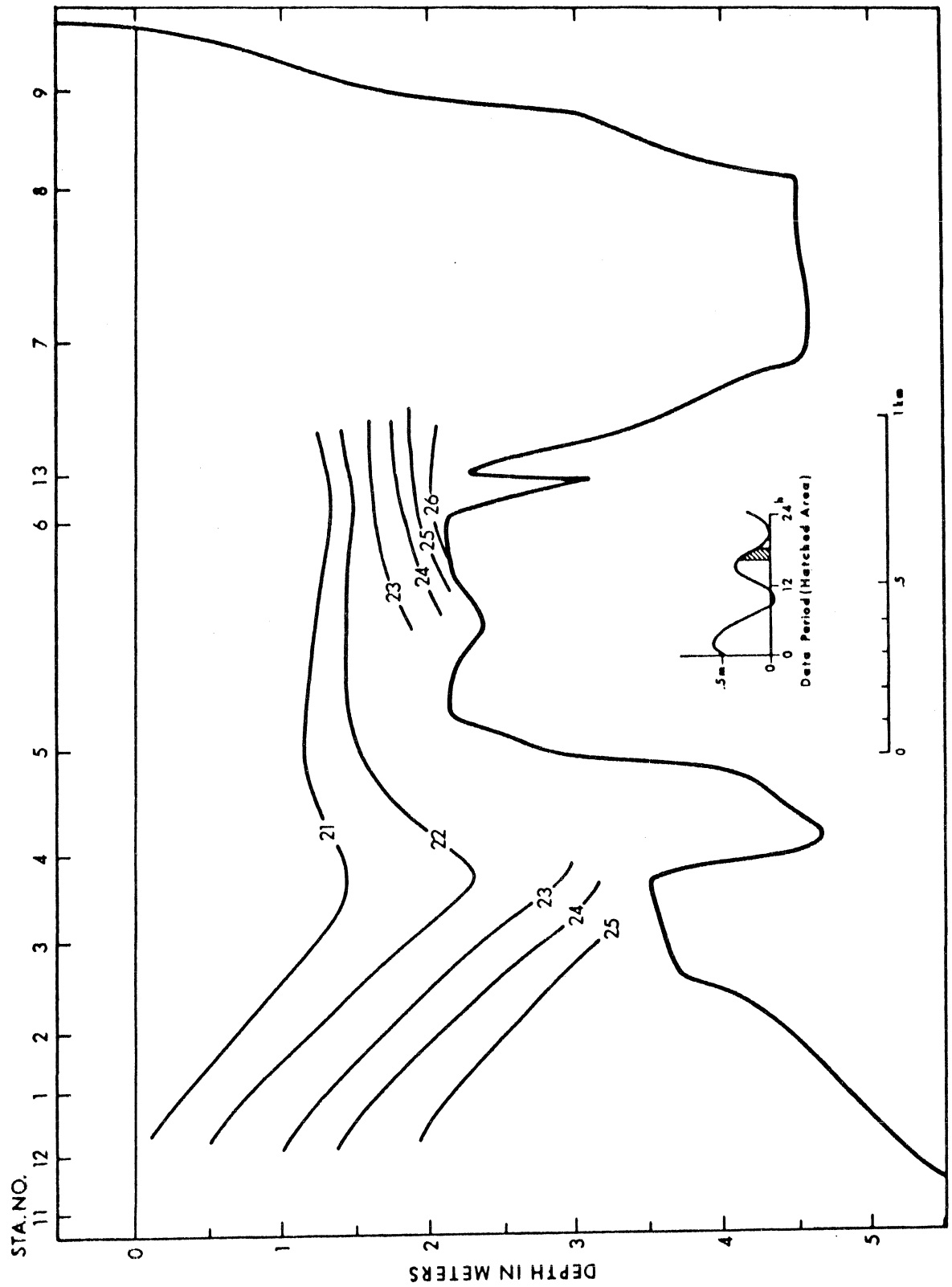
STA. NO.
11 12 1 2 3 4 5 6 13 7 8 9
DEPTH IN METERS
0 1 2 3 4 5
21
22
23
24
25
23
24
25
26
.5m
0
12
24h
Date Period (Hatched Area)
0
.5
1 km

Figure 22(c). Longitudinal section of sigma-t in gm/cm^3. March 16, 1969.


STA. NO.
11 12 1 2 3 4 5 6 13 7 8 9
DEPTH IN METERS
0 1 2 3 4 5
2 4 6 8 10 12 16 20
12 16 20
.5m
0
12
24h
Data Period (Hatched Area)
0 .5 1 km

Figure 23(a). Longitudinal section of salinity in °/oo. March 29, 1969.

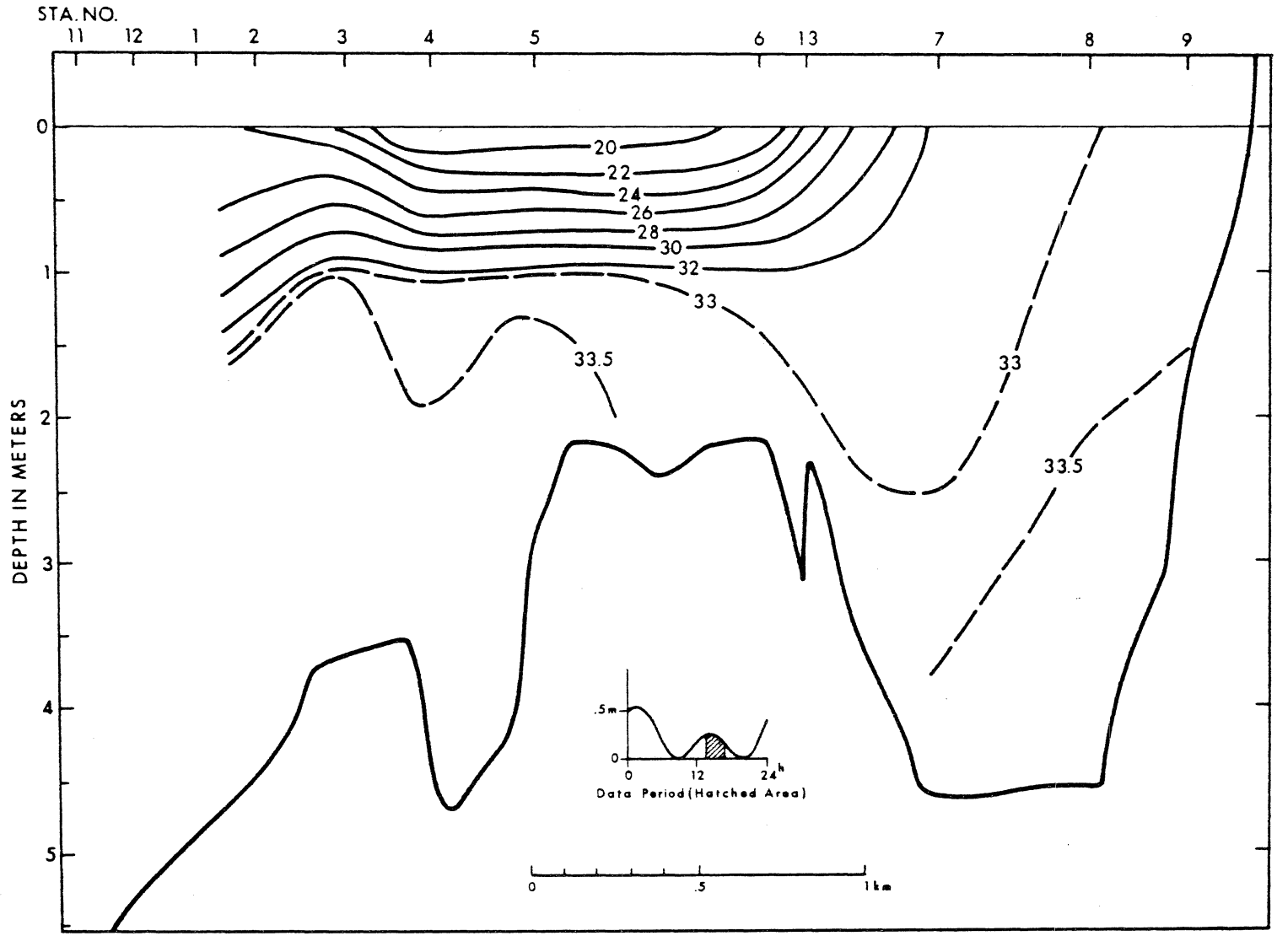
STA. NO.
11
12
1
2
3
4
5
6
13
7
8
9
0
1
2
3
4
5
DEPTH IN METERS
20
22
24
26
28
30
32
33
33.5
33
33.5
.5m
0
0
12
24h
Data Period (Hatched Area)
0
.5
1km

Figure 23(b). Longitudinal section of temperature in °C. March 29, 1969.

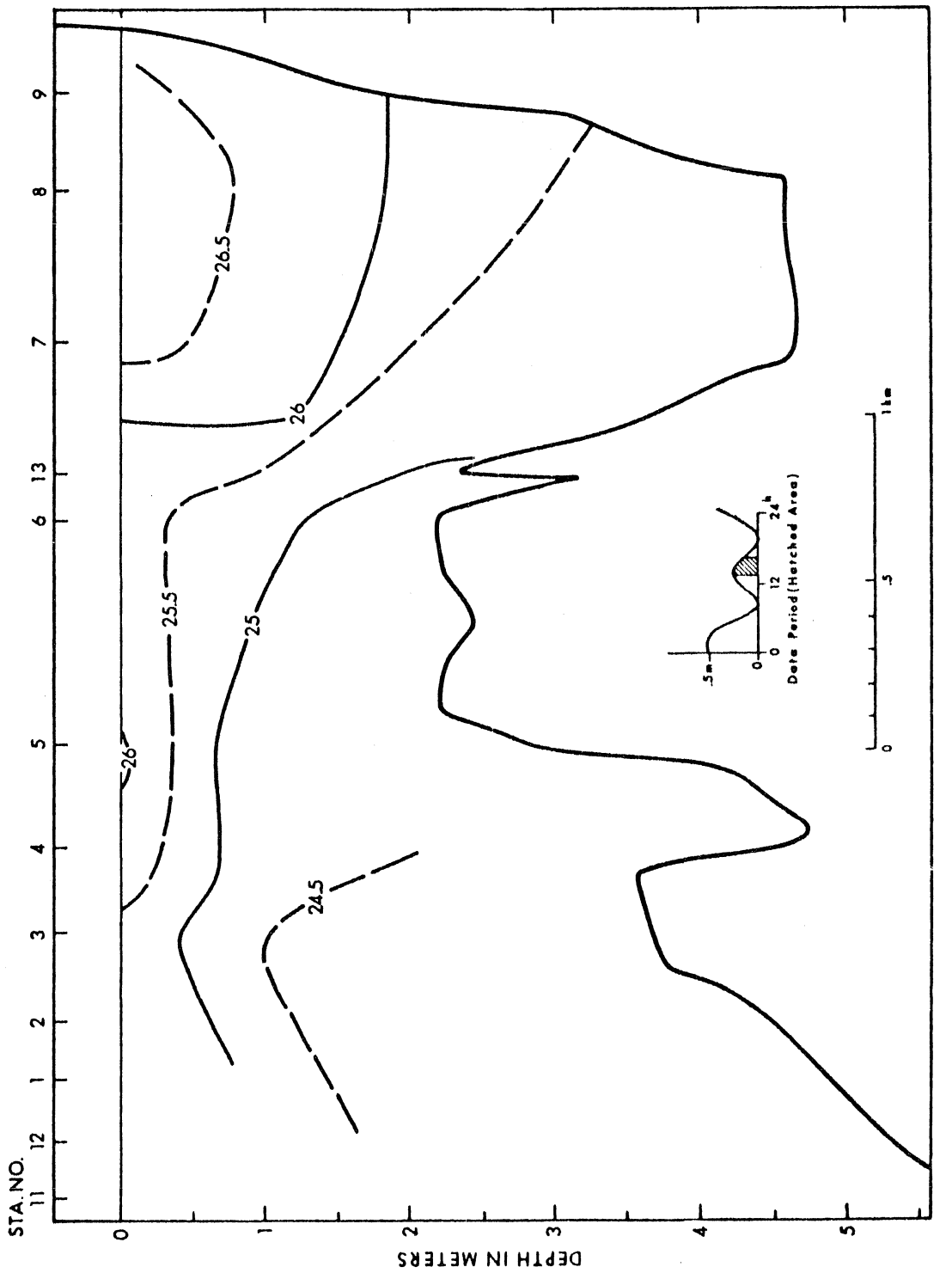
STA. NO.
11 12 1 2 3 4 5 6 13 7 8 9
DEPTH IN METERS
0 1 2 3 4 5
26.5
26
25.5
25
24.5
26
.5m
0
12
24h
Data Period (Hatched Area)
0
.5
1km

Figure 23(c). Longitudinal section of sigma-t in gm/cm^3. March 29, 1969.

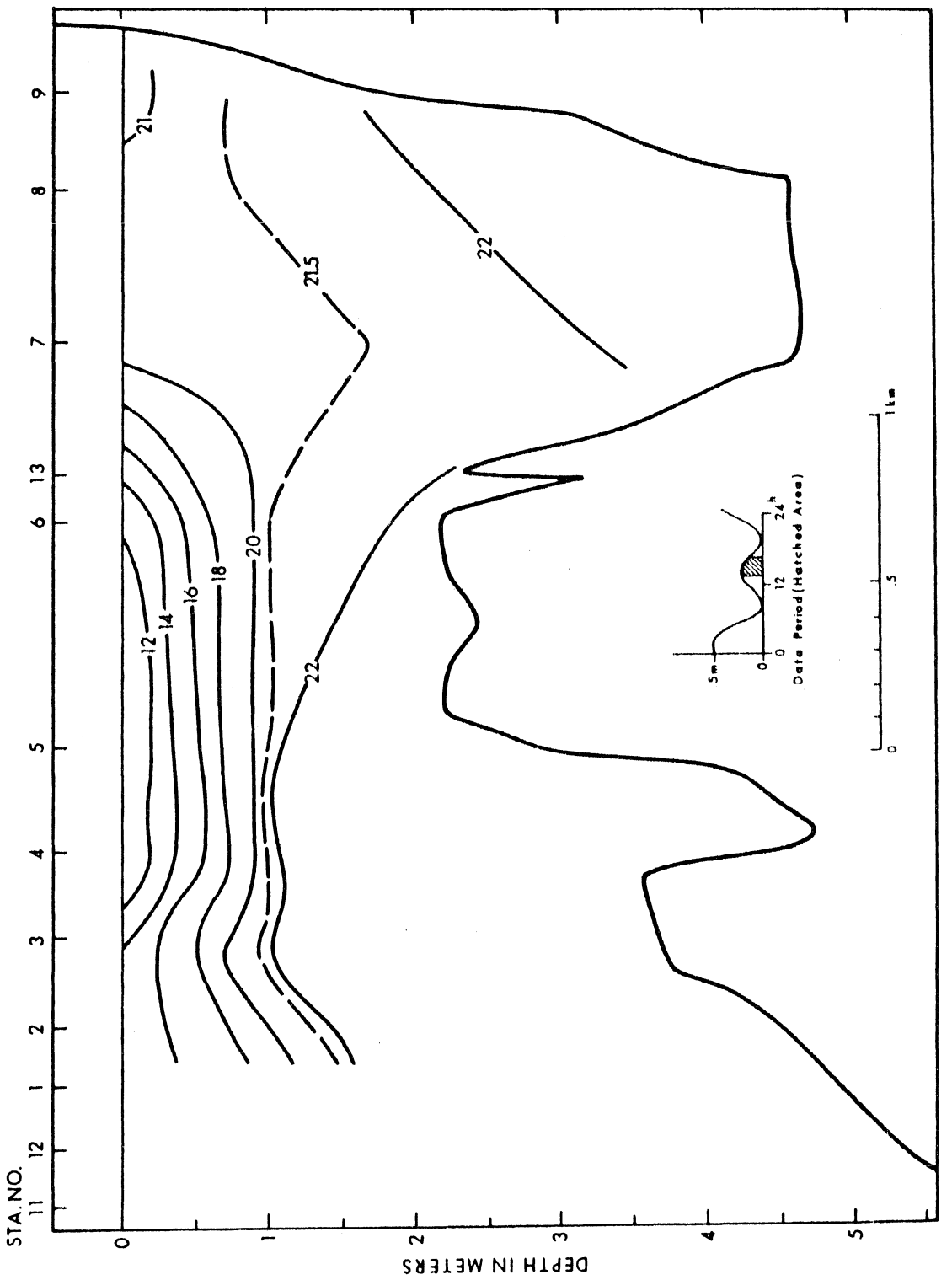
STA. NO.
11 12 1 2 3 4 5 6 13 7 8 9
DEPTH IN METERS
0 1 2 3 4 5
12
14
16
18
20
21
21.5
22
22
5m
0
0
12
24h
Date Period (Hatched Area)
0
.5
1 km

Figure 23(d). Longitudinal section of dissolved oxygen in ml/l. March 29, 1969.

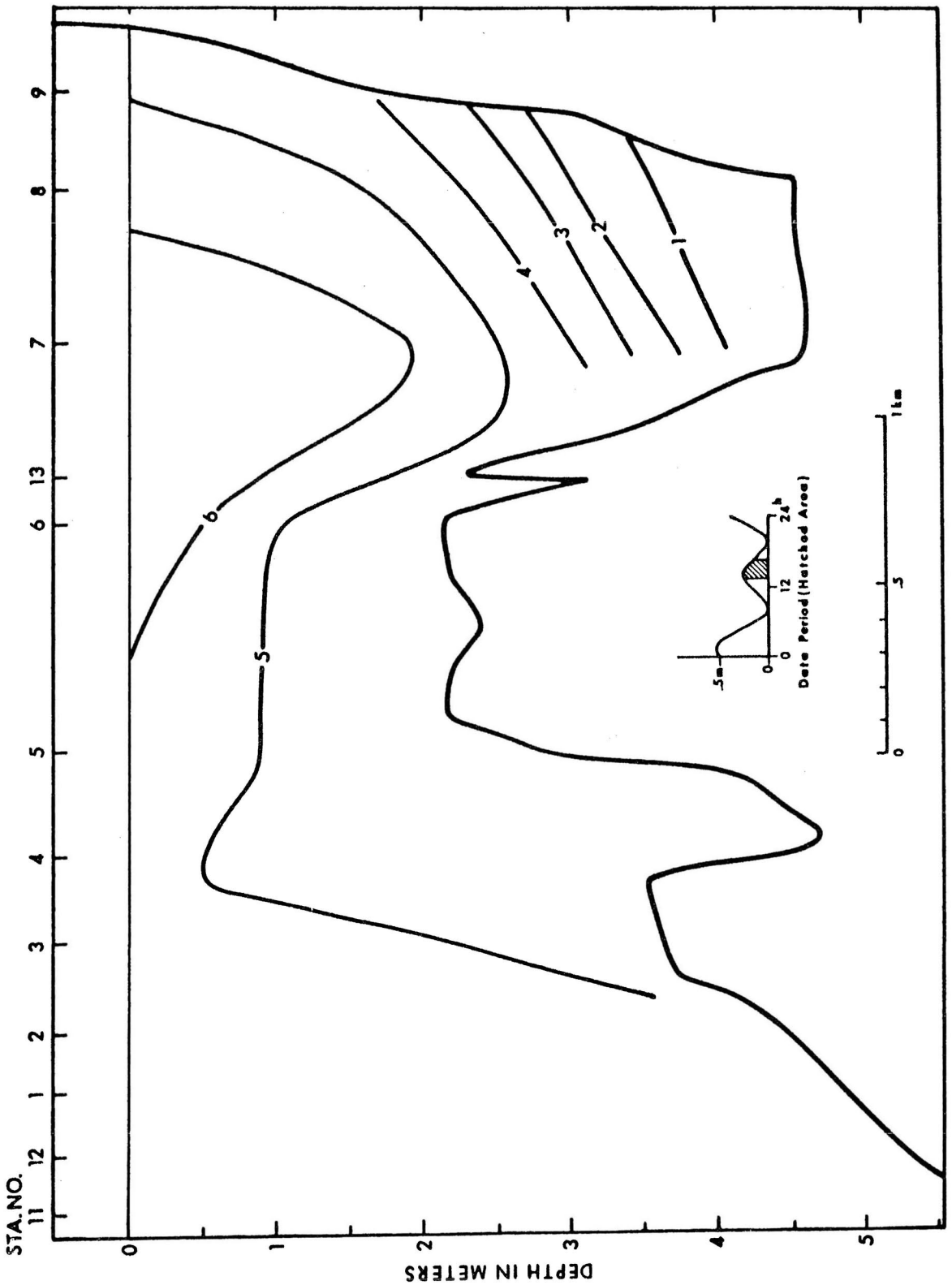
STA. NO.
11 12 1 2 3 4 5 6 13 7 8 9
DEPTH IN METERS
0 1 2 3 4 5
6
5
4
3
2
1
-.5m
0
12
24h
Data Period (Hatched Area)
0
.5
1km

Figure 24(a). Longitudinal section of salinity in $^{o}/oo$. April 1, 1969.

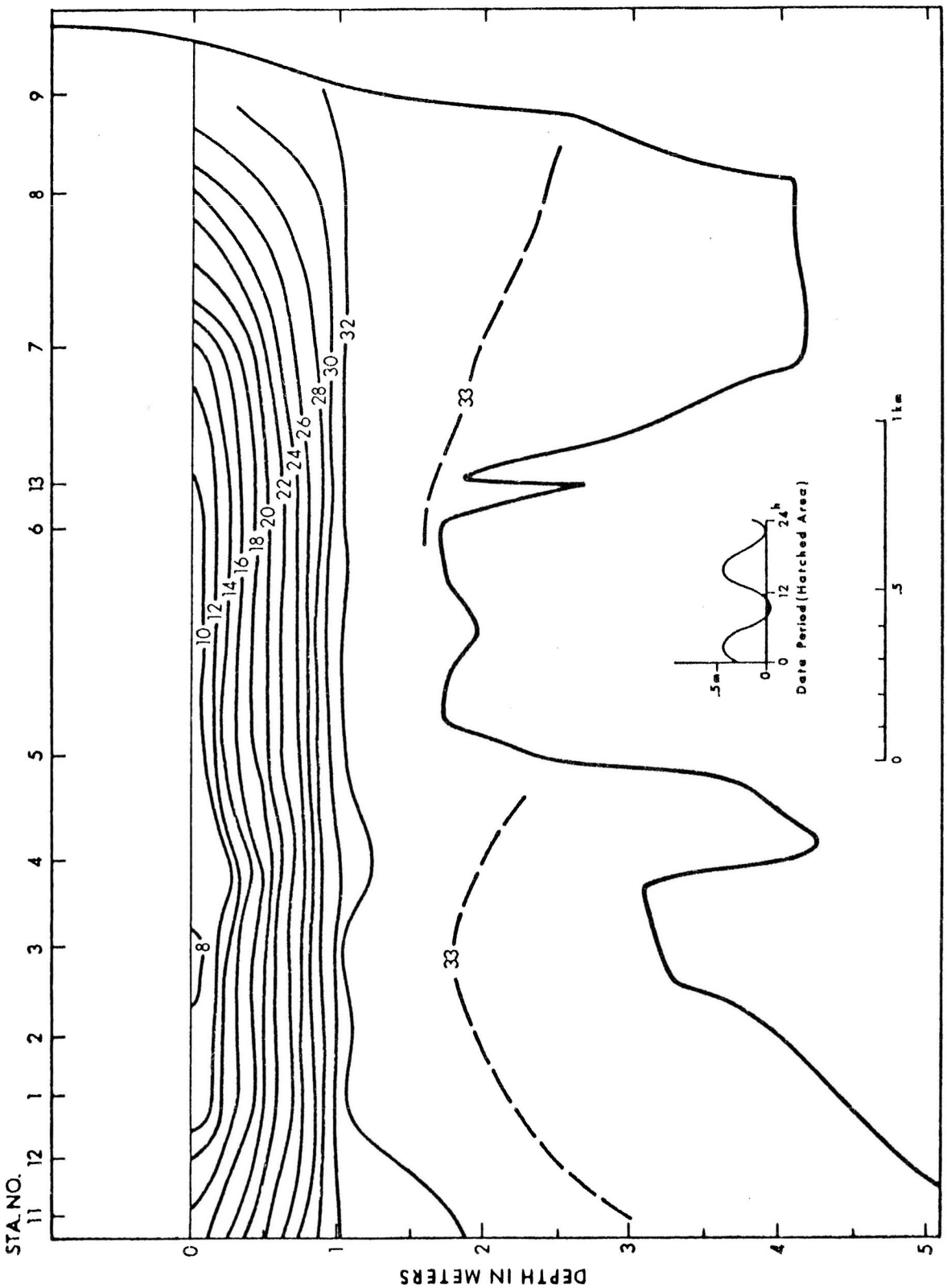
STA. NO.
11 12 1 2 3 4 5 6 13 7 8 9
DEPTH IN METERS
0 1 2 3 4 5
8 10 12 14 16 18 20 22 24 26 28 30 32
33
33
.5m
0 12 24h
Date Period (Hatched Area)
0 .5 1 km

Figure 24(b). Longitudinal section of temperature in °C. April 1, 1969.


STA. NO.
11 12 1 2 3 4 5 6 13 7 8 9
DEPTH IN METERS
0 1 2 3 4 5
26
25.5
25
24
23
22
.5m
0
12
24h
Data Period (Hatched Area)
0
.5
1 km

Figure 24(c). Longitudinal section of sigma-t in gm/cm^3. April 1, 1969.

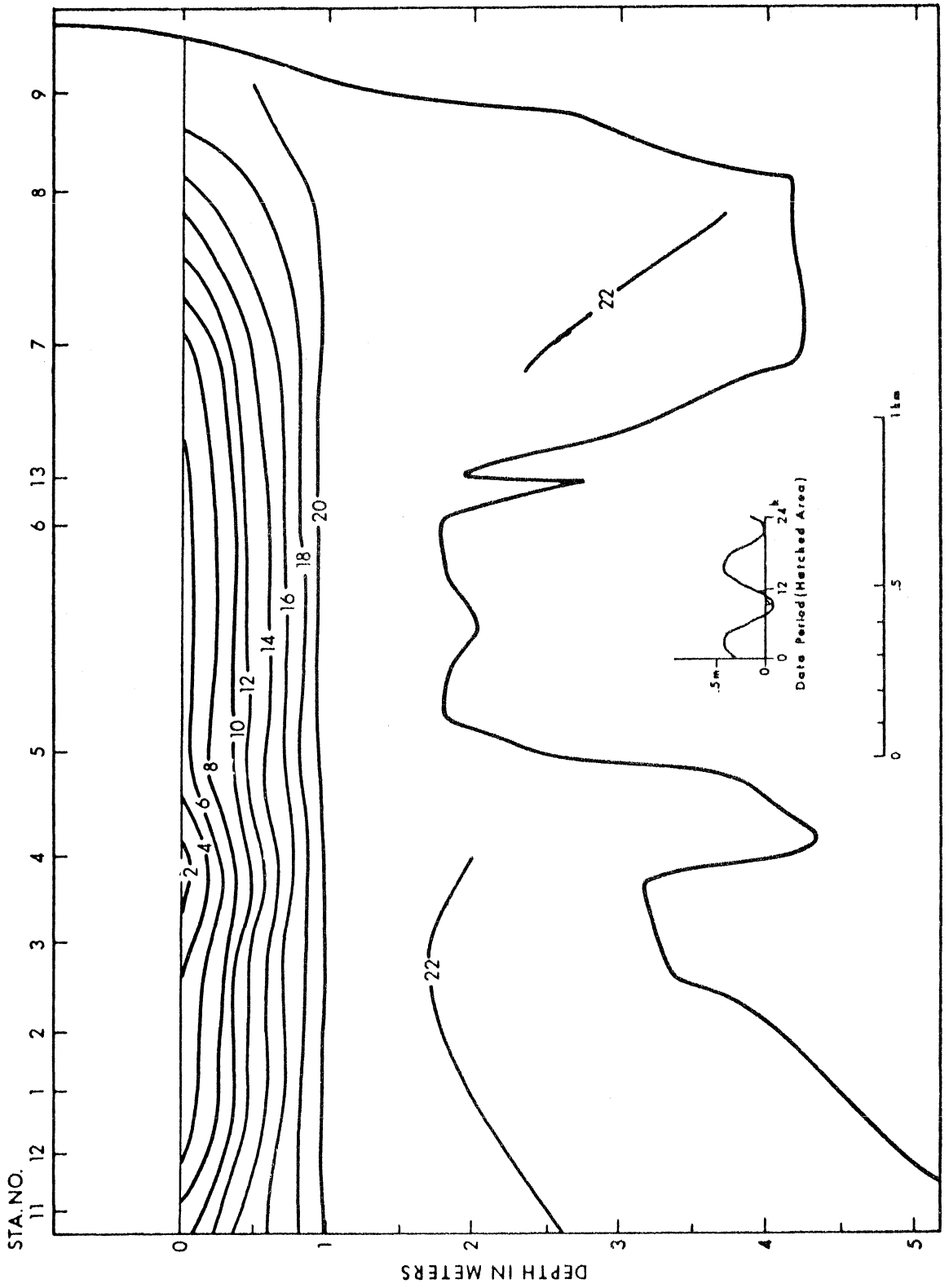
STA. NO.
11 12 1 2 3 4 5 6 13 7 8 9
DEPTH IN METERS
0 1 2 3 4 5
2 4 6 8 10 12 14 16 18 20
22
22
.5m
0
12
24h
Data Period (Hatched Area)
0 .5 1km

Figure 24(d). Longitudinal section of dissolved oxygen in ml/l. April 1, 1969.

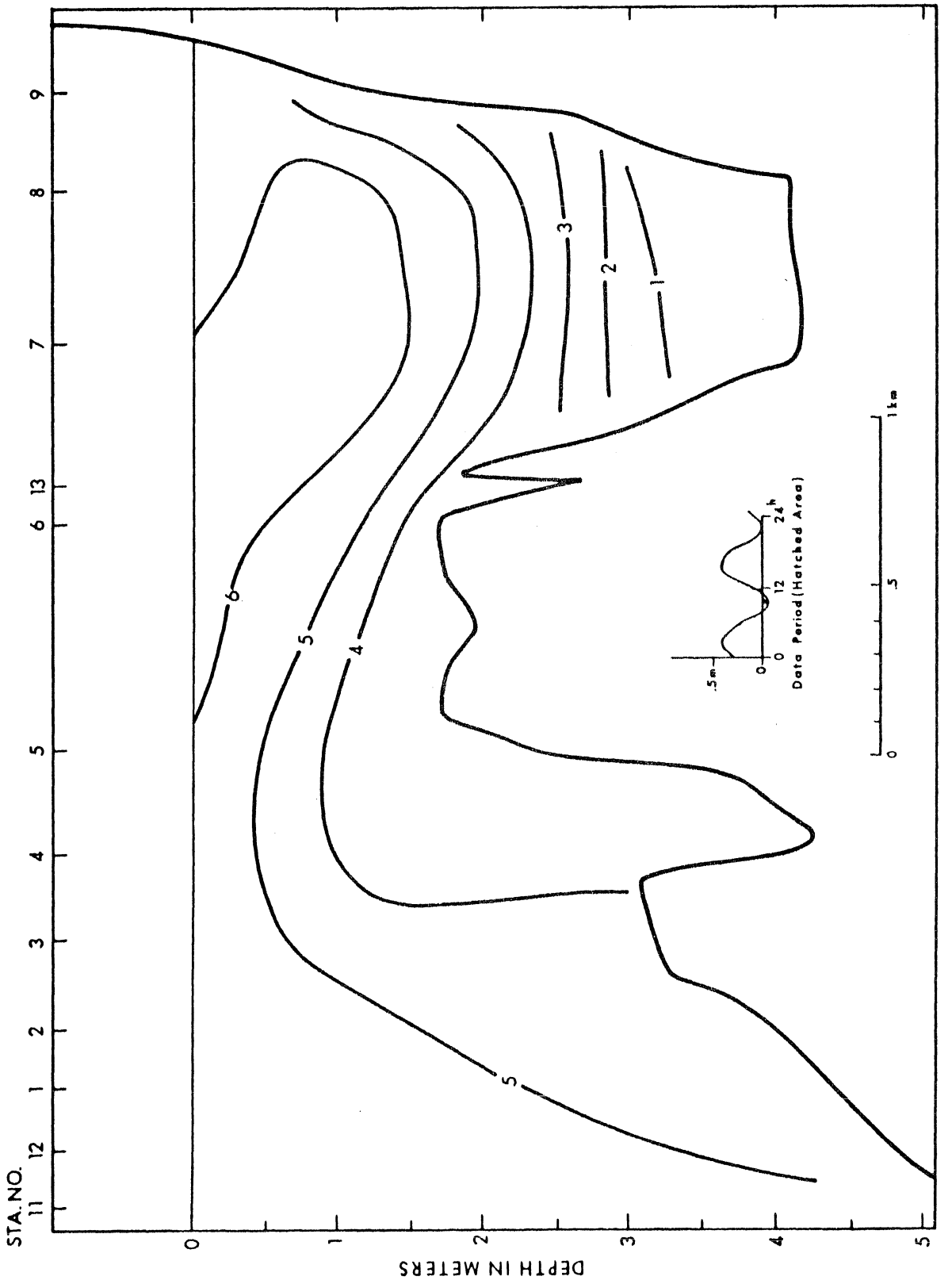
STA. NO.
11 12 1 2 3 4 5 6 13 7 8 9
DEPTH IN METERS
0 1 2 3 4 5
1
2
3
4
5
6
5
Data Period (Hatched Area)
-.5m
0
12
24h
0
.5
1km

Figure 25(a). Longitudinal section of salinity in $^{o}/oo$. May 9, 1969.

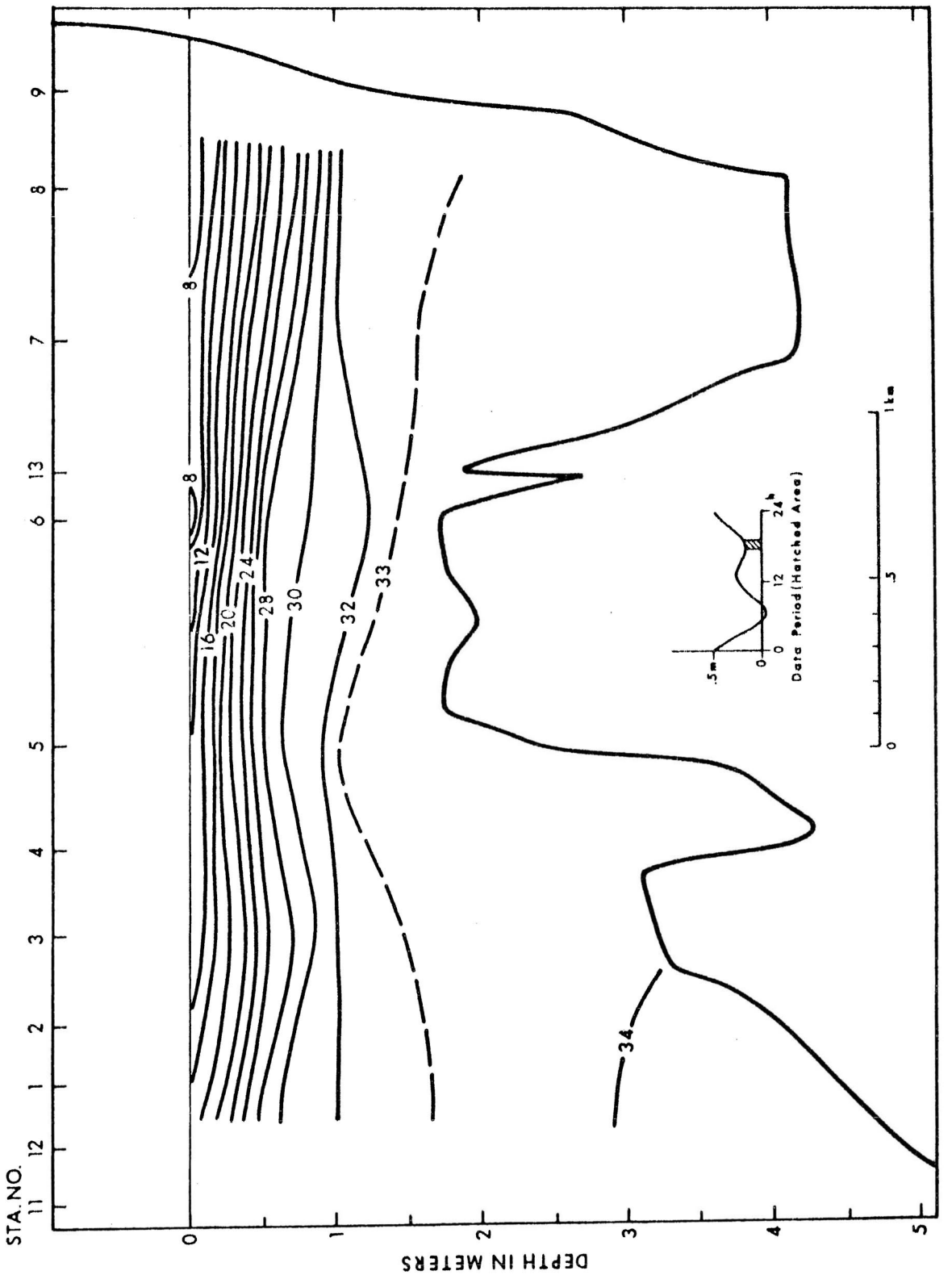
STA. NO.
11 12 1 2 3 4 5 6 13 8 9
DEPTH IN METERS
0 1 2 3 4 5
8
8
12
16
20
24
28
30
32
33
34
.5m
0
0
12
24h
Data Period (Hatched Area)
1 km
.5
0

Figure 25(b). Longitudinal section of temperature in °C. May 9, 1969.

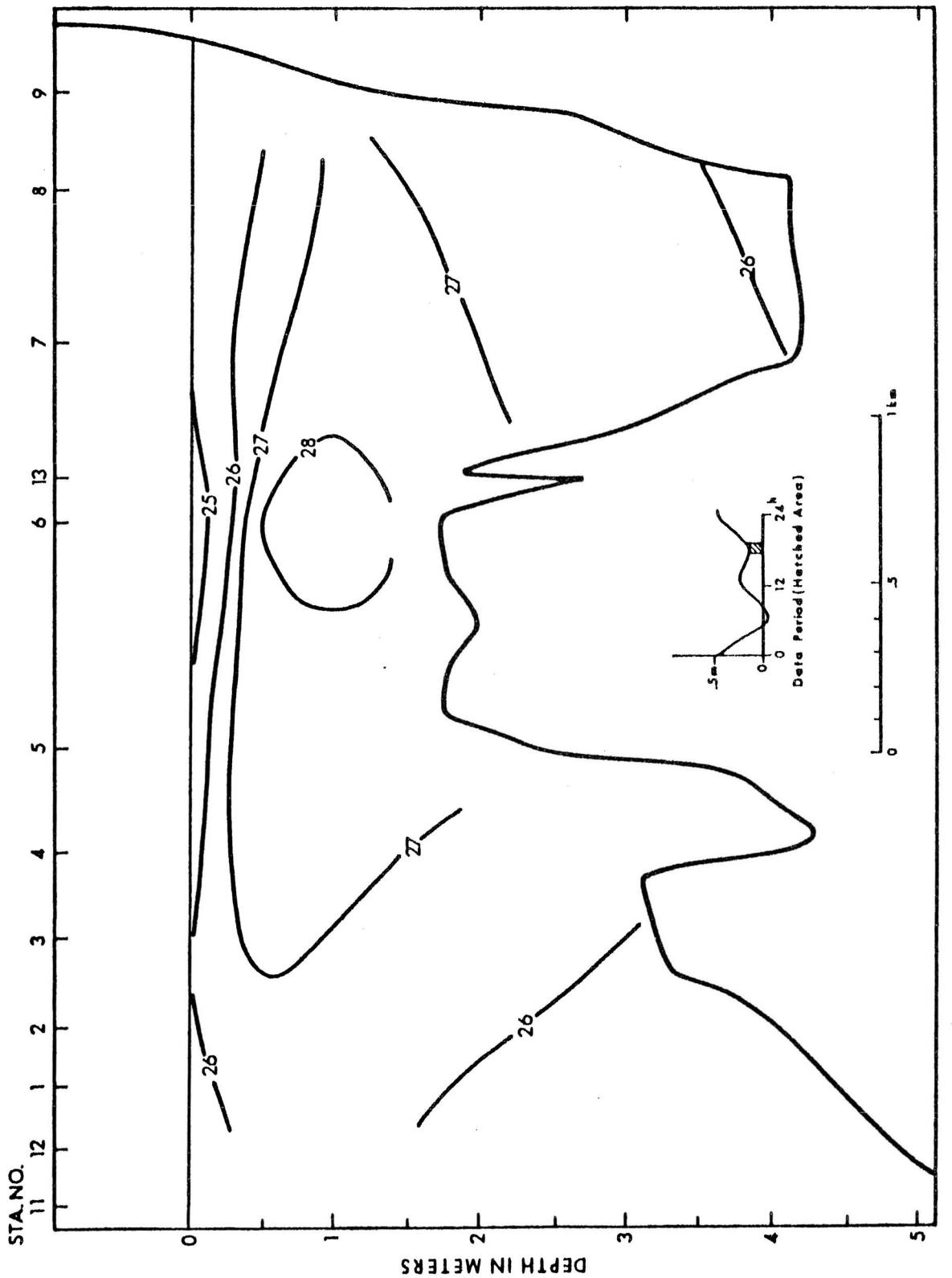
STA. NO.
11 12 1 2 3 4 5 6 13 7 8 9
DEPTH IN METERS
0 1 2 3 4 5
25
26
27
28
26
27
27
26
.5m
0
12
24h
Data Period (Hatched Area)
0
.5
1 km

Figure 25(c). Longitudinal section of sigma-t in gm/cm^3. May 9, 1969.

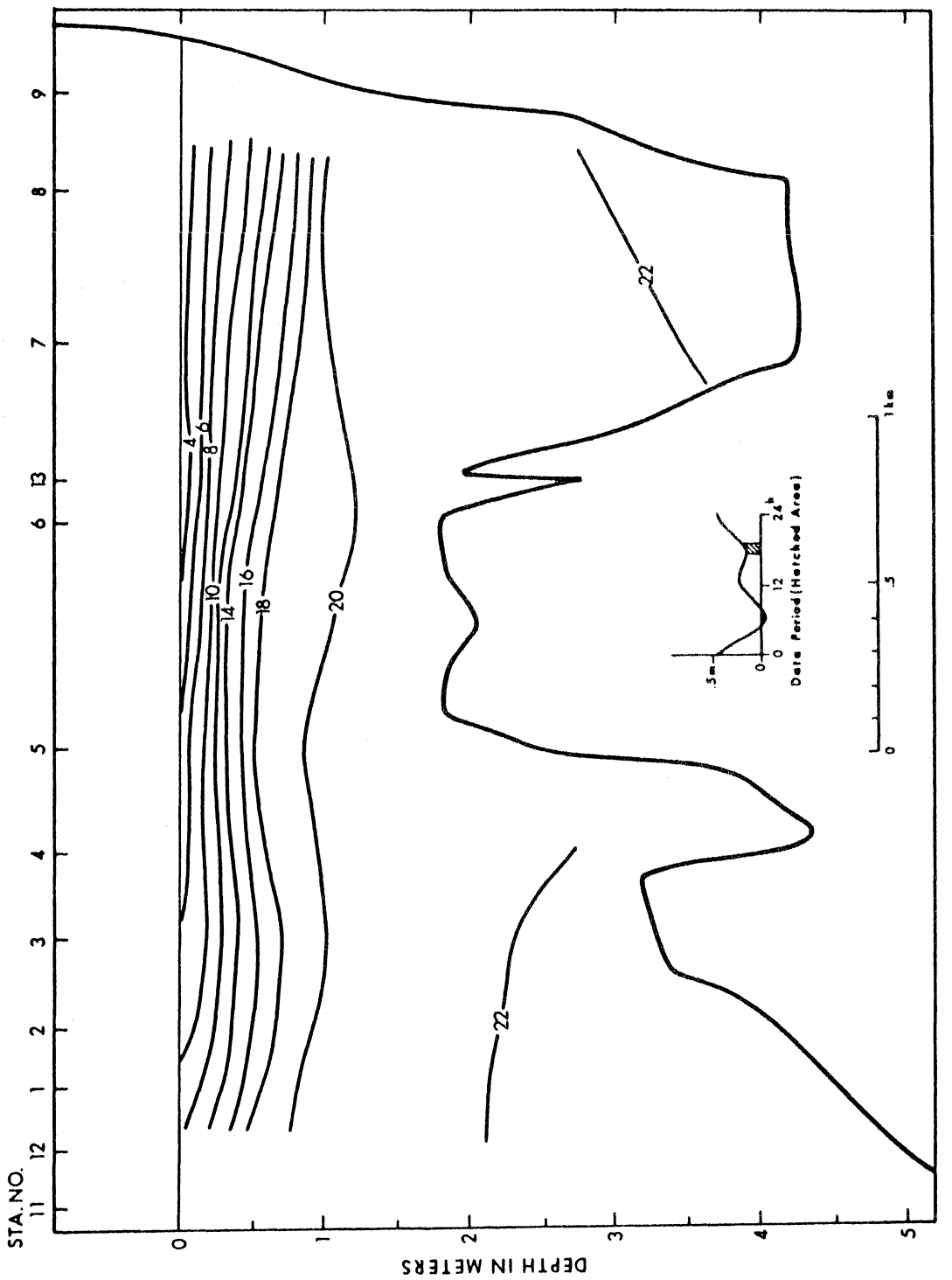
STA. NO.
11 12 1 2 3 4 5 6 13 7 8 9
DEPTH IN METERS
0 1 2 3 4 5
4
6
8
10
14
16
18
20
22
22
.5m
0
0
12
24h
Data Period (Hatched Area)
0
.5
1 Lo

Figure 26(a). Longitudinal section of salinity in $^{o}/oo$. June 10, 1969.

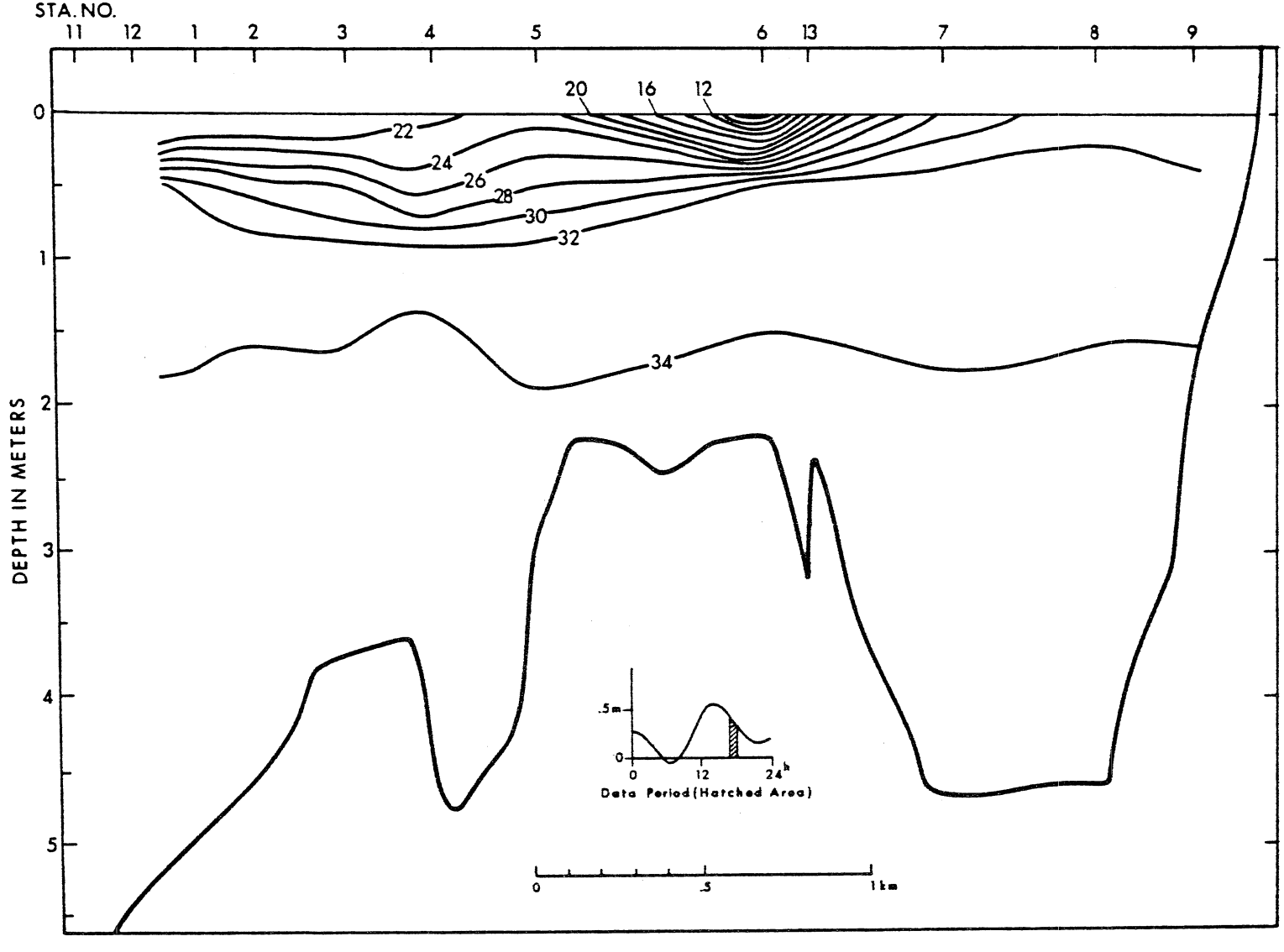
STA. NO.
11
12
1
2
3
4
5
6
13
7
8
9
20
16
12
22
24
26
28
30
32
34
DEPTH IN METERS
0
1
2
3
4
5
.5m
0
0
12
24h
Data Period (Hatched Area)
0
.5
1 km

Figure 26(b). Longitudinal section of temperature in °C. June 10, 1969.

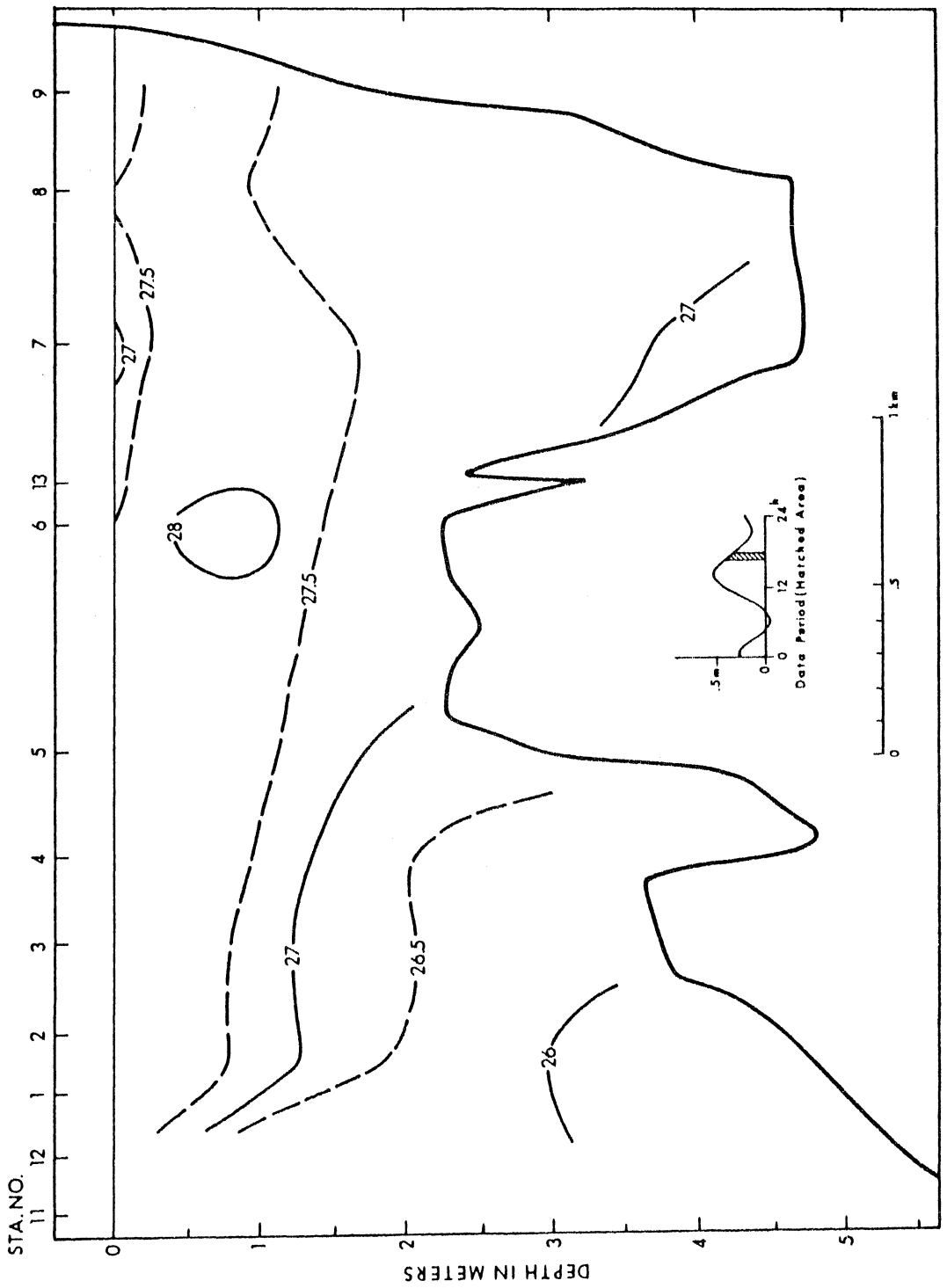
STA. NO.
11 12 1 2 3 4 5 6 13 7 8 9
DEPTH IN METERS
0 1 2 3 4 5
28
27.5
27
26.5
26
.5m
0
12
24h
Data Period (Hatched Area)
0 .5 1km

Figure 26(c). Longitudinal section of sigma-t in gm/cm^3. June 10, 1969.

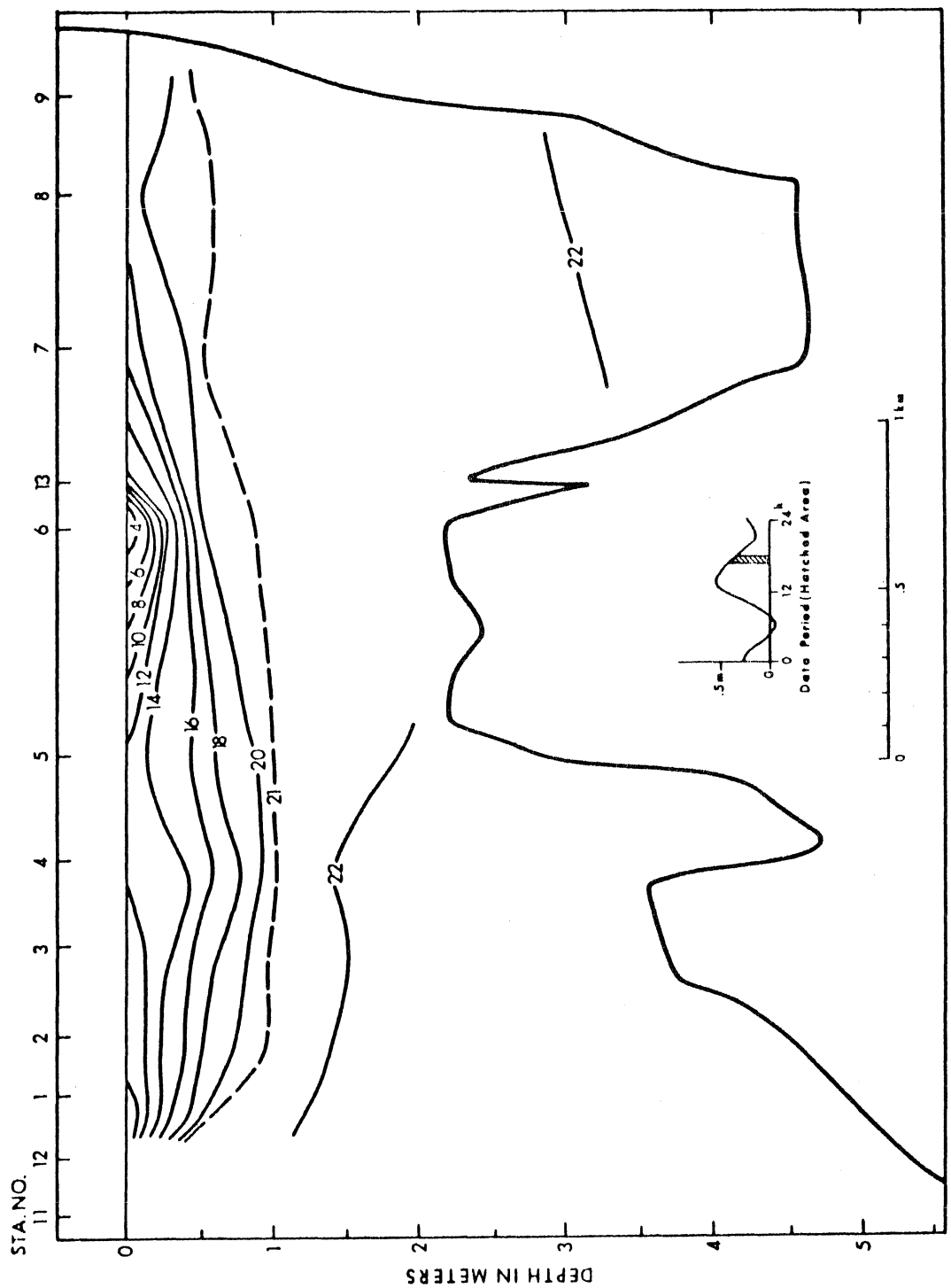
STA. NO.
11 12 1 2 3 4 5 6 13 7 8 9
DEPTH IN METERS
0 1 2 3 4 5
4
6
8
10
12
14
16
18
20
21
22
22
.5m
0
12
24h
Data Period (Hatched Area)
1 km
.5
0

Figure 27(a). Longitudinal section of salinity in $^{o}/oo$. June 25, 1969

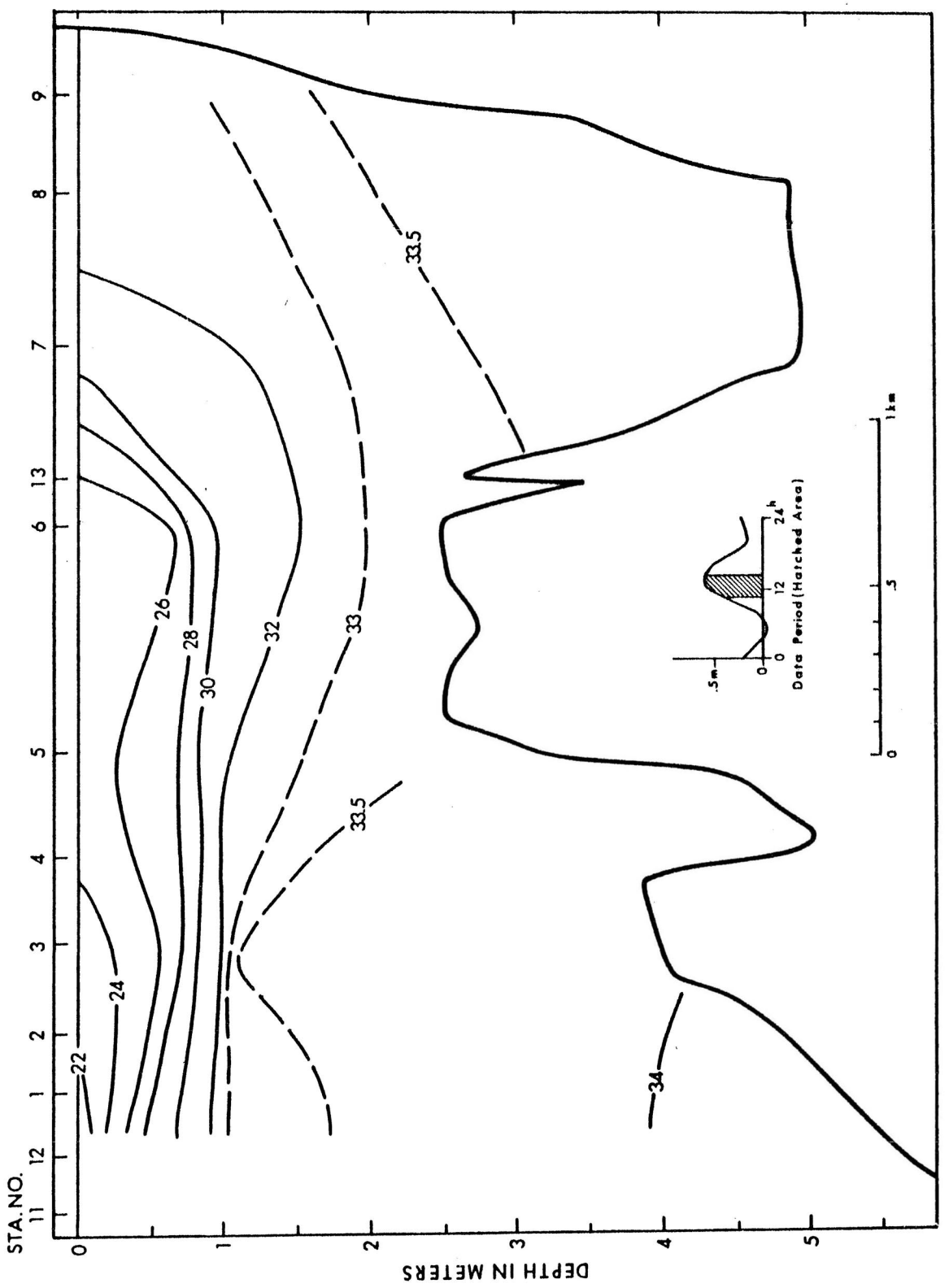
STA. NO.
11 12 1 2 3 4 5 6 13 7 8 9
DEPTH IN METERS
0 1 2 3 4 5
22
24
26
28
30
32
33
33.5
33.5
34
.5m
0
0
12
24h
Data Period (Hatched Area)
0
.5
1km

Figure 27(b). Longitudinal section of temperature in °C. June 25, 1969.

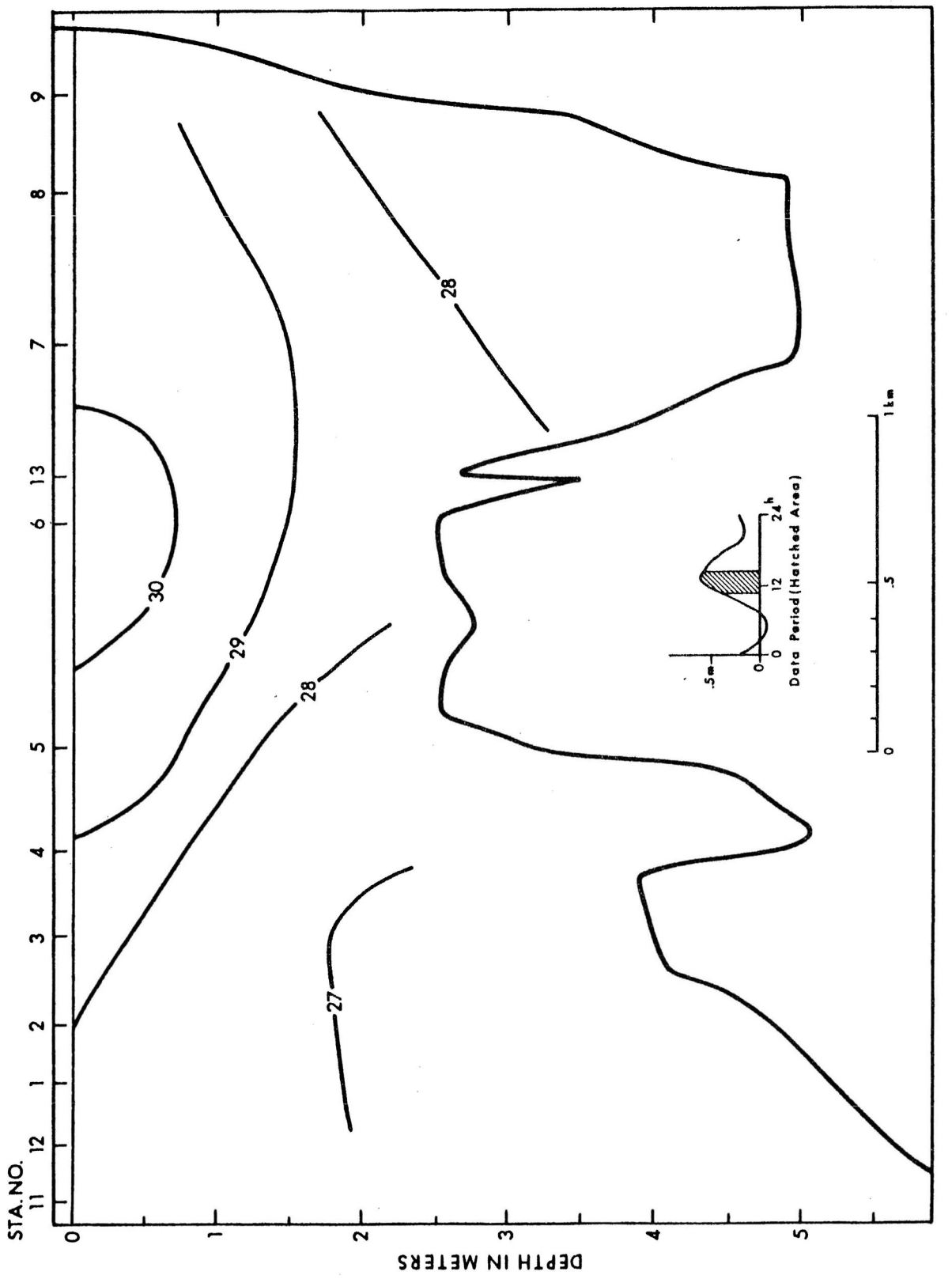
STA. NO.
11 12 1 2 3 4 5 6 13 7 8 9
DEPTH IN METERS
0 1 2 3 4 5
30
29
28
28
27
.5m
0
12
24h
Data Period (Hatched Area)
0
.5
1 km

Figure 27(c). Longitudinal section of sigma-t in gm/cm^3. June 25, 1969.

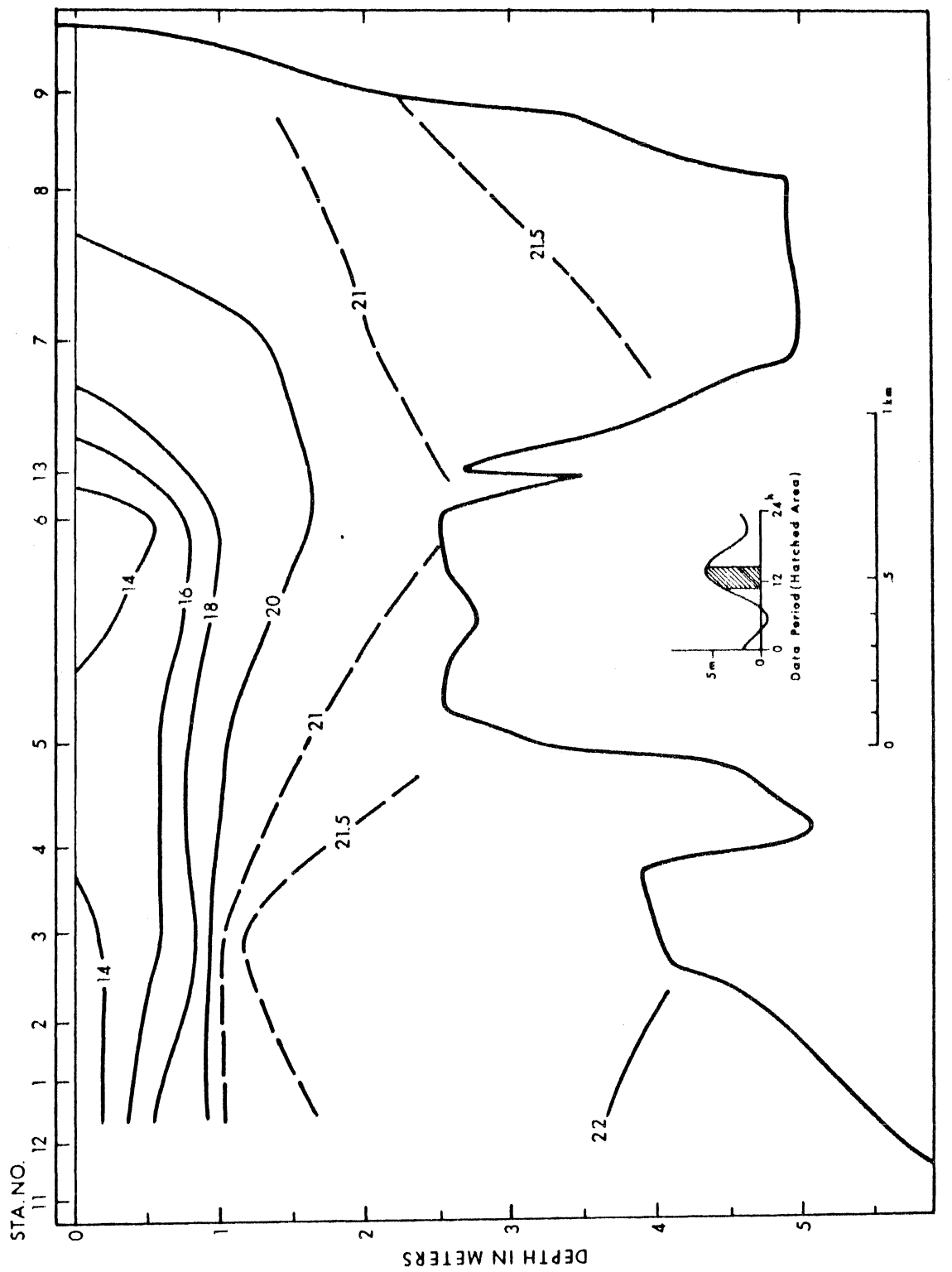
STA. NO.
11 12 1 2 3 4 5 6 13 7 8 9
DEPTH IN METERS
0 1 2 3 4 5
14
14
16
18
20
21
21.5
21
21.5
22
5m
0
12
24h
Data Period (Hatched Area)
0
.5
1km

Figure 28(a). Longitudinal section of salinity in $^{o}/oo$. July 12, 1969.

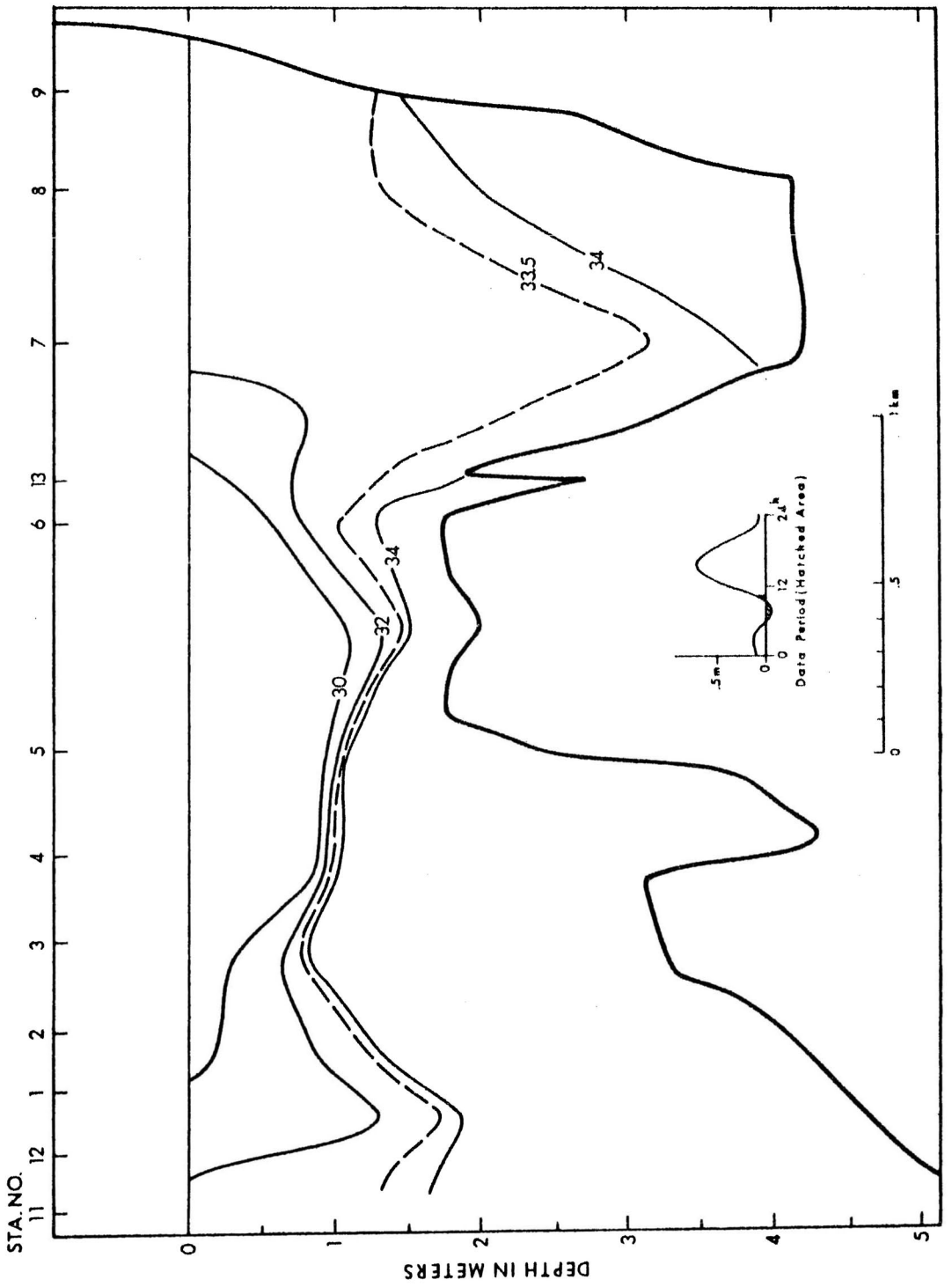
STA. NO.
11 12 1 2 3 4 5 6 13 7 8 9
DEPTH IN METERS
0 1 2 3 4 5
30
32
34
33.5
34
.5m
0
12
24h
Data Period (Hatched Area)
0
.5
1 km

Figure 28(b). Longitudinal section of temperature in °C. July 12, 1969.

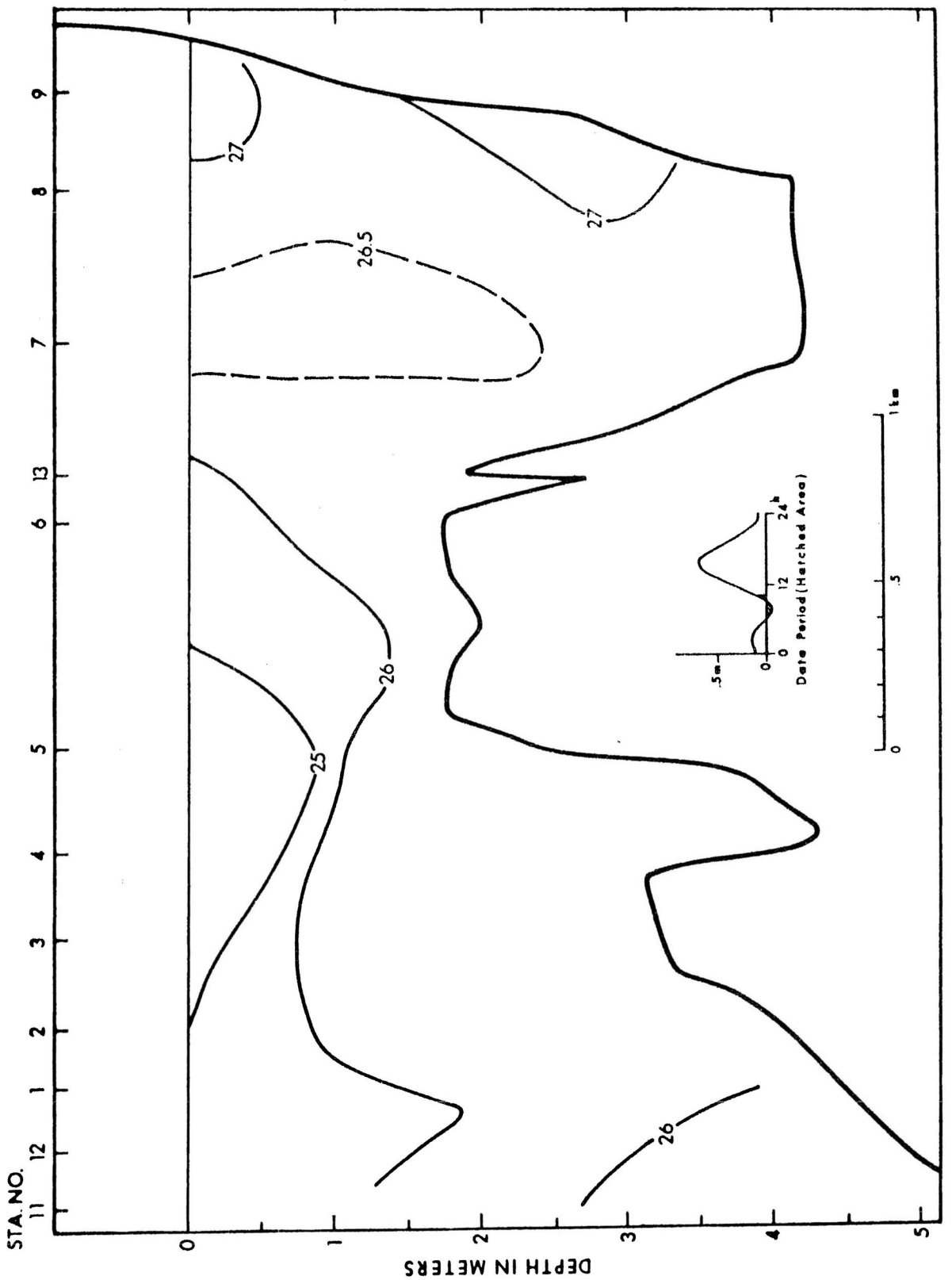
STA. NO.
11 12 1 2 3 4 5 6 13 7 8 9
DEPTH IN METERS
0 1 2 3 4 5
27
26.5
27
26
25
26
.5m
0 12 24h
Date Period (Hatched Area)
0 .5 1 km

Figure 28(c). Longitudinal section of sigma-t in gm/cm^3. July 12, 1969.

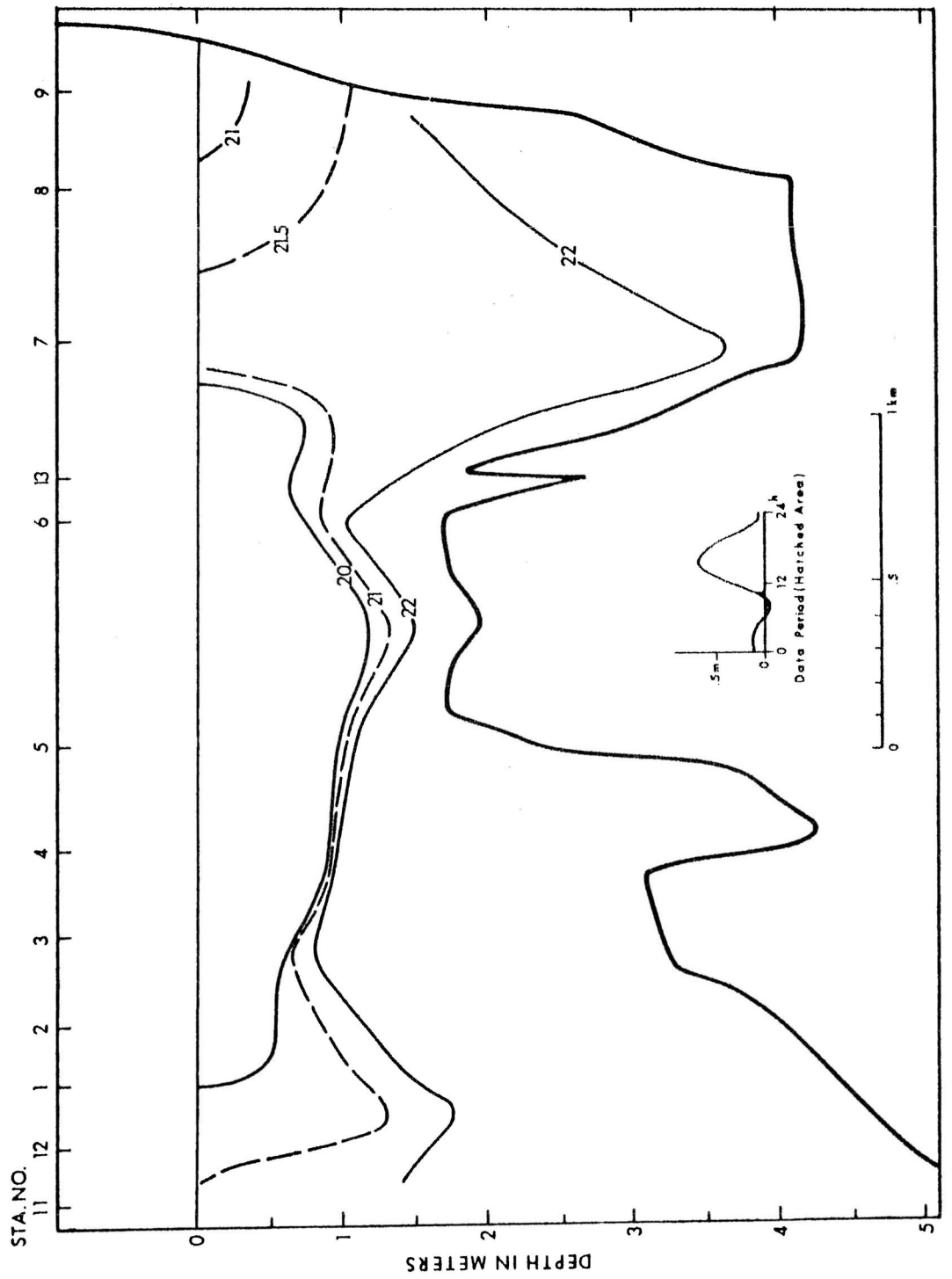
STA. NO.
11
12
1
2
3
4
5
6
13
7
8
9
DEPTH IN METERS
0
1
2
3
4
5
21
21.5
22
20
21
22
.5m
0
12
24h
Data Period (Hatched Area)
0
.5
1 km

Figure 28(d). Longitudinal section of dissolved oxygen in ml/l. July 12, 1969

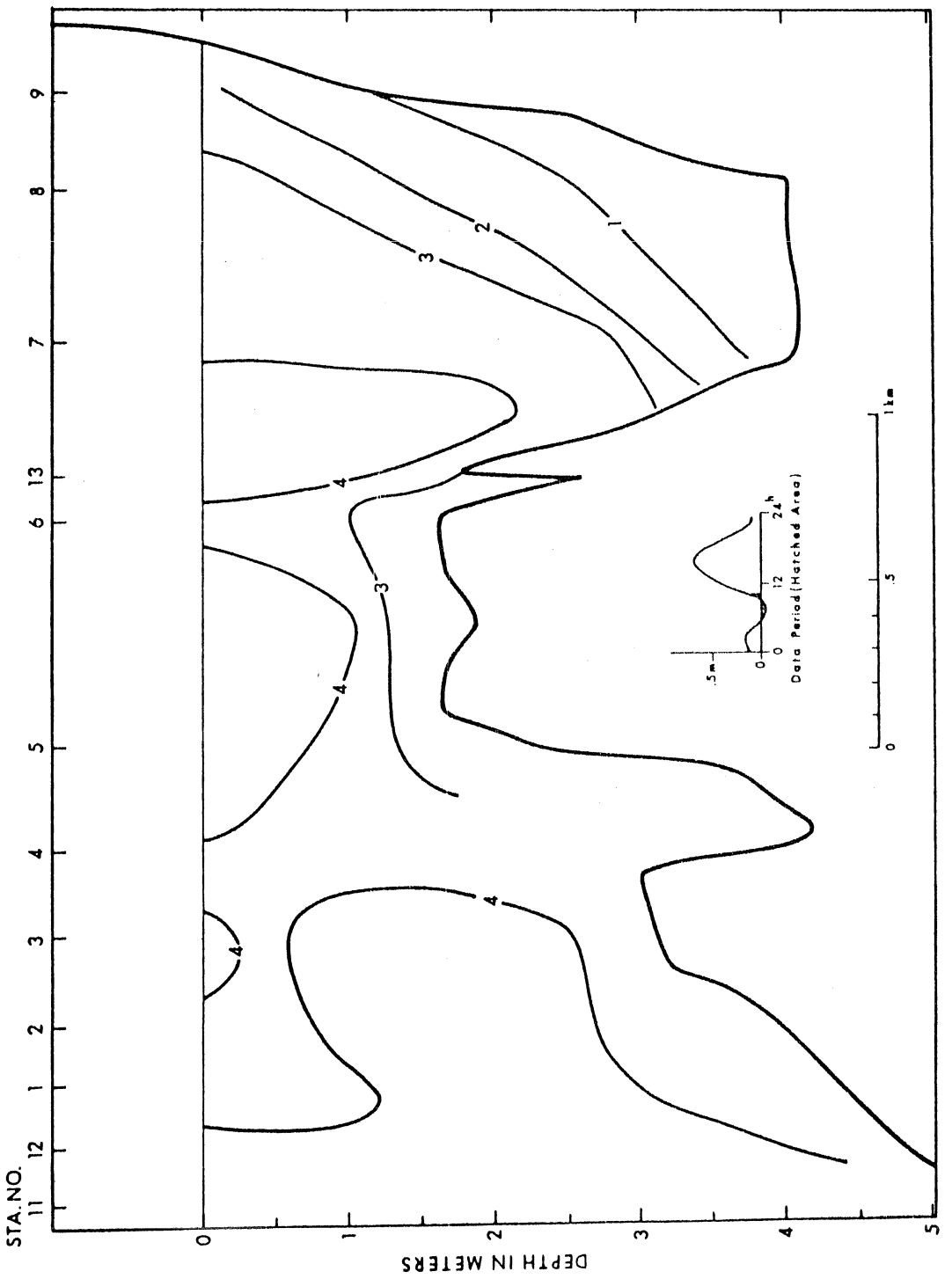
STA. NO.
11 12 1 2 3 4 5 6 13 7 8 9
DEPTH IN METERS
0 1 2 3 4 5
1
2
3
4
4
4
4
3
.5m
0
12
24 h
Data Period (Hatched Area)
0
.5
1 km

Figure 28(e). Longitudinal section of limits of the halocline. July 12, 1969. Vertical lines indicate uncertainty in individual determinations.

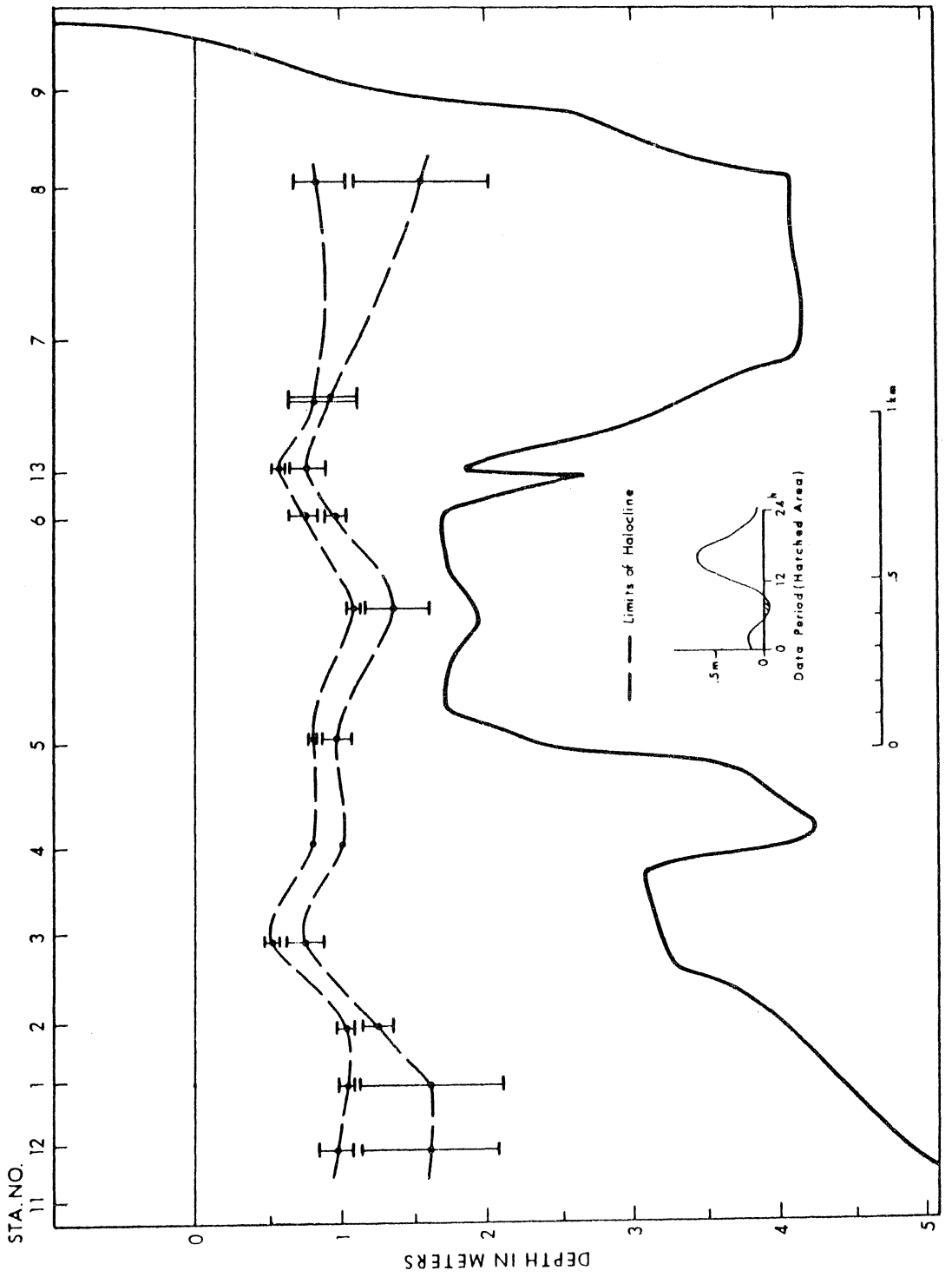
STA. NO.
11 12 1 2 3 4 5 6 13 7 8 9
DEPTH IN METERS
0 1 2 3 4 5
Limits of Halocline
.5m
0
12
24 h
Data Period (Hatched Area)
1 km
.5
0

Figure 29(a). Longitudinal section of salinity in °/oo. July 12, 1969.

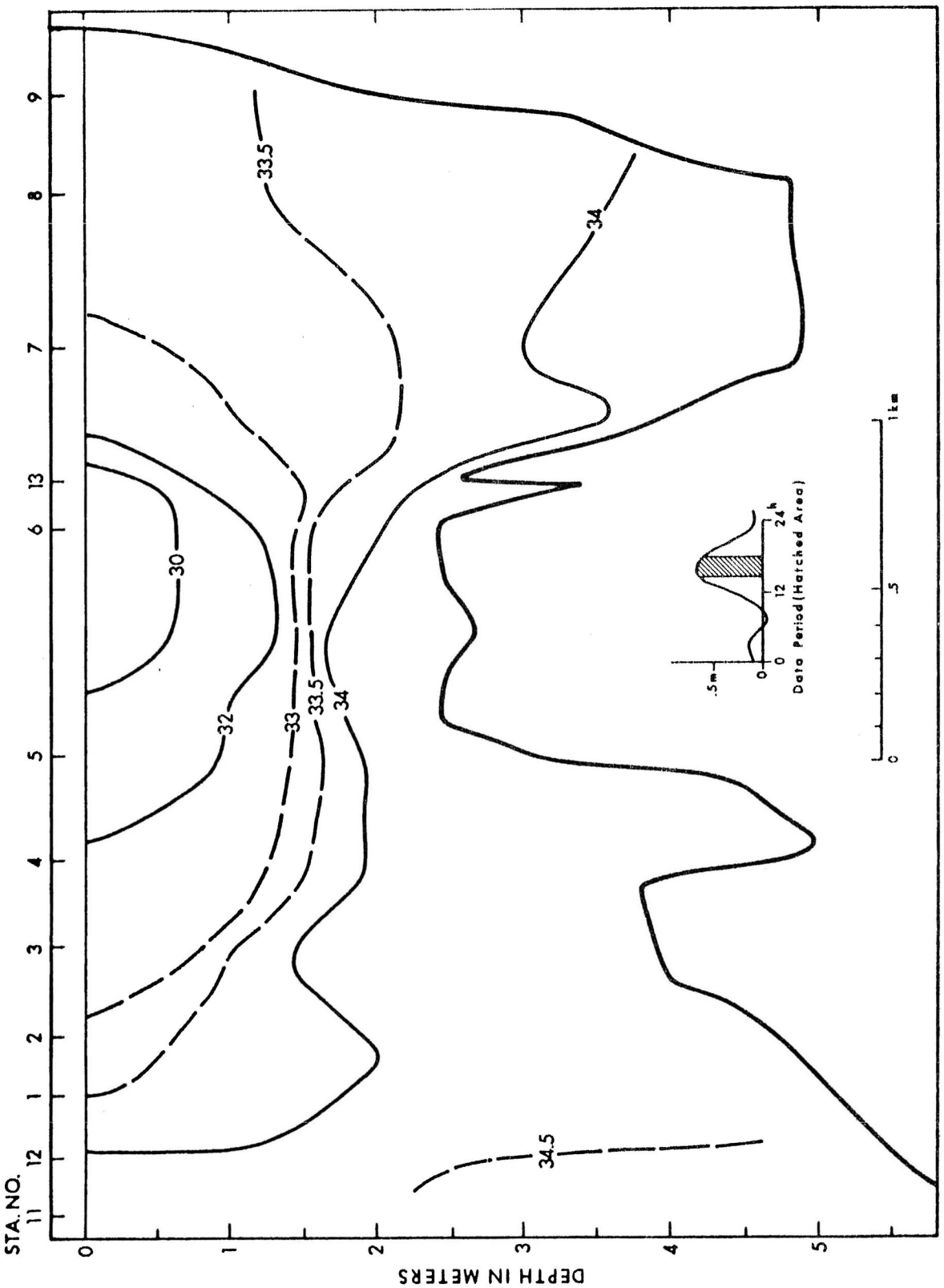
STA. NO.
11 12 1 2 3 4 5 6 13 7 8 9
DEPTH IN METERS
0 1 2 3 4 5
30
32
33
33.5
34
34.5
33.5
34
.5m
0
12
24 h
Data Period (Hatched Area)
0
.5
1 km

Figure 29(b). Longitudinal section of temperature in °C. July 12, 1969.

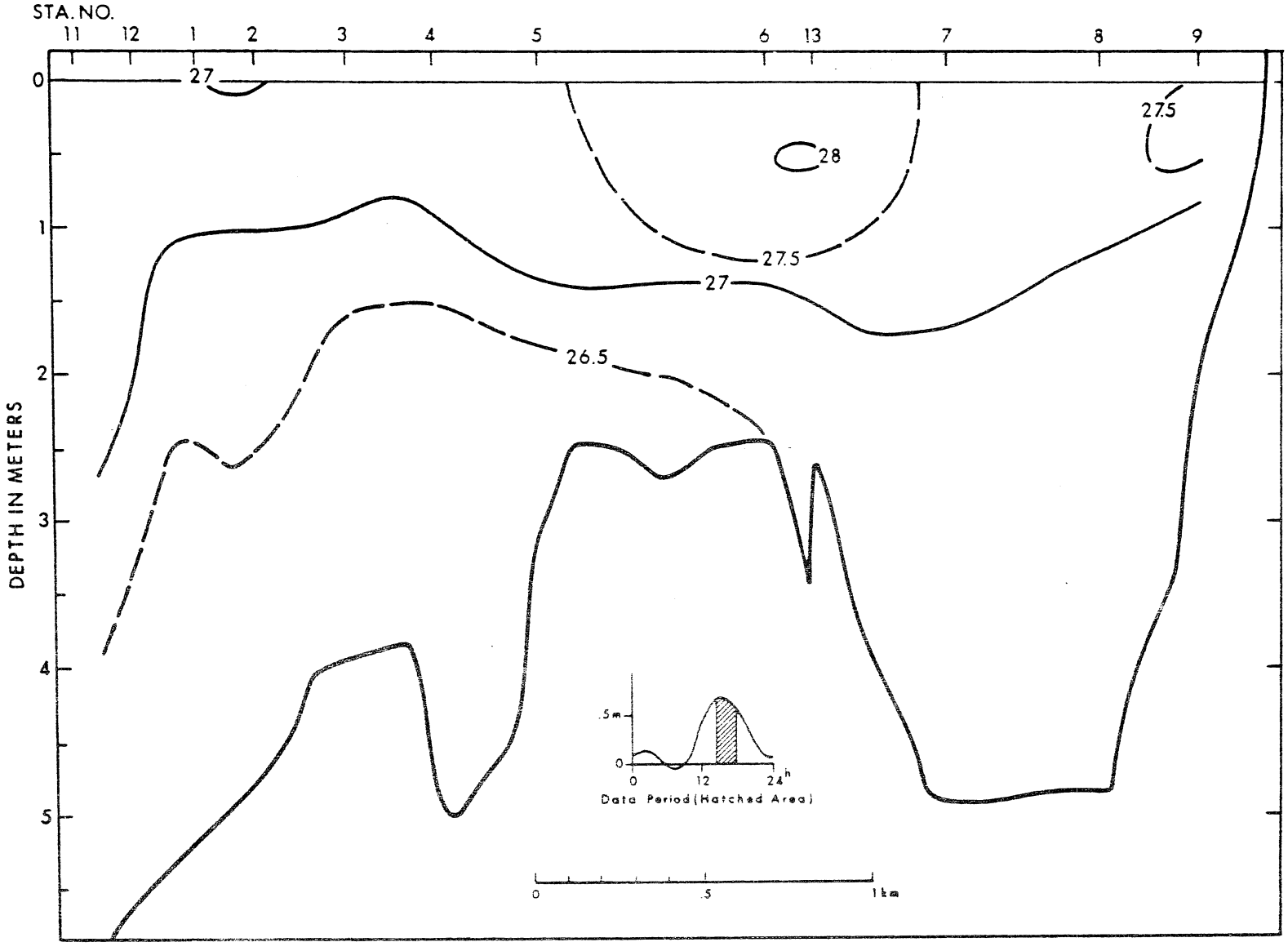
STA. NO.
11
12
1
2
3
4
5
6
13
7
8
9
0
1
2
3
4
5
DEPTH IN METERS
27
28
27.5
27.5
27
26.5
.5m
0
0
12
24h
Data Period (Hatched Area)
0
.5
1km

Figure 29(c). Longitudinal section of sigma-t in gm/cm^3. July 12, 1969.

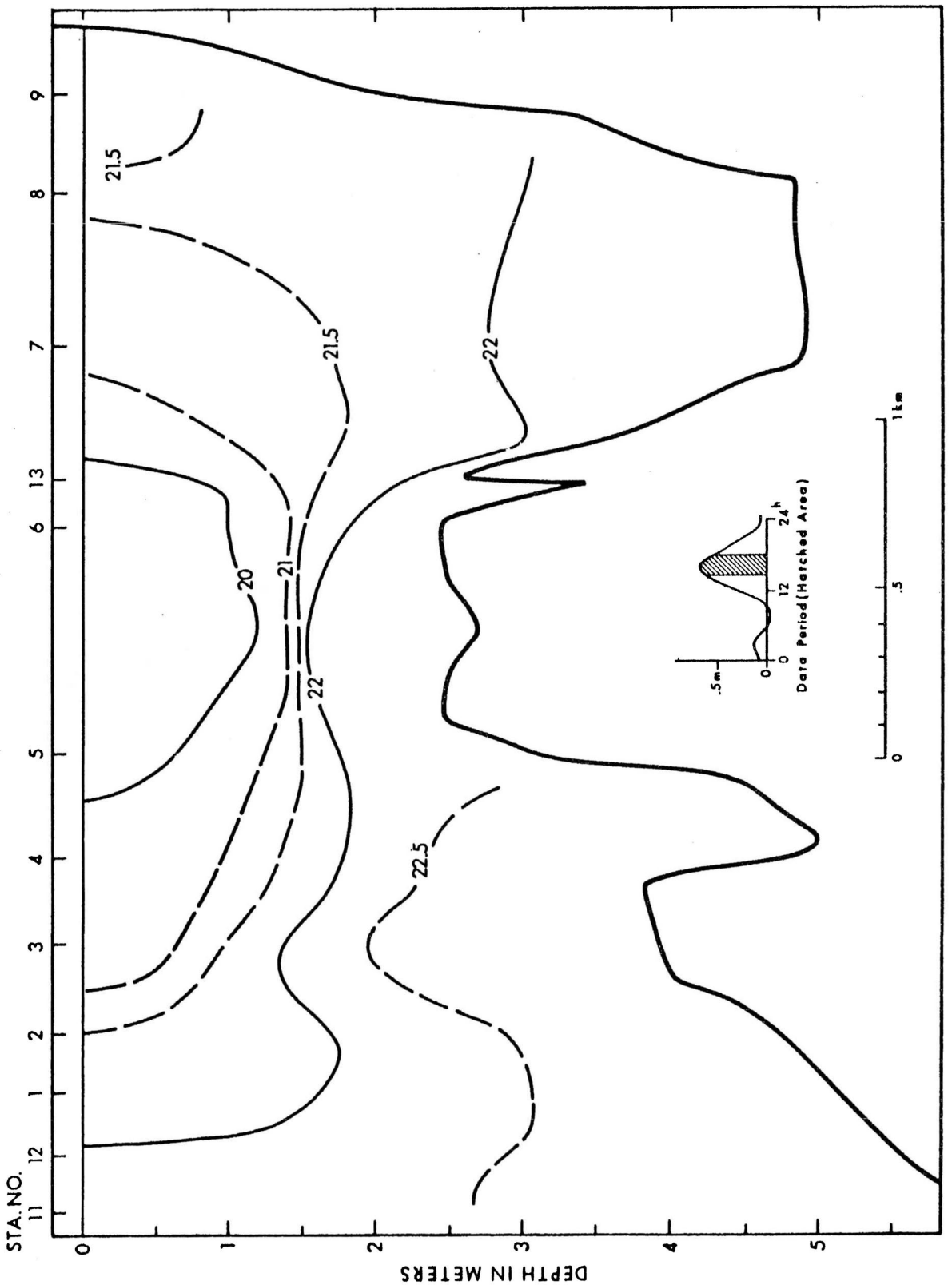
STA. NO.
11 12 1 2 3 4 5 6 13 7 8 9
DEPTH IN METERS
0 1 2 3 4 5
21.5
21.5
22
20
21
22
22.5
.5m
0
0
12
24 h
Data Period (Hatched Area)
0
.5
1 km

Figure 29(d). Longitudinal section of dissolved oxygen in ml/l. July 12, 1969.


STA. NO.
11 12 1 2 3 4 5 6 13 7 8 9
DEPTH IN METERS
0 1 2 3 4 5
1
2
3
4
5
6
6
5
5
.5m
0
12
24h
Data Period (Hatched Area)
0
.5
1kn

Figure 29(e). Longitudinal section of limits of the halocline. July 12, 1969. Vertical lines indicate uncertainty in individual determinations.

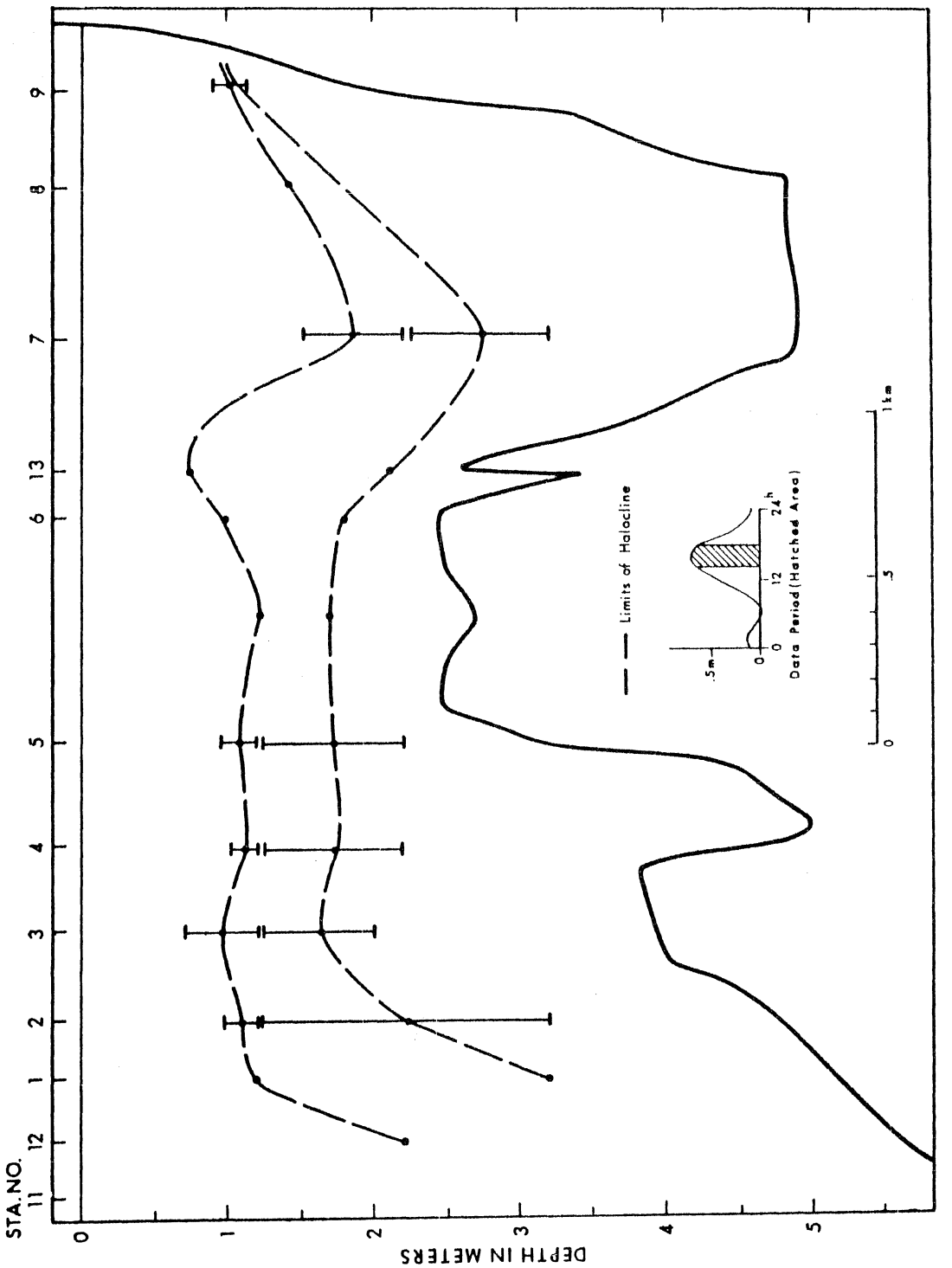
STA. NO.
11 12 1 2 3 4 5 6 13 7 8 9
DEPTH IN METERS
0 1 2 3 4 5
Limits of Halocline
.5m
0
12
24h
Data Period (Hatched Area)
0
.5
1 km

Figure 30(a). Longitudinal section of salinity in $^{o}/oo$. October 20, 1969.

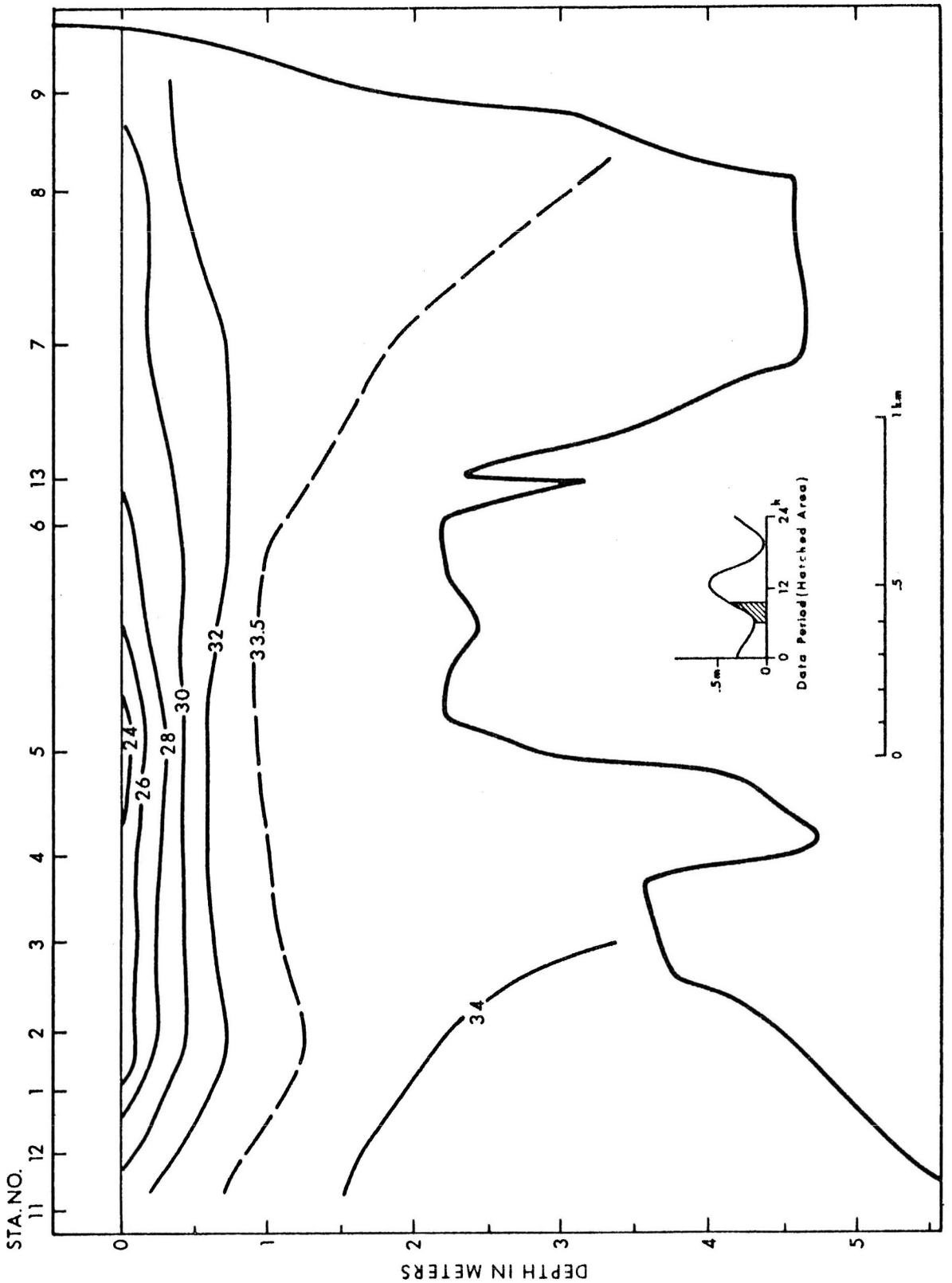
STA. NO.
11 12 1 2 3 4 5 6 13 7 8 9
DEPTH IN METERS
0 1 2 3 4 5
24
26
28
30
32
33.5
34
.5m
0
12
24h
Data Period (Hatched Area)
0
.5
1 km

Figure 30(b). Longitudinal section of temperature in °C. October 20, 1969.

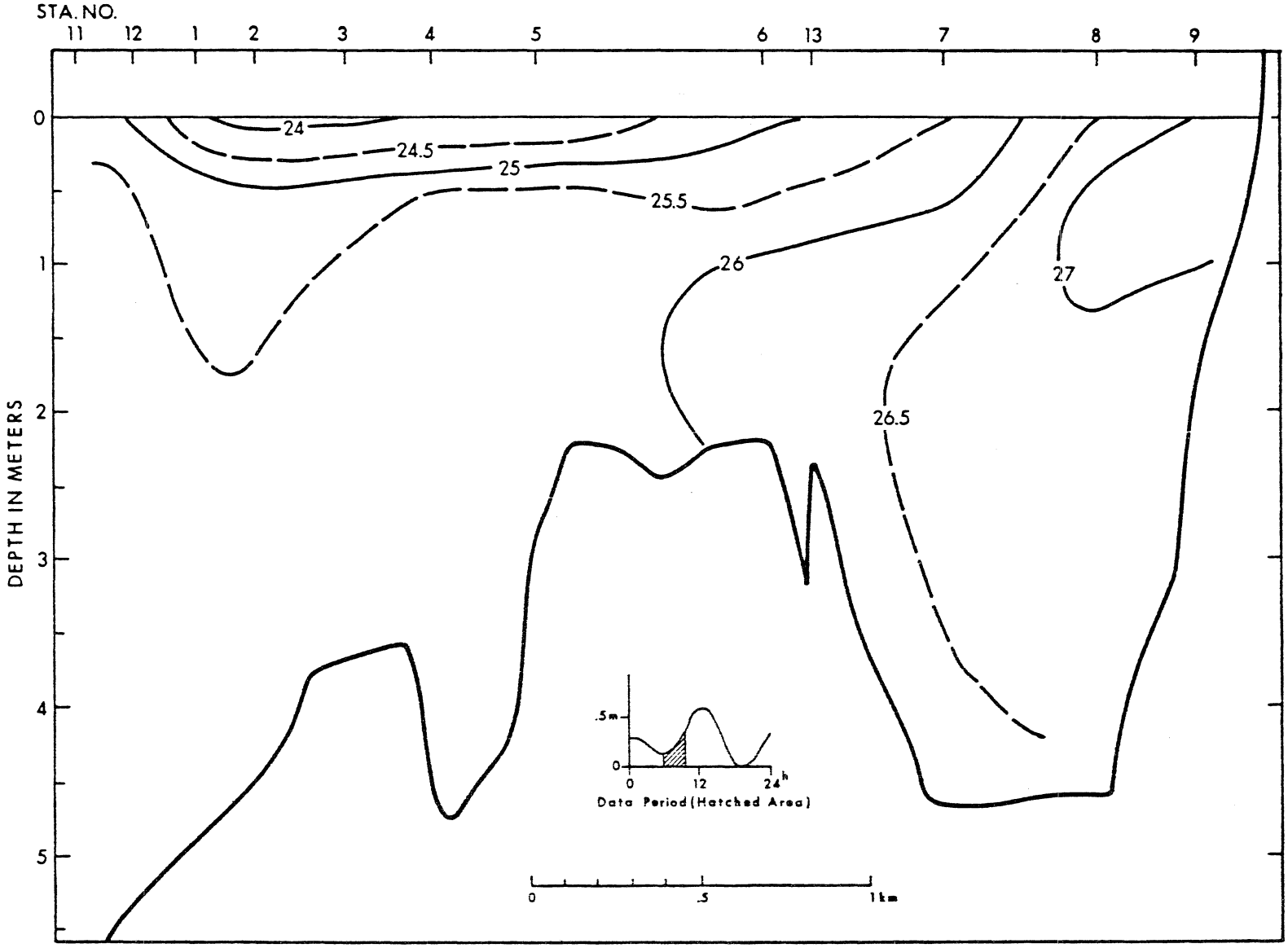
STA. NO.
11
12
1
2
3
4
5
6
13
7
8
9
0
1
2
3
4
5
DEPTH IN METERS
24
24.5
25
25.5
26
26.5
27
.5m
0
0
12
24h
Data Period (Hatched Area)
0
.5
1km

Figure 30(c). Longitudinal section of sigma-t in gm/cm^3. October 20, 1969.

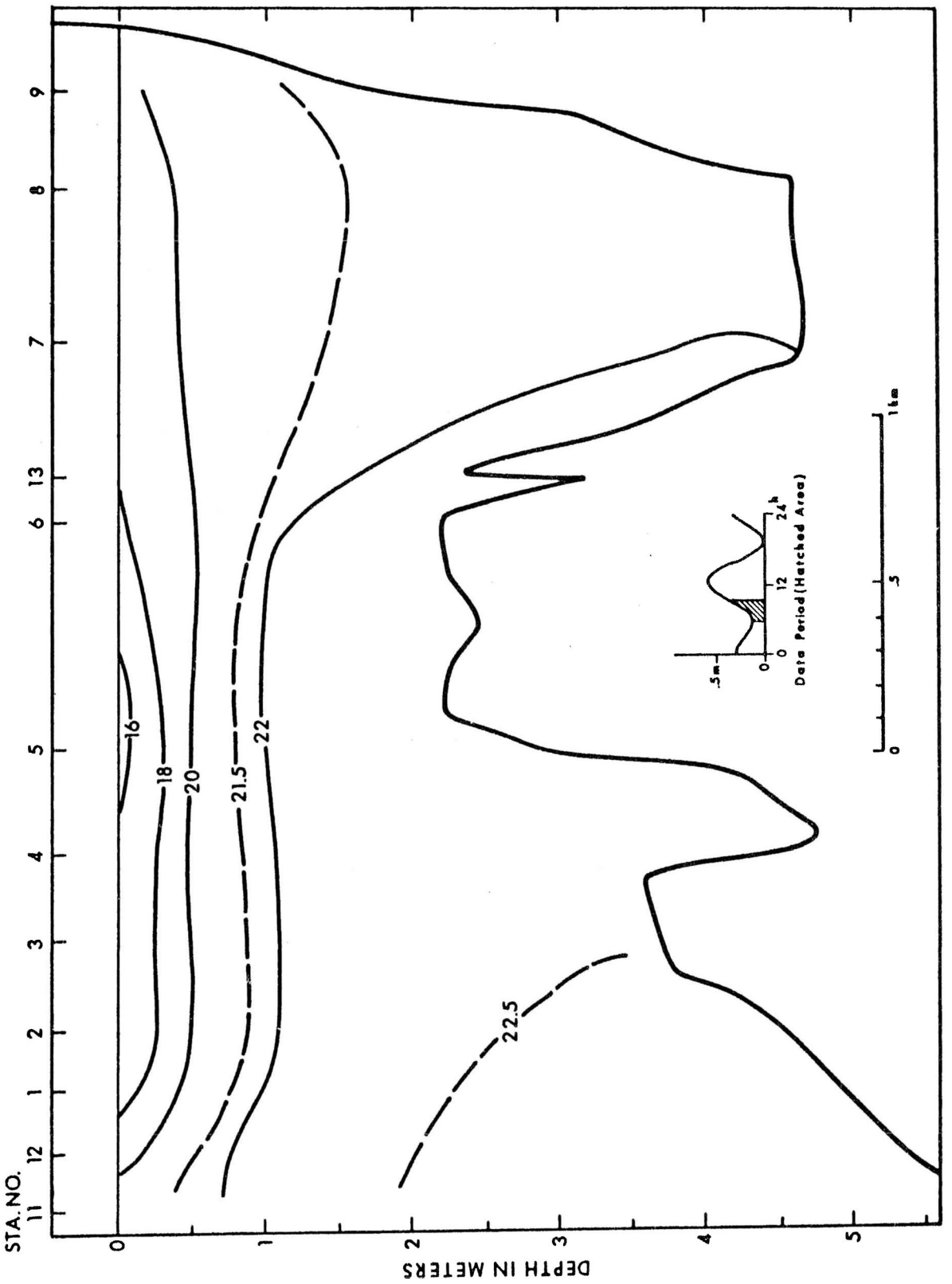
STA. NO.
11 12 1 2 3 4 5 6 13 7 8 9
DEPTH IN METERS
0 1 2 3 4 5
16
18
20
21.5
22
22.5
-5m
0
12
24 h
Data Period (Hatched Area)
0
.5
1 km

Figure 30(d). Longitudinal section of dissolved oxygen in ml/l. October 20, 1969.

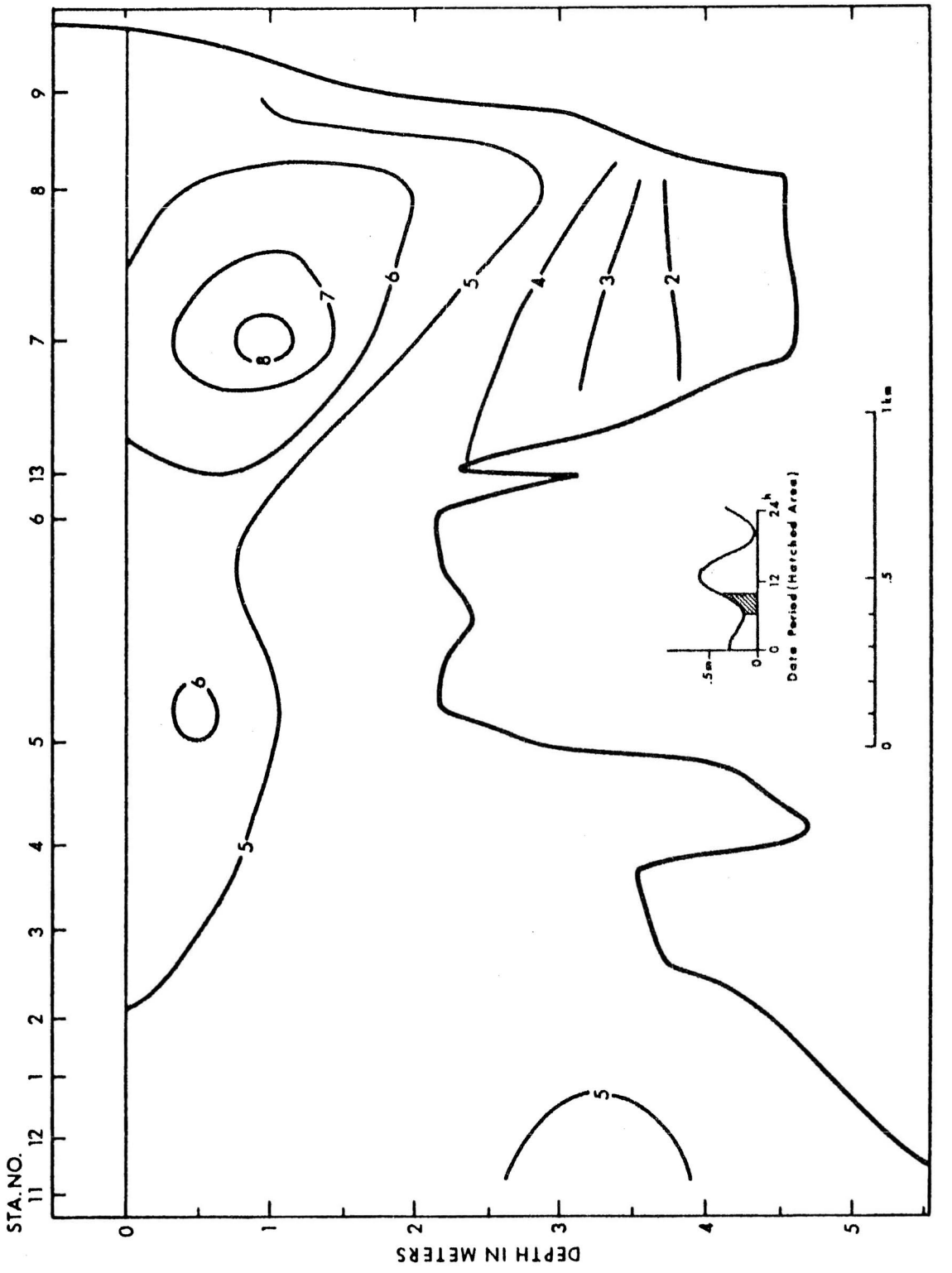
STA. NO.
11 12 1 2 3 4 5 6 13 7 8 9
DEPTH IN METERS
0 1 2 3 4 5
C6
8
7
6
5
4
3
2
5
5
.5m
0
0
12
24h
Data Period (Hatched Area)
0
.5
1m

Figure 30(e). Longitudinal section of phosphate in µg-at/l. October 20, 1969.

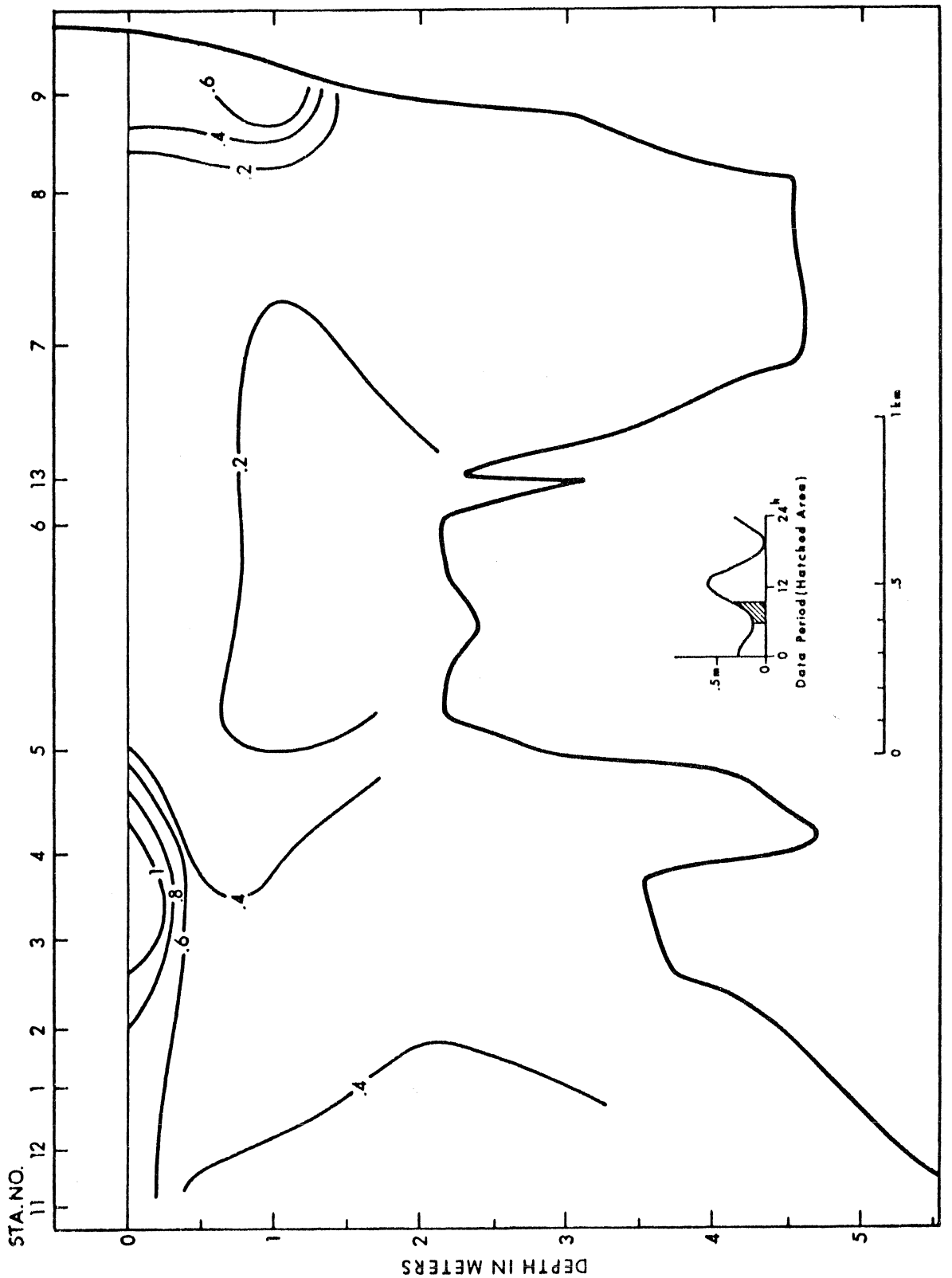
STA. NO.
11 12 1 2 3 4 5 6 13 7 8 9
DEPTH IN METERS
0 1 2 3 4 5
.6
.4
.2
.2
.4
1
.8
.6
.4
.5m
0
0
12
24h
Data Period (Hatched Area)
0
.5
1km

Figure 30(f). Longitudinal section of nitrate in µg-at/l. October 20, 1969.

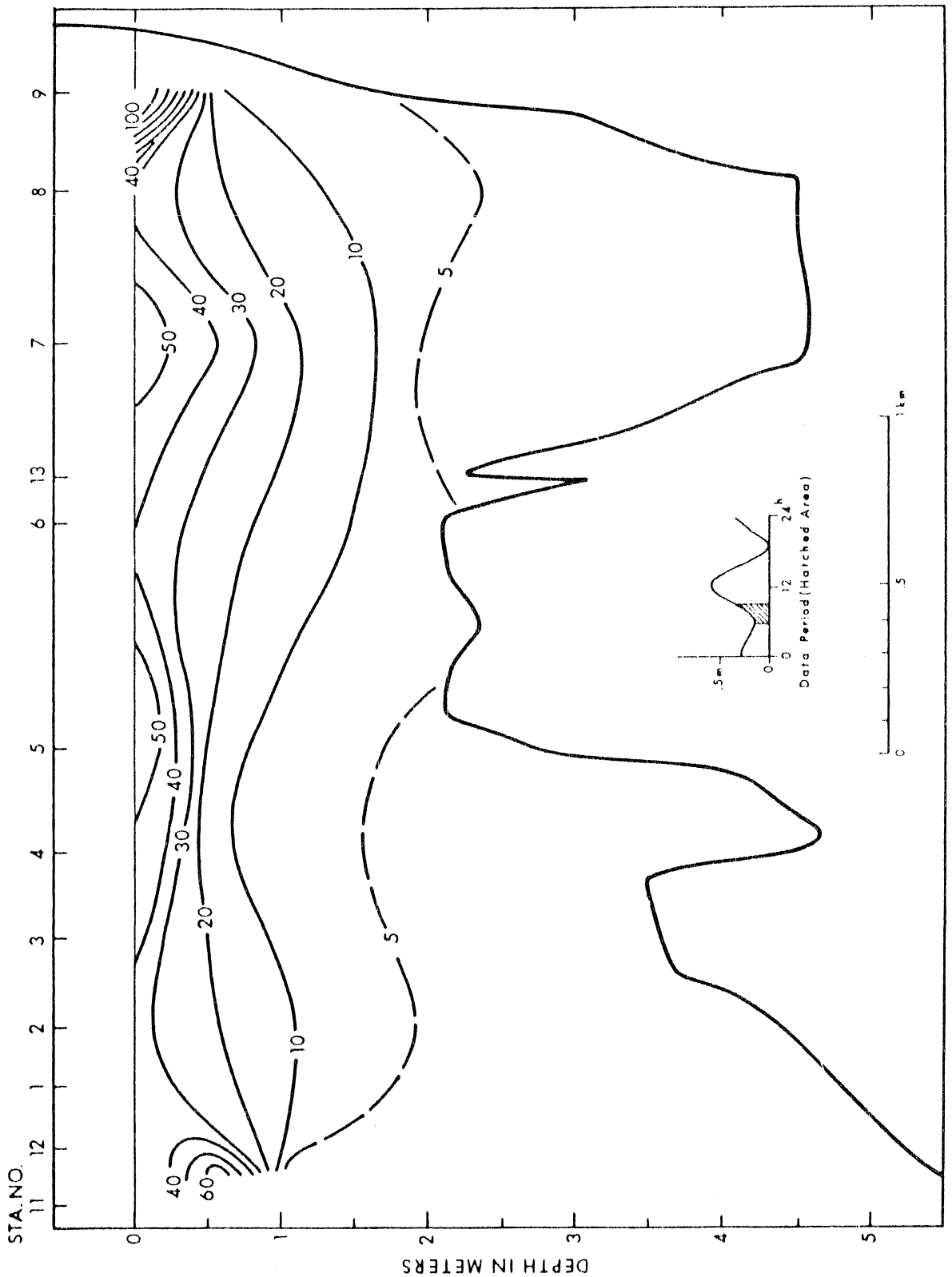
STA. NO.
11 12 1 2 3 4 5 6 13 7 8 9
0 1 2 3 4 5
DEPTH IN METERS
100
40
60
50
40
30
20
10
5
.5m
0
12
24 h
Data Period (Hatched Area)
0
.5
1 km

Figure 30(g). Longitudinal section of nitrite in µg-at/l. October 20, 1969.

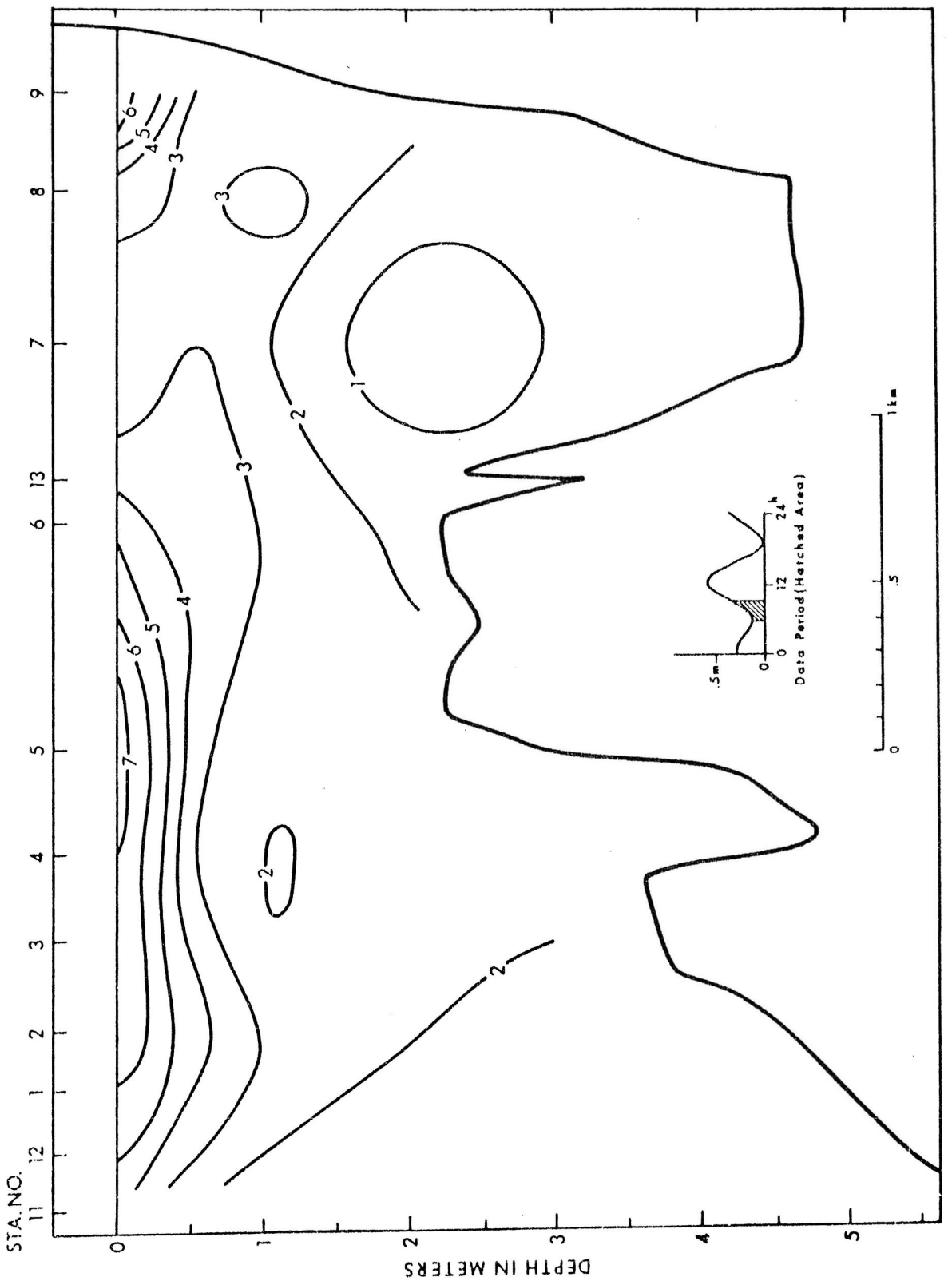
STA. NO.
11 12 1 2 3 4 5 6 13 7 8 9
DEPTH IN METERS
0 1 2 3 4 5
1
2
3
4
5
6
7
.5m
0
12
24h
Data Period (Hatched Area)
0
.5
1km

Figure 30(h). Longitudinal section of suspended load in mg/l. October 20, 1969.

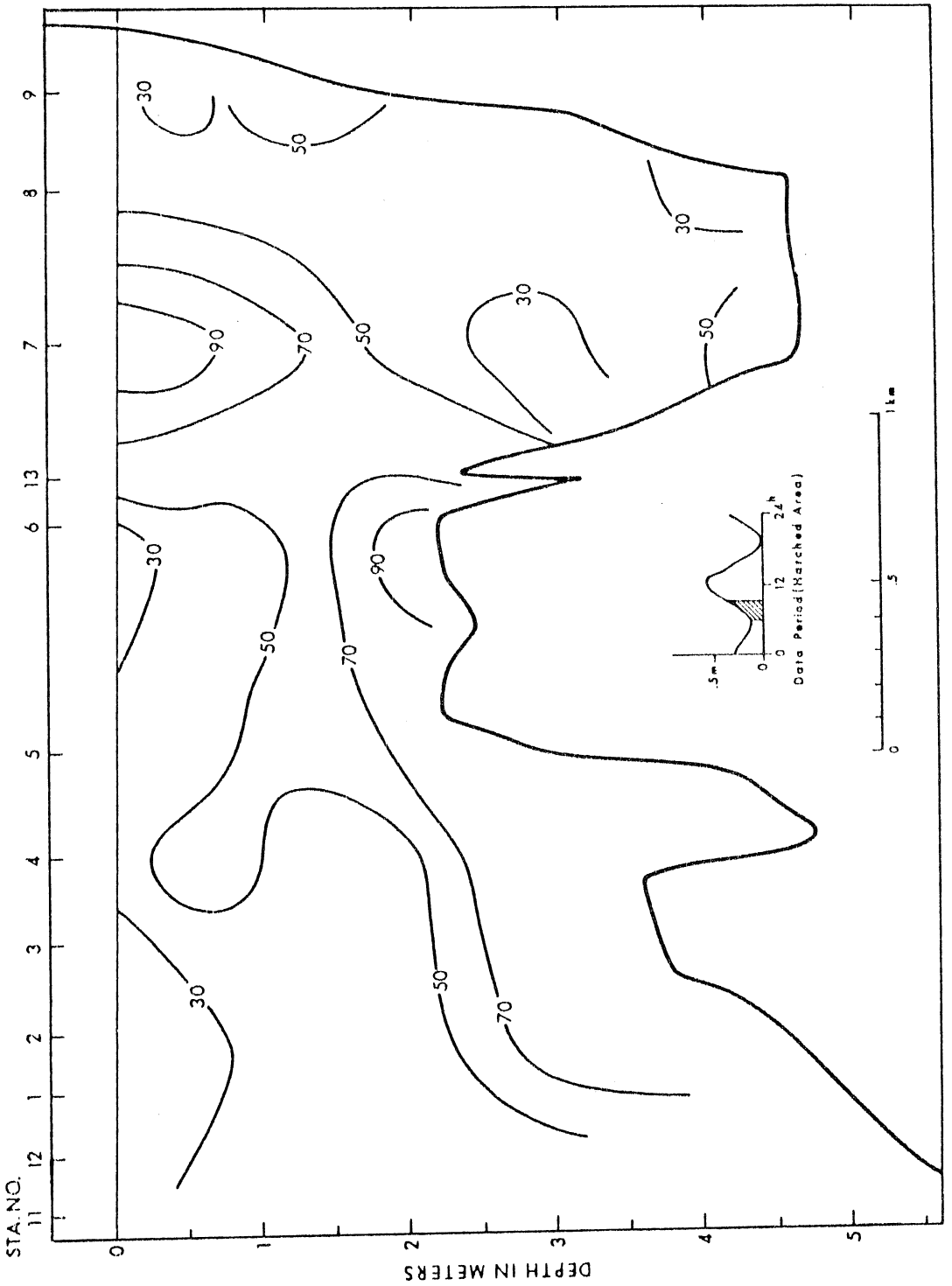
STA. NO.
11 12 1 2 3 4 5 6 13 7 8 9
DEPTH IN METERS
0 1 2 3 4 5
30
50
70
90
.5m
0
12
24 h
Data Period (Hatched Area)
0
.5
1 km

Figure 31(a). Longitudinal section of salinity in $^{o}/oo$. December 9, 1969.

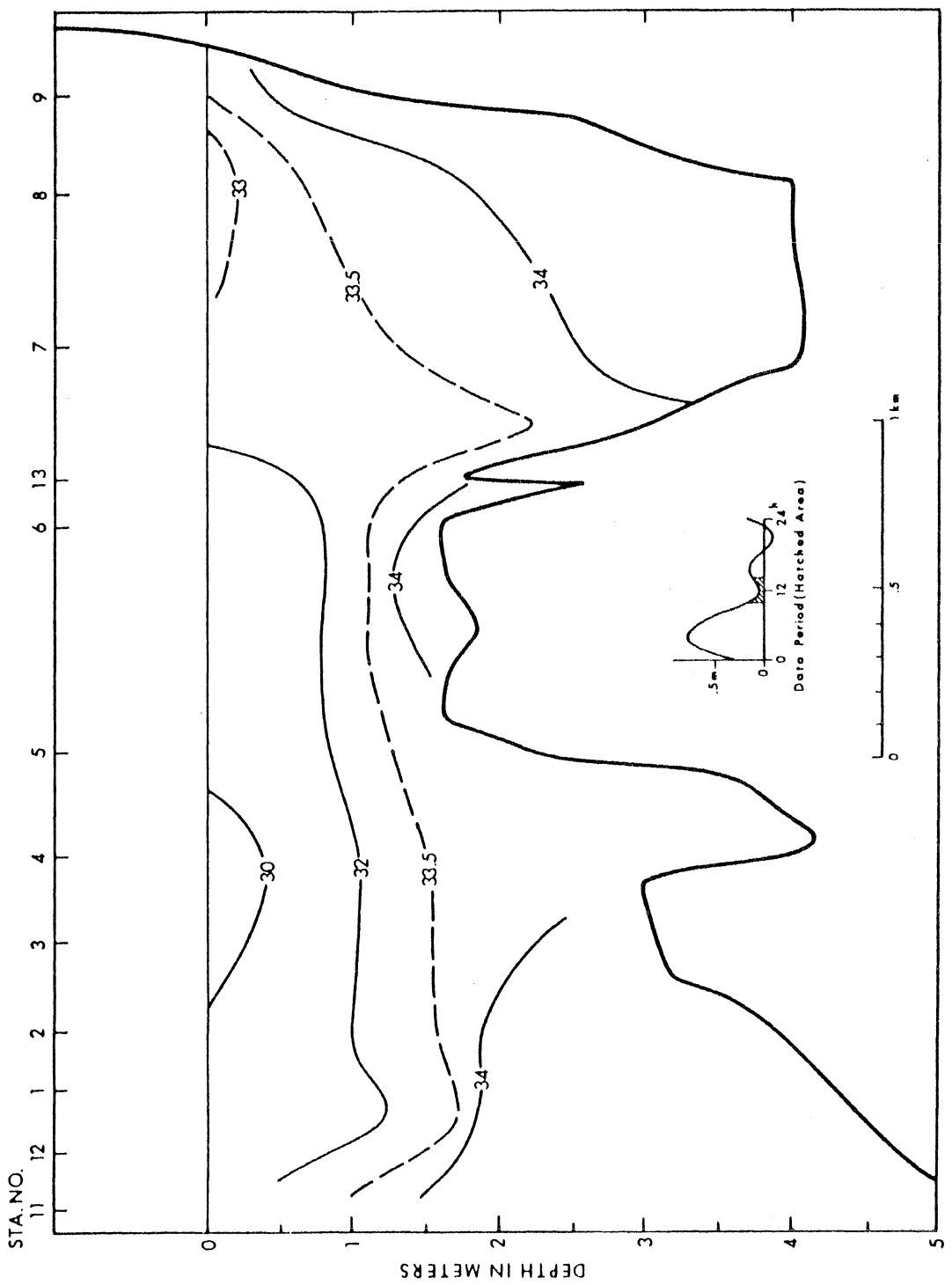
STA. NO.
11 12 1 2 3 4 5 6 13 7 8 9
DEPTH IN METERS
0 1 2 3 4 5
30
32
33.5
34
33
33.5
34
34
.5m
0
12
24h
Data Period (Hatched Area)
0
.5
1km

Figure 31(b). Longitudinal section of temperature in °C. December 9, 1969.

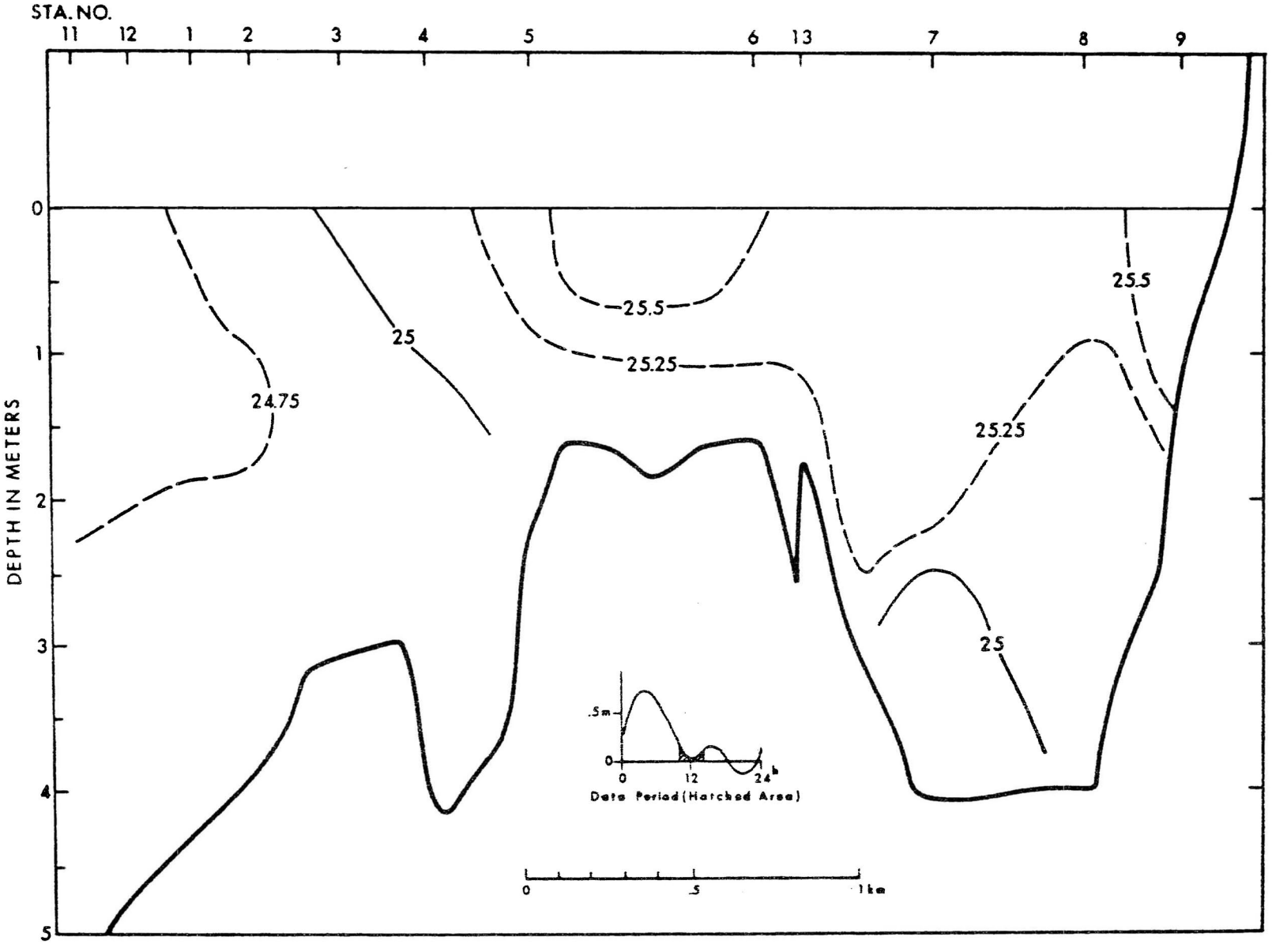
STA. NO.
11
12
1
2
3
4
5
6
13
7
8
9
0
1
2
3
4
5
DEPTH IN METERS
24.75
25
25.5
25.25
25.5
25.25
25
.5m
0
0
12
24h
Data Period (Hatched Area)
0
.5
1km

Figure 31(c). Longitudinal section of sigma-t in gm/cm^3. December 9, 1969.

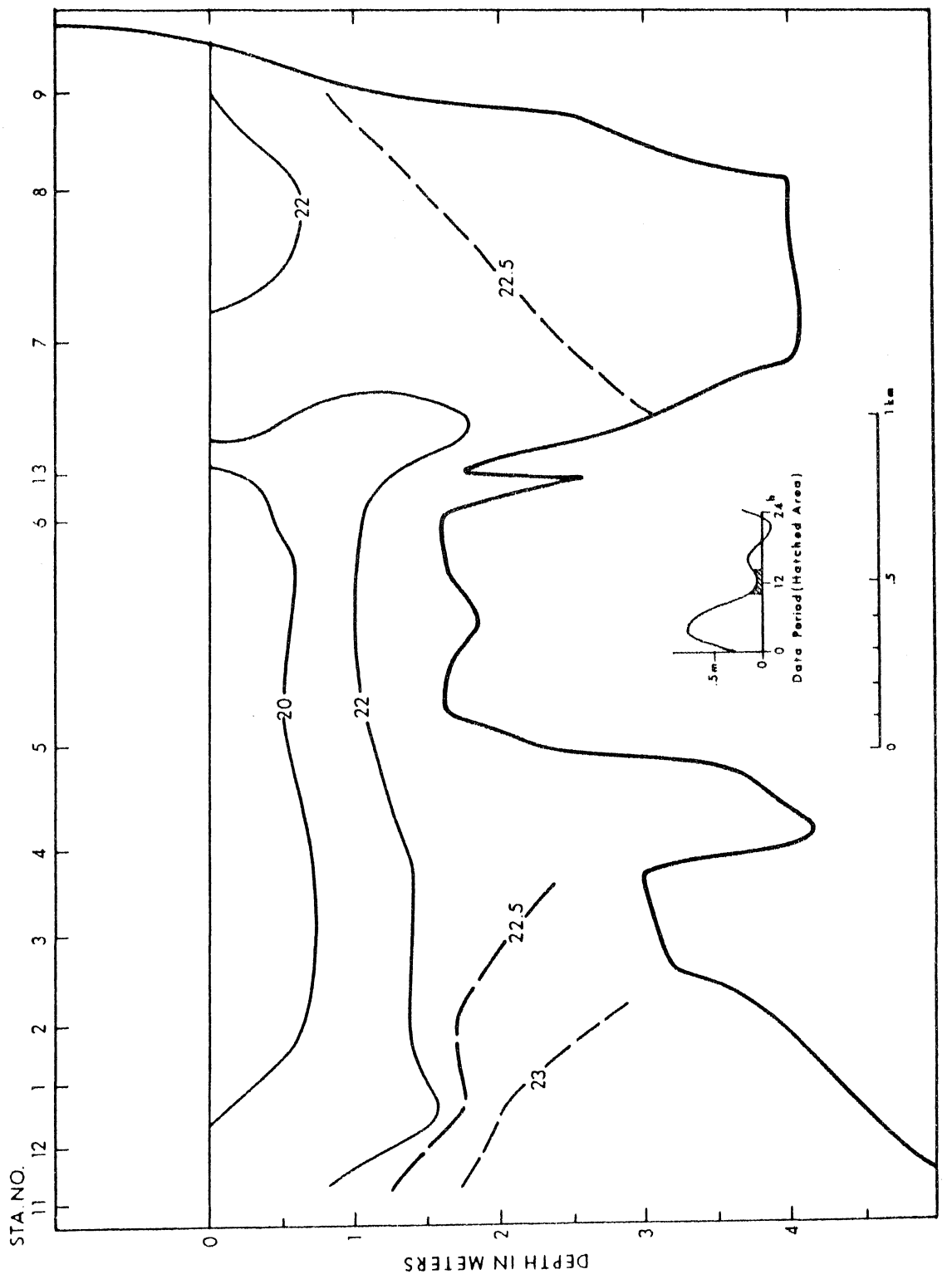
STA. NO.
11 12 1 2 3 4 5 6 13 7 8 9
DEPTH IN METERS
0 1 2 3 4
22
22.5
20
22
22.5
23
.5m
0 12 24h
Data Period (Hatched Area)
0 .5 1km

Figure 31(d). Longitudinal section of dissolved oxygen in ml/l. December 9, 1969.

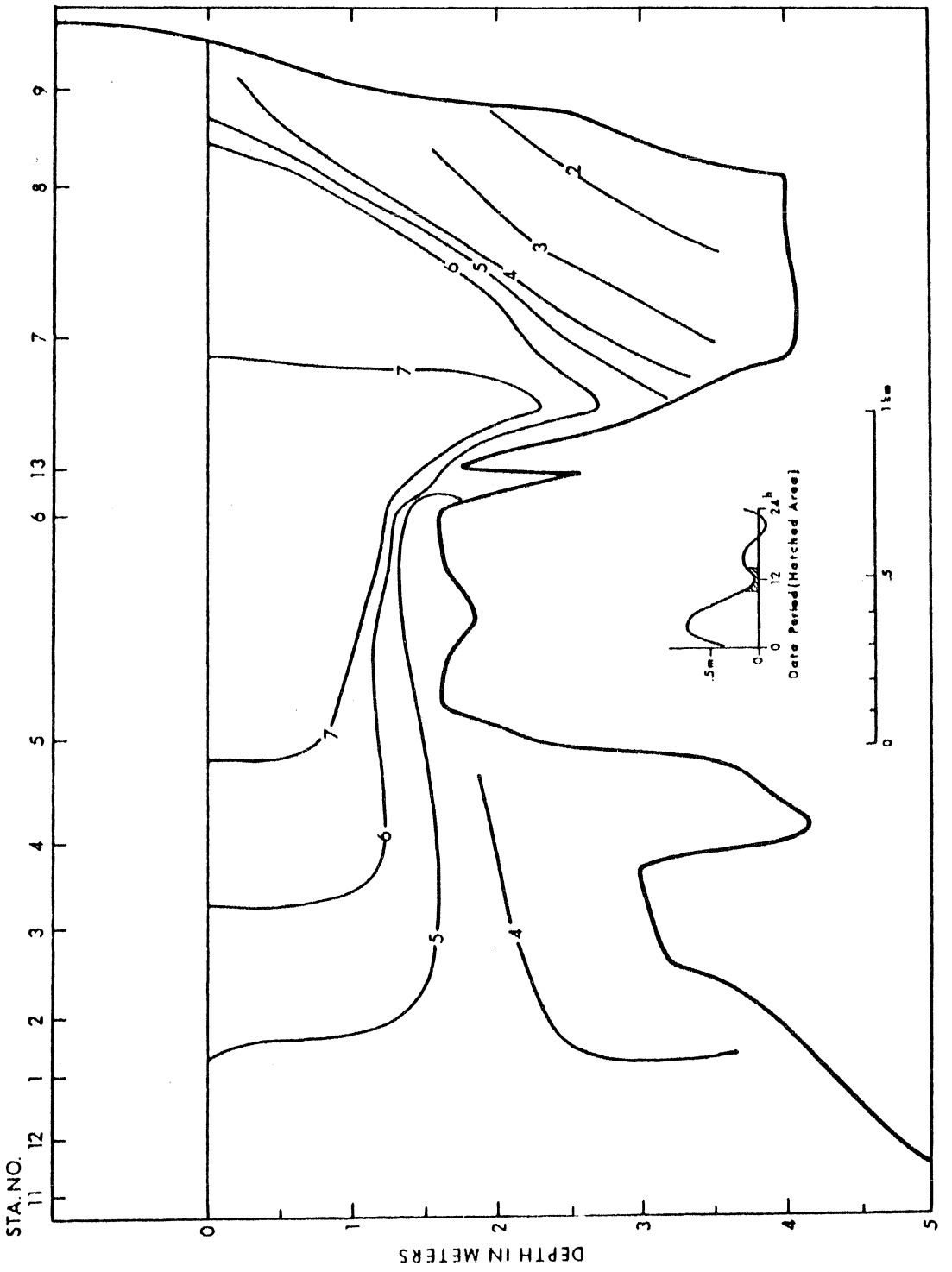
STA. NO.
11 12 1 2 3 4 5 6 13 7 8 9
DEPTH IN METERS
0 1 2 3 4 5
2
3
4
5
6
7
7
6
5
4
.5m
0
0
12
24h
Date Period (Hatched Area)
0
.5
1km

Figure 31(e). Longitudinal section of phosphate in µg-at/1. December 9, 1969.

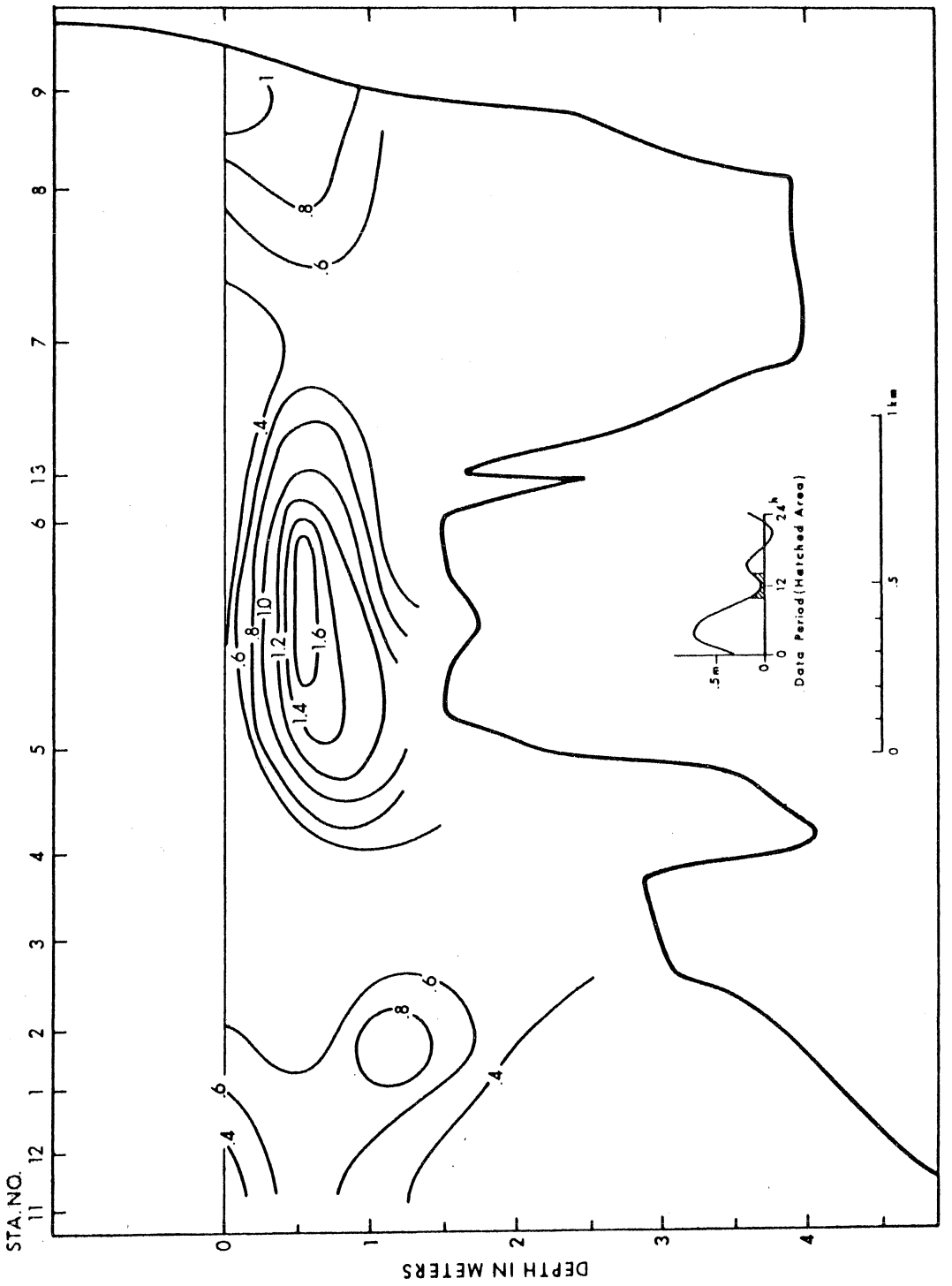
STA. NO.
11 12 1 2 3 4 5 6 13 7 8 9
DEPTH IN METERS
0 1 2 3 4
.4
.6
.8
1
1.2
1.4
1.6
.5m
0 12 24h
Data Period (Hatched Area)
0 .5 1km

Figure 31(f). Longitudinal section of nitrite in µg-at/1. December 9, 1969.

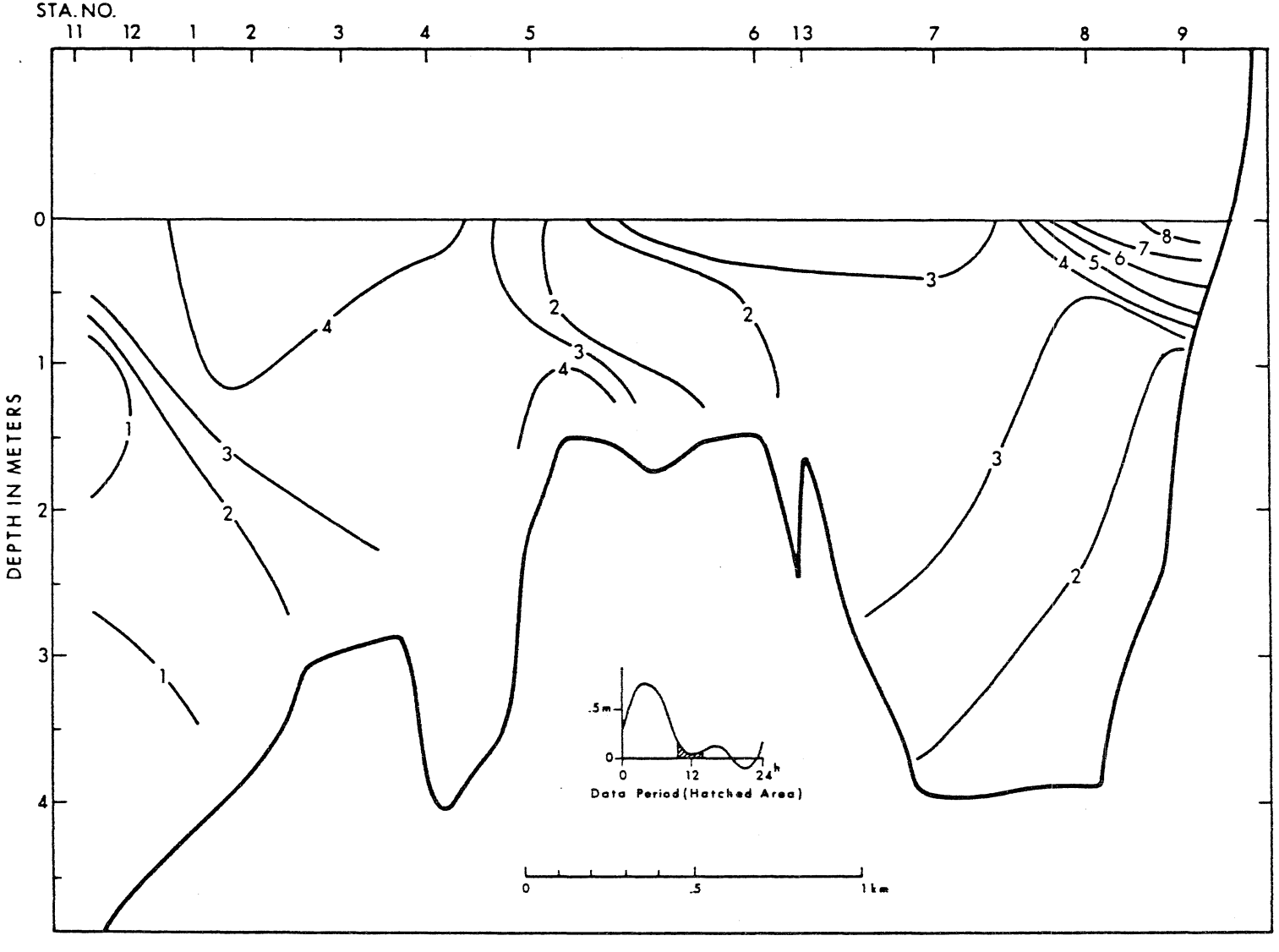
STA. NO.
11
12
1
2
3
4
5
6
13
7
8
9
DEPTH IN METERS
0
1
2
3
4
.5m
0
0
12
24h
Data Period (Hatched Area)
0
.5
1km

Figure 31(g). Longitudinal section of suspended load in mg/l. December 9, 1969.

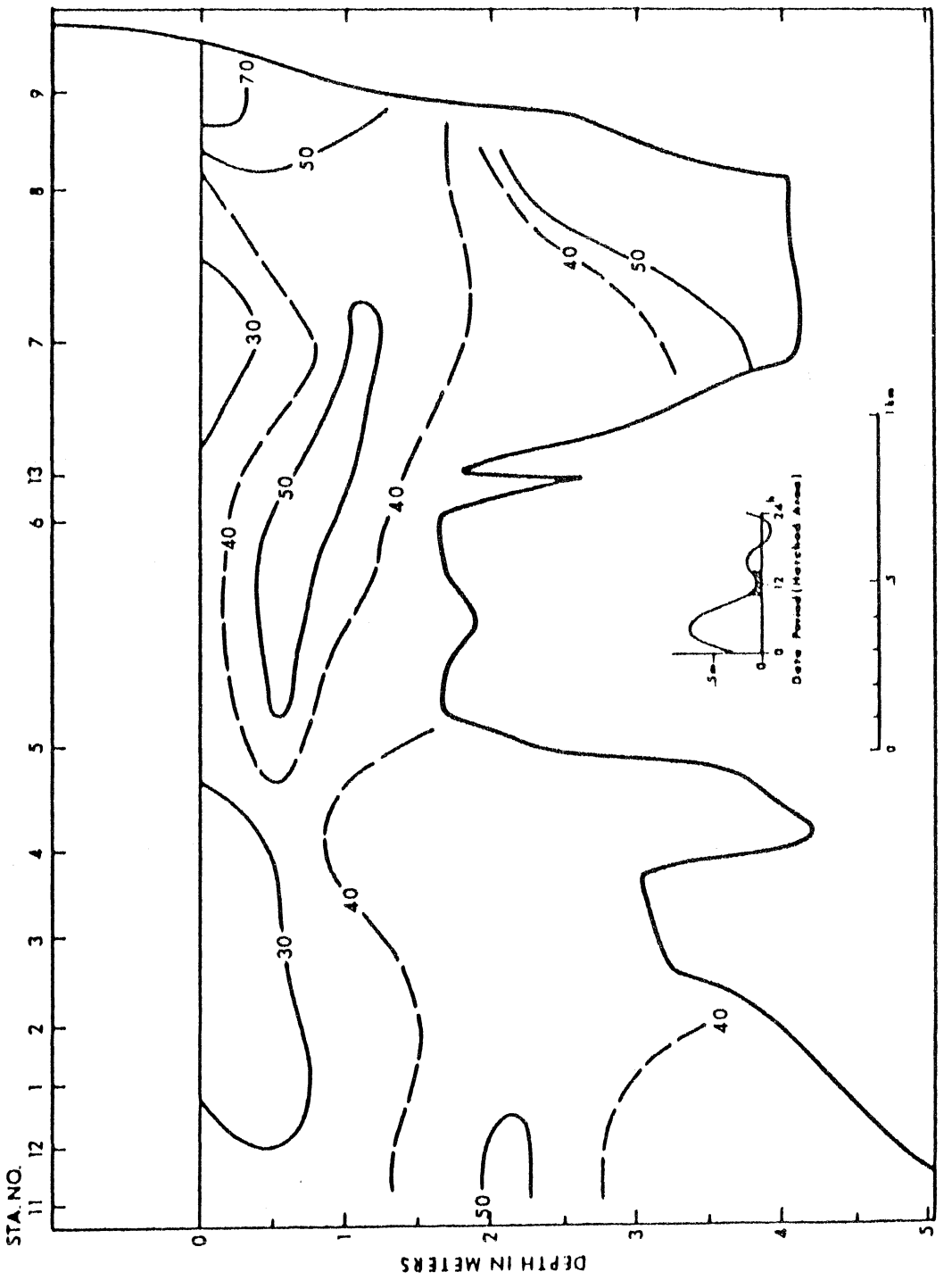
STA. NO.
11 12 1 2 3 4 5 6 13 7 8 9
DEPTH IN METERS
0 1 2 3 4 5
70
50
40
30
50
40
40
50
40
30
40
50
40
Data Period (Hatched Area)
-5m
0
12
24 h
0
5
1 km

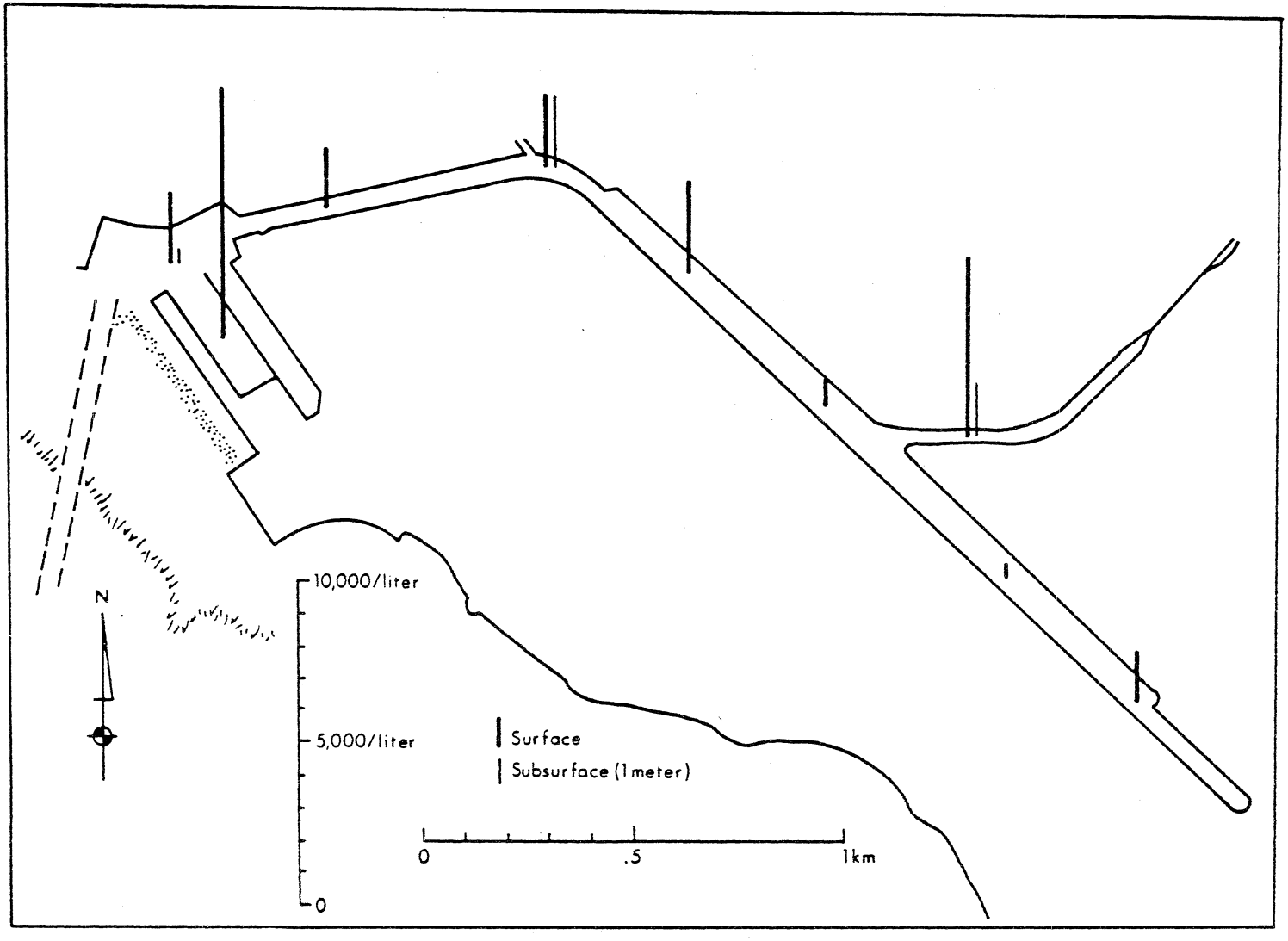

Figure 32. Total coliform distribution. December 9, 1969.

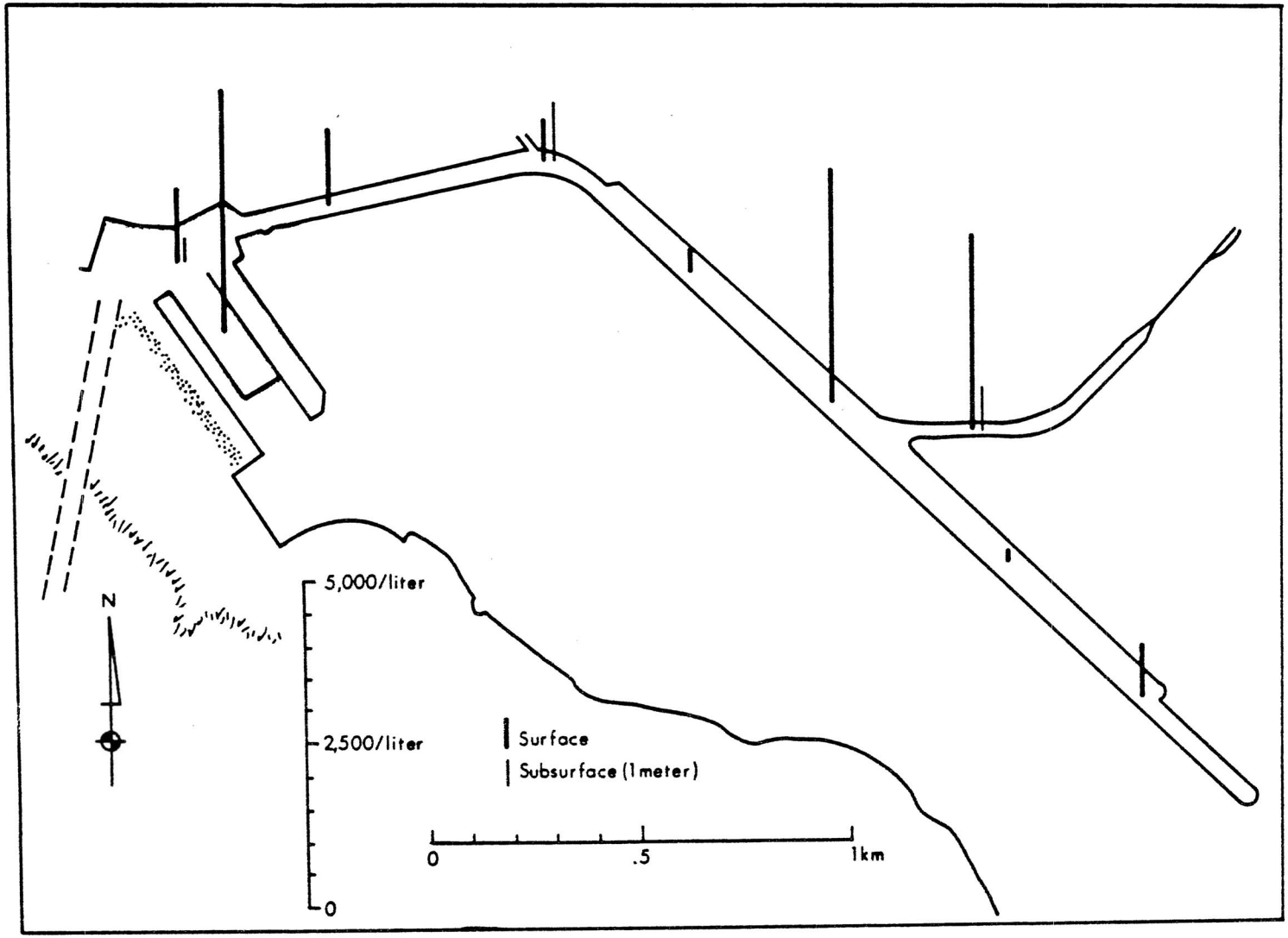

Figure 33. Fecal coliform distribution. December 9, 1969.

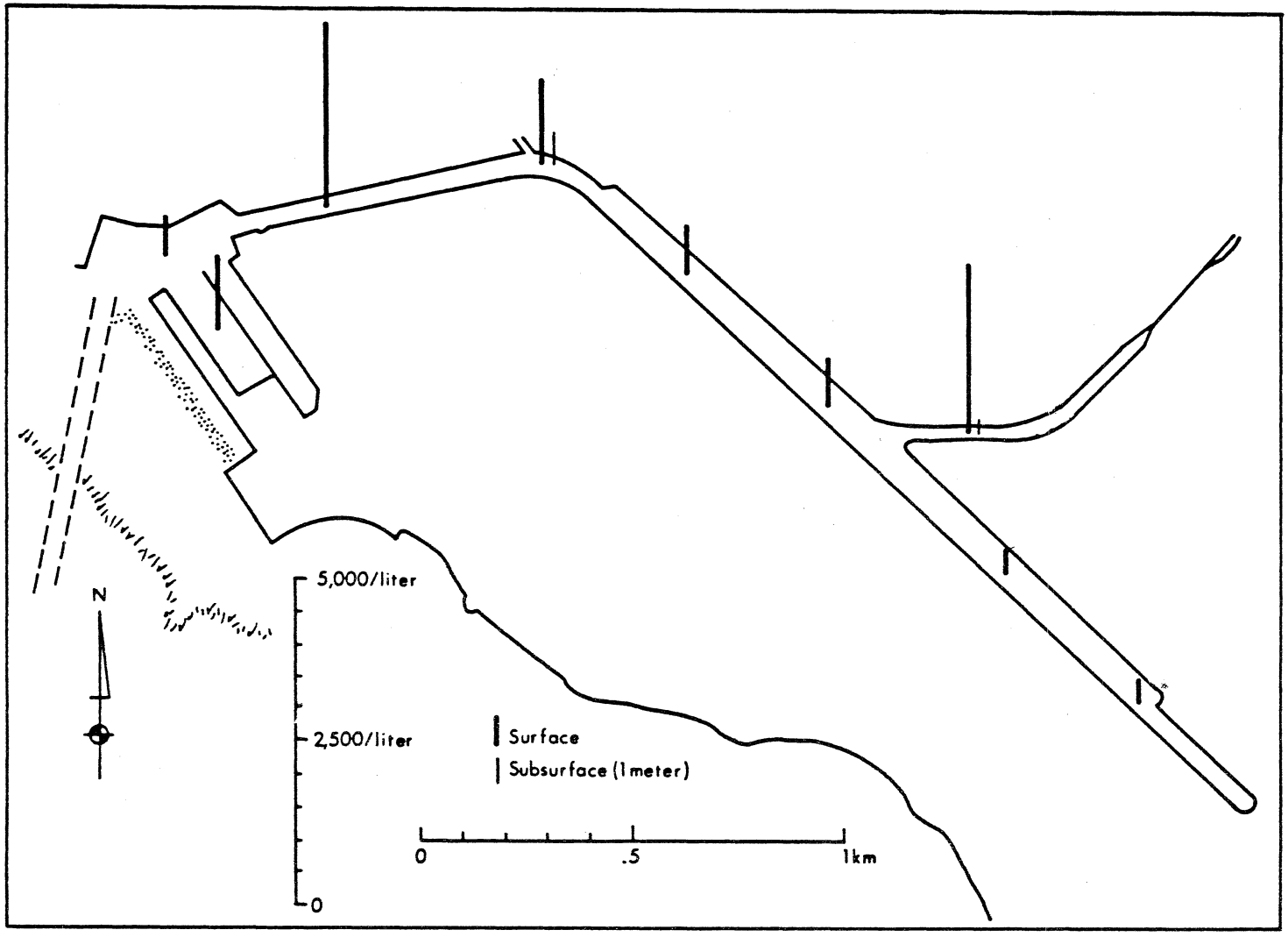

Figure 34. Fecal streptococci distribution. December 9, 1969.

BIBLIOGRAPHY

Bigelow, L. H. 1927. Report of the Superintendent of Public Works to the Governor of the Territory of Hawaii for the year ending June 30, 1927. Honolulu Star Bulletin.

Bowden, K. F. 1967. Circulation and diffusion. In Estuaries, edited by G. H. Lauff, pp. 15-36. Publication No. 83, American Association for the Advancement of Science. Washington, D. C.

Chinn, S. S. W. 1965. Water supply potential from an asphalt-lined catchment near Holualoa Kona, Hawaii. Geological Survey Water-Supply paper 1809-P.

Cox, D. C. 1969. Estuarine pollution in the state of Hawaii. University of Hawaii Water Resources Research Center, Technical Report No. 31.

Honolulu Advertiser. 1957. Houseboats must move from Ala Wai Harbor. Section A1, p. 2, April 2, 1957.

Honolulu Department of Public Works. 1969. Storm drainage standards. Division of Engineering.

Millipore Corporation. 1969. Microbiological analysis of water. Millipore Application Report AR-81.

Mink, J. F. 1962. Rainfall and runoff in the leeward Koolau Mountains, Oahu, Hawaii. Pacific Science, Vol. XVI, April, 1962.

Postma, H. 1967. Sediment transport and sedimentation in the estuarine environment. In Estuaries, edited by G. H. Lauff, pp. 158-179. Publication No. 83, American Association for the Advancement of Science. Washington, D. C.

Pritchard, D. W. 1967. Observations of circulation in coastal plain estuaries. In Estuaries, edited by G. H. Lauff, pp. 37-44. Publication No. 83, American Association for the Advancement of Science. Washington, D. C.

Proudman, J. 1953. Dynamical oceanography. John Wiley and Sons, Inc. New York.

Strickland, J. and Parsons, T. 1965. A manual of sea water analysis. Fisheries Research Board of Canada, Bulletin No. 125, 2nd Revised Edition.

Tully, J. P. 1953. Some characteristics of sea water structure. Proceedings of 8th Pacific Science Congress, Philippines (1953), 3:643-662.

Tully, J. P. 1958. On structure, entrainment, and transport in estuarine embayments. Journal of Marine Research, 17:523-535.

Wyrtki, K., Burks, J. B., Latham, R. C. and Patzert, Wm. 1967. Oceanographic observation during 1965-1967 in the Hawaiian Archipelago. Hawaii Institute of Geophysics Report 67-15.